

# **Modeling of Cardiac Uptake, Binding Kinetics and Inotropic Response of Amiodarone, Verapamil and $\alpha_1$ -Adrenergic Agents in Isolated Perfused Rat Heart**

## **D i s s e r t a t i o n**

zur Erlangung des akademischen Grades  
*doctor rerum naturalium* (Dr. rer. nat)

vorgelegt der

Naturwissenschaftlichen Fakultät I  
Biowissenschaften

der Martin-Luther-Universität Halle-Wittenberg

von

Frau Pakawadee Sermsappasuk  
geb. am 24.01.1976 in Bangkok, Thailand

Gutachter:

1. Prof. Dr. Michael Weiss
2. Prof. Dr. Reinhard Neubert
3. PD Dr. Willi Weber

Halle (Saale), 19. Dezember 2007

**urn:nbn:de:gbv:3-000012862**

[<http://nbn-resolving.de/urn/resolver.pl?urn=nbn%3Ade%3Agbv%3A3-000012862>]

## Table of Contents

<b>1.</b>	<b>Introduction .....</b>	<b>1</b>
1.1.	Pharmacokinetic/ Pharmacodynamic Modeling Concept .....	1
1.2.	Cardiophysiology.....	3
<b>2.</b>	<b>Langendorff Heart.....</b>	<b>7</b>
2.1.	Principle .....	7
2.2.	Langendorff Isolated Perfused Rat Heart System .....	9
2.3.	Langendorff Isolated Perfused Heart Preparation .....	11
<b>3.</b>	<b>Model Development Process.....</b>	<b>12</b>
3.1.	Measurement Model .....	13
3.2.	Parameter Estimation .....	13
3.3.	Model Selection.....	14
<b>4.</b>	<b>Amiodarone.....</b>	<b>15</b>
4.1.	Background .....	15
4.2.	Materials and Methods.....	16
4.2.1.	Drugs and Chemicals .....	16
4.2.2.	Experimental Protocol.....	16
4.2.3.	Quantification of Amiodarone.....	17
4.2.4.	PK/PD Model and Data Analysis .....	18
4.3.	Results.....	22
4.4.	Discussion .....	29
<b>5.</b>	<b>Verapamil.....</b>	<b>31</b>
5.1.	Background .....	31
5.2.	Materials and Methods.....	33
5.2.1.	Drugs and Chemicals .....	33
5.2.2.	Experimental Protocol.....	33
5.2.3.	Quantification of Verapamil.....	35
5.2.4.	PK/PD Model and Data Analysis .....	35
5.3.	Results and Discussion .....	40
5.3.1.	Effect of Amiodarone on PK/PD Modeling of Verapamil.....	40
5.3.2.	Effect of Endotoxemia on PK/PD Modeling of Verapamil .....	53
<b>6.</b>	<b><math>\alpha_1</math>-Adrenergic Agents.....</b>	<b>61</b>
6.1.	Background .....	61
6.2.	Materials and Methods.....	63
6.2.1.	Drugs and Chemicals .....	63
6.2.2.	Experimental Protocol.....	63
6.2.3.	Quantification of Prazosin.....	64
6.2.4.	Cumulative Dose-Response Curve of Phenylephrine .....	64
6.2.5.	PK/PD Model and Data Analysis .....	64
6.3.	Results.....	71
6.4.	Discussion .....	76
<b>7.</b>	<b>Summary.....</b>	<b>79</b>
<b>8.</b>	<b>Zusammenfassung .....</b>	<b>81</b>
<b>9.</b>	<b>References .....</b>	<b>83</b>

## Abbreviations

AIC	Akaike information criteria
AR	Agonist receptor occupation
Ca <sup>2+</sup>	Calcium
Ci	Curie
CL <sub>P</sub>	Permeation clearance (distribution clearance, transcapillary uptake clearance)
C(t)	Concentration at time <i>t</i>
C <sub>e</sub> (t)	Concentration in effect site
C <sub>in</sub> (t)	Input concentration to the heart
C <sub>out</sub> (t)	Output concentration from the heart
CV	Approximate coefficient of variation of parameter estimate
CVR	Coronary vascular resistance
DMSO	Dimethyl sulfoxide
E <sub>0</sub>	Baseline effect
EC	Excitation-contraction
EC <sub>50</sub>	Concentration required to produce 50% maximal response
E <sub>D</sub> (t)	Direct negative inotropic effect
E <sub>max</sub>	Maximum response
E(t)	Inotropic effect
E <sub>T</sub> (t)	rebound inotropic effect
f <sub>u</sub>	Free fraction in plasma
g	Extent of tolerance development
h	Hour
HR	Heart rate
HPLC	High-performance liquid chromatography
I	Dosing rate
ip	Intraperitoneal
K <sub>A</sub>	Equilibrium dissociation constant
K <sub>E</sub>	AR producing 50% of $\phi_{max}$
k <sub>in</sub>	First-order uptake rate constant
k <sub>ir</sub>	First-order rate constant of irreversible tissue binding
k <sub>on</sub>	Association rate constant
k <sub>off</sub>	Dissociation rate constant
k <sub>out</sub>	First-order rate constant of transport from extravascular compartment to vascular compartment
K <sub>p</sub>	Partition coefficient
K <sub>pu</sub>	Partition coefficient related to unbound drug concentration
l	Liter
LPS	Lipopolysaccharides

<i>LVDP</i>	Left ventricular developed pressure
<i>LVEDP</i>	Left ventricular enddiastolic pressure
<i>LVSP</i>	Left ventricular systolic pressure
<i>M</i>	Molar
<i>min</i>	Minute
<i>ML</i>	Maximum likelihood
<i>mol</i>	Mole
$M_i$	Transit compartment <i>i</i>
<i>MTT</i>	Mean transit time
<i>N</i>	Hill coefficient
<i>PE</i>	Phenylephrine
<i>PK/PD</i>	Pharmacokinetic/pharmacodynamic
<i>Pgp</i>	P-glycoprotein
<i>PRZ</i>	Prazosin
<i>Q</i>	Flow rate
$R^2$	Coefficient of determination
$R_{tot}$	Amount of receptor sites available for binding
<i>s</i>	Second
<i>S.D.</i>	Standard deviation
<i>S.E.M.</i>	Standard error of mean
<i>SR</i>	Sarcoplasmic reticulum
$\tau$	Delay time constant
$t_{1/2}$	Half-life
$V_0$	Volume of an additional compartment to account for the mixing in nonexchanging elements of system
$V_{ss}$	Volume of distribution at steady state
$V_{vas}$	Vascular volume
$x_i$	drug amount in compartment <i>i</i>
$\phi$	Chain of cellular process

# 1. Introduction

## 1.1. Pharmacokinetic/ Pharmacodynamic Modeling Concept

Pharmacokinetics involves the kinetics of drug absorption, distribution, metabolism and excretion, or in other words, it is defined as the use of mathematical models to quantitate the time course of drug absorption and disposition in man and animals (Riviere, 1999). Pharmacodynamics has been defined as the study of the biologic effects resulting from the interaction between drugs and biologic systems (Holford and Sheiner, 1981). Modeling “provides a systematic way of organizing data and observations of a system at cell, tissue, organ, or whole animal (human) levels” and “affords the opportunity to better understand and predict physiological phenomena” (Epstein, 1994). Pharmacokinetic/pharmacodynamic modeling has been used as a tool to understand the impact of dose or drug concentration on pharmacological response.

Assuming a compartmental structure, pharmacokinetic models can be written in form of sums of exponentials, or differential equations based on mass-balance, or mass-action principles. For pharmacodynamics, many mathematical models have been proposed. The most widely used pharmacodynamic models are the  $E_{max}$ -model and the sigmoid  $E_{max}$ -model which are often regarded as empiric mathematical functions that describe the shape of the concentration-effect relationship for a particular drug. However, these models cannot distinguish between the occupation and the activation of a receptor by an agonist. In contrast, the operation model proposed by Black & Leff (1983) can relate receptor occupancy and pharmacologic effect using two successive saturable hyperbolic functions. The first is the binding of the agonist to the receptor, and the second is the stimulus-response relationship between the agonist-receptor complex ( $[AR]$ ) and the pharmacological effect (Kenakin, 1993).

The PK/PD modeling is a mathematical approach that correlates the mass transfer embedded in pharmacokinetic model to drug effect (Riviere, 1999). The drug effect cannot be directly correlated to the drug concentration in a pharmacokinetic compartment, since due to an equilibrium delay with the site of drug action (Sheiner

et al., 1979) or post receptor transduction system (Mager and Jusko, 2001), it becomes necessary to identify a biophase as an effect compartment so that concentration-time profile in biophase can be correlated to drug effect.

Model parameters estimated are normally built using experimentally data that contain information on the system (systematic component) and are subject to errors. Therefore, one objective of mathematical modeling is to differentiate the systematic component in the system from the noise or random component in the system. Hence, models usually consist of a structure model that derived from systematic component plus a statistical model that describe the error component of the model (Bonate, 2006).

One can choose either an empirical or mechanism-based model. The empirical model is useful when little is known about the underlying physical process, whereas the mechanism-based model is based on physical and physiological principles. Factors such as transport to tissues dependent on blood flow, kinetics of receptor binding, and intracellular diffusion processes may all play a role. In order to increase knowledge in pharmacologic mechanism, researchers have established many useful mechanism-based models. For example, mechanism-based pharmacokinetic model for paclitaxel (Henningsson et al., 2001), digoxin (Baek and Weiss, 2005), idarubicin (Weiss and Kang, 2002), midazolam (Cleton et al., 2004), etc. One objective of our present research is also to establish the mechanism-based model for amiodarone, verapamil and  $\alpha$ -adrenergic agonist/antagonist in isolated heart.

## 1.2. **Cardiophysiology**

The heart is one of the vital organs in the body. In order to maintain its proper function, it requires highly controlled regulation of calcium concentration inside cardiomyocyte (Marks and Marx, 2001), and the control from the sympathetic and parasympathetic nervous systems (Brodde and Michel, 1999; Marks and Marx, 2001), which act via adrenoceptors and muscarinic acetylcholine receptors, respectively.

Excitation-contraction (EC) coupling is a process that regulates the heart contraction (Fig. 1.1). Its initial signal is an electrical one known as the depolarization, triggered by the cardiac action potential. The electrical signal travels into the heart muscle via specialized membranes known as the transverse (T) tubule system. These membranes contain the voltage-dependent calcium channel or L-type calcium channel that is the molecular target for the widely used calcium channel antagonists such as verapamil.

During the action potential, L-type calcium channel is activated by membrane depolarization, then, a small amount of calcium enters the heart muscle cell due to the large chemical gradient of calcium across the plasma membrane. However, the amount is insufficient to trigger heart muscle cell contraction, but it sufficient to activate much larger intracellular calcium release channels, ryanodine receptors, on the sarcoplasmic reticulum (SR) membrane within the cardiac muscle cells (Marks and Marx, 2001).

Once calcium binds troponin C, it undergoes a conformation change that permits actin and myosin to form crossbridges and causes contraction of the heart muscle cells. During the relaxation phase, when the heart cell membrane is repolarized, calcium channels in the SR membrane pump the calcium back into the SR. This results to decrease the calcium concentration in the cytosol of the muscle; then calcium no longer binds to troponin C and heart muscle relaxation occurs.

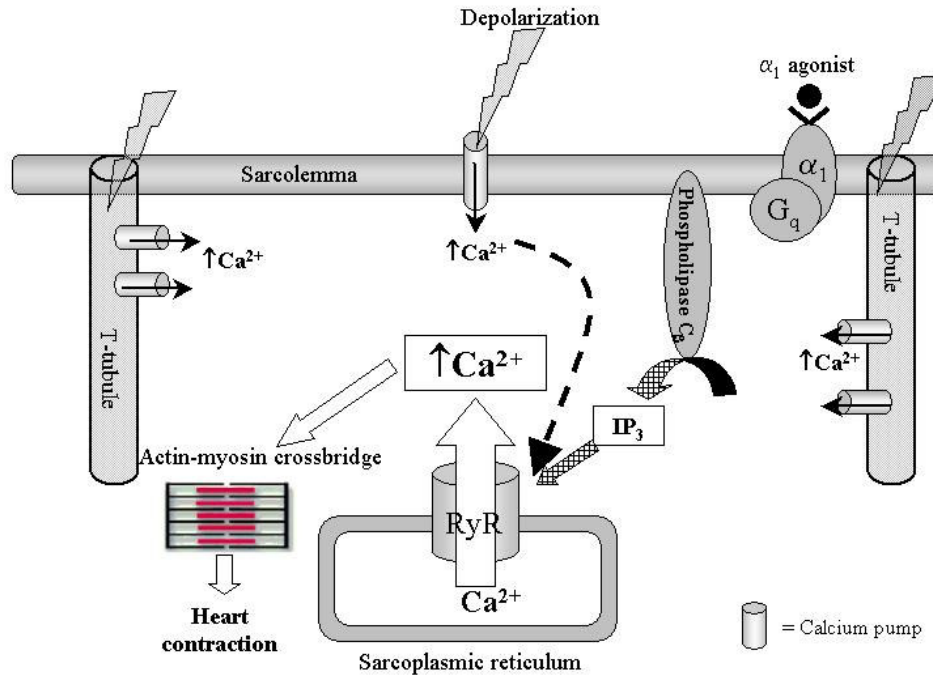


**Figure 1.1** The Excitation-contraction (EC) coupling process and the  $\alpha_1$  signal transduction pathway in cardiac cell. The EC process initiated by depolarization leads to small amount of  $\text{Ca}^{2+}$  inflow from outside cell which activates larger amount of  $\text{Ca}^{2+}$  inflow from sarcoplasmic reticulum (SR) via ryanodine receptors (RyR). Then,  $\text{Ca}^{2+}$  induces crossbridge formation of actin-myosin, which leads to heart contraction. The  $\alpha_1$  stimulation promotes the contraction by activating via  $G_q$  protein and phospholipase  $C_\beta$ . It results in an increasing amount of inositol-1,4,5-trisphosphate ( $\text{IP}_3$ ) which stimulates the influx of  $\text{Ca}^{2+}$  from SR.

The heart contains many subtypes of adrenoceptors such as  $\beta_1$ -,  $\beta_2$ -,  $\beta_3$ -, and  $\alpha_1$ -adrenoceptors (Van Zwieten, 1994; Westfall and Westfall, 2005); however, because of high density of  $\beta_1$ -adrenoceptors,  $\beta$ -adrenoceptors are predominant in normal physiological condition. The receptors regulate positive inotropic and positive chronotropic functions through stimulatory G ( $G_s$ ) protein which activates adenylate cyclase to produce cyclic AMP (cAMP).

In contrast with  $\beta$ -adrenoceptors, the stimulation of  $\alpha_1$ -adrenoceptors with appropriate agonists will cause a rise in contractility but not in heart rate (Van Zwieten, 1994). Such effects can only be demonstrated appropriately *in vitro*, since *in vivo* or the isolated perfused heart the picture is greatly complicated by the simultaneously occurring vasoconstriction, also induced by  $\alpha_1$ -adrenoceptor stimulation. Positive inotropic effect of  $\alpha_1$  receptor stimulation is not thought to be of major importance in myocardium; however, in pathological conditions where  $\beta$ -adrenergic activity is compromised such as congestive heart failure, hypothyroidism and hypoxia,  $\alpha_1$ -adrenoceptor pathway may act as a reserve mechanism to maintain the myocardial responsiveness to endogenous catecholamines.

A primary mode of signal transduction of  $\alpha_1$ -adrenoceptors involve activation of the  $G_q$ -PLC $\beta$ -IP $_3$ -Ca $^{2+}$  pathway which is shown in Fig. 1.1 (Westfall and Westfall, 2005). The pathway involves activation of a phospholipase C $\beta$  (PLC $\beta$ ), apparently through a  $G_q$  protein, and the hydrolysis of membrane-bound phosphatidylinositol-4,5-bisphosphate; the result is generation of two second messengers-diacylglycerol and inositol-1,4,5-triphosphate (IP $_3$ ). The latter compound stimulates the release of Ca $^{2+}$  from intracellular stores, which might be involved in increases in force of contraction (Lefkowitz et al., 1990). In addition,  $\alpha_1$ -adrenoceptor stimulation increases the Ca $^{2+}$  sensitivity of myofilaments and the transsarcolemmal Ca $^{2+}$  influx and causes intracellular alkalinization via activation of the Na $^+$ /H $^+$  exchanger (Fuller et al., 1991), at least in part, due to diacylglycerol-induced activation of protein kinase C. The receptor has also shown to couple other transduction pathways including phospholipase A $_2$ , phospholipase D and calcium channel (Perez et al., 1993).

In the present study, inotropic effect of cardiovascular drugs were measured and related to outflow concentration using PK/PD modeling. Verapamil and amiodarone, are the calcium antagonists that inhibit an influx of calcium ions by binding voltage-dependent L-type calcium channels (Fig 1.1), consequently induce negative inotropic effect. Phenylephrine (PE) is the  $\alpha_1$ -adrenoceptor agonist that induces positive inotropic effect via the mechanism described above, while prazosin,  $\alpha_1$ -adrenoceptor antagonist, reduces this positive inotropic effect when administered together with PE.

## 2. Langendorff Heart

### 2.1. Principle

Langendorff heart is one type of isolated perfused heart which is widely used for biochemical, physiological, morphological and pharmacological researches. It provides detailed analysis of intrinsic ventricular mechanics, metabolism and coronary vascular responses.

Langendorff heart (Fig. 2.1) is the isolated perfused heart of which the coronary arteries are perfused by retrograde flow from aorta. For maintaining cardiac activity, the basic principle of Langendorff isolated heart is to perfuse oxygenated perfusate via coronary arteries using a cannula inserted in the ascending aorta. Then, during diastole when the aortic valves are closed, the perfusate flows through the coronary arteries. After passing through the coronary vascular system, the perfusate enters the right atrium via coronary sinus and finally flows out via the right ventricle and pulmonary artery. The perfusate might be blood, Tyrode, Locke or Krebs-Henseleit bubbled with carbogen at physiological temperature. The perfusate flow rate is controlled by hydrostatic pressure for constant pressure model, or by roller pump for constant flow model. The latter model was used for our experiments.

Like other isolated organs, the certain advantage of the Langendorff heart is that measurements can be obtained without many complications such as feedback effects and hormonal and neural controls that originate outside of the heart. This allows an investigation of more specific response to the cardiac drug.

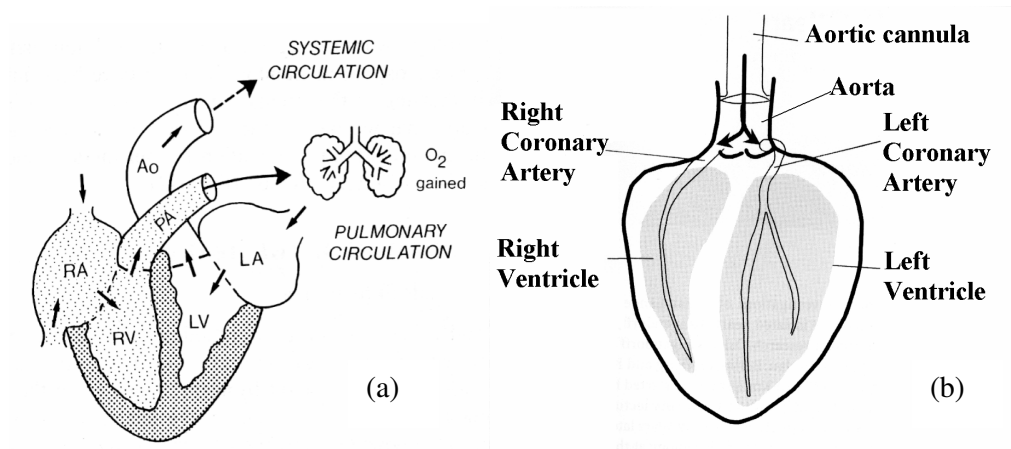


**Figure 2.1** (a) Normal circulaion (Opie, 1997). (b) Circulation in Langendorff perfused heart (Dhein, 2005). In Langendorff perfused heart, perfusate fluid enters the heart via the aorta. RA, right atrium; RV, right ventricle; PA, pulmonary artery; LA, left atrium; LV, left ventricle; Ao, aorta; O<sub>2</sub>, oxygen.

### 2.2. Langendorff Isolated Perfused Rat Heart System

For the Langendorff preparation, the model of isolated heart size3 (HSE-Harvard, March-Hugstetten, Germany), as shown in Fig. 2.2, was used in our experiments. The main part of Langendorff apparatus consists of a gear pump, an oxygenator, a roller pump, a heat exchanger, a thermostatic heart chamber and transducers. The gear pump is used for delivering the perfusate fluid from the reservoir to the oxygenator which produces thin film of the perfusate fluid in a carbogen (95% O<sub>2</sub> and 5% CO<sub>2</sub>) atmosphere. Then, the saturated carbogen perfusate fluid is supplied to the heart by means of a roller pump, which generates a constant perfusion flow. This will produce a corresponding perfusion pressure, which is measured by transducer no.1 (Fig. 2.2). The perfusion solution is delivered to a heat-exchanger chamber (normally a double walled cylinder connected to the thermostat) with an aortic cannula at its bottom. When the heart is attached to the cannula, the thermostatic heart chamber is moved to cover the heart. By transducer no.2 (Fig. 2.2), left ventricular pressure is recorded isovolumetrically supplied via a balloon catheter.

#### Modified Krebs-Henseleit Buffer

The perfusate fluid used in this research was a modified Krebs-Henseleit buffer containing NaCl (118 mM), KCl (4.7 mM), CaCl<sub>2</sub> (1.5 mM), MgSO<sub>4</sub> (1.66 mM), NaHCO<sub>3</sub> (24.88 mM), KH<sub>2</sub>PO<sub>4</sub> (1.18 mM), glucose (5.55 mM), Na-pyruvate (2 mM), and bovine albumin (0.1%w/v). The perfusate buffer was freshly prepared and filtered by 0.45 µm hydrophilic microfiltration membrane based on polyether sulfone (Sartorius AG, Gottingen).

## 2. Langendorff Heart

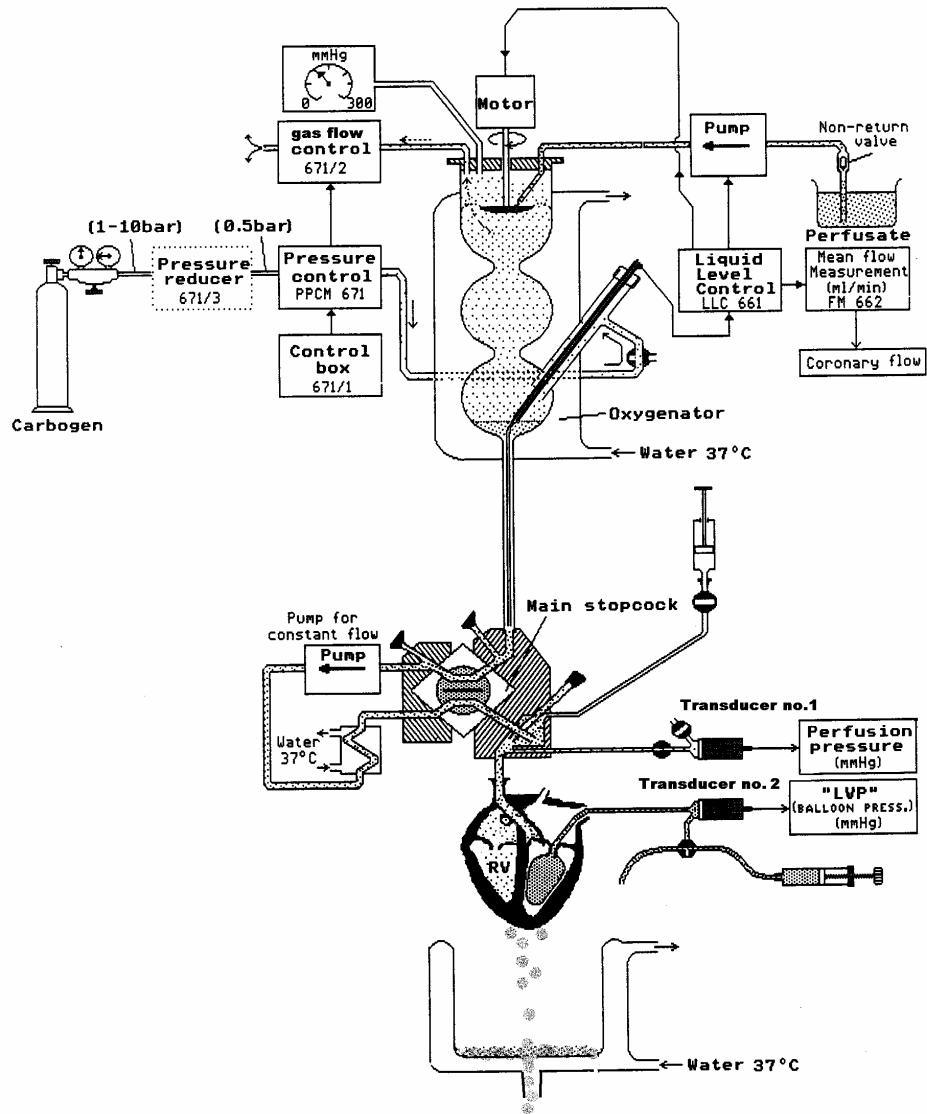


**Figure 2.2** Model of Langendorff heart at constant flow (modified from operating instructions for the experimental apparatus isolated heart size3 type 830, HSE-Harvard, March-Hugstetten, Germany)

### 2.3. Langendorff Isolated Perfused Heart Preparation

Rat was intraperitoneal (ip) injected with 500 IU heparin and anesthetized by ip injection of 50-80 mg/kg pentobarbital. After the rat became unconscious and lost pedal reflex activity, the heart surgery was started. First, its trachea was cannulated with an artificial ventilator, and then a midsternal thoracotomy was performed to open its chest. Second, the heart was hastened to excise and to transfer into oxygenated ice-cold modified Krebs-Henseleit buffer. Then, the cannula filled with oxygenated modified Krebs-Henseleit buffer was tied to its aorta. Finally, the heart attached cannula was rapidly switched to connect with the Langendorff perfusion apparatus. The apparatus had been previously set for constant flow rate ( $9.7 \pm 0.5$  ml/min) of the modified Krebs-Henseleit buffer saturated with carbogen (95% O<sub>2</sub> and 5% CO<sub>2</sub>), and its temperature was controlled at 37°C.

In order to measure pharmacodynamic response, a latex balloon tied to the end of a polyethylene tube, which was connected with pressure transducer, was carefully inserted into a left ventricle of the isolated heart. The balloon was inflated with 50% methanol to create a diastolic pressure of 5 to 6 mmHg. Four pharmacodynamic endpoints, left ventricular systolic pressure (*LVSP*), left ventricular enddiastolic pressure (*LVEDP*), heart rate (*HR*) and coronary perfusion pressure, were measured and monitored continuously by a physiological recording system (HSE Harvard, March-Hugstetten, Germany). Additionally, left ventricular developed pressure (*LVDP*) is defined as  $LVDP = LVSP - LVEDP$ , and coronary vascular resistance (*CVR*) is calculated from perfusion pressure divided by coronary flow.

### 3. Model Development Process

To develop models in the present study, many processes as shown in Fig. 3.1 have been involved. First, we needed to identify research problems, designed and performed experiment, and then collected the data. Second, based on scientific knowledge, measurement models that describe the time course of observed data (consisting of structure model and variance model) were formulated. Third, data were simultaneously fitted with the model using ADAPT II version 4 with Maximum Likelihood (ML) estimation. Then, the model was evaluated and selected using goodness of fit, model discrimination criteria such as AIC, and the approximate coefficients of variation of individual parameter estimates (*CV*). If the model was rejected, a new model was generated and evaluated again. Finally, when a final model was found, the results were interpreted.

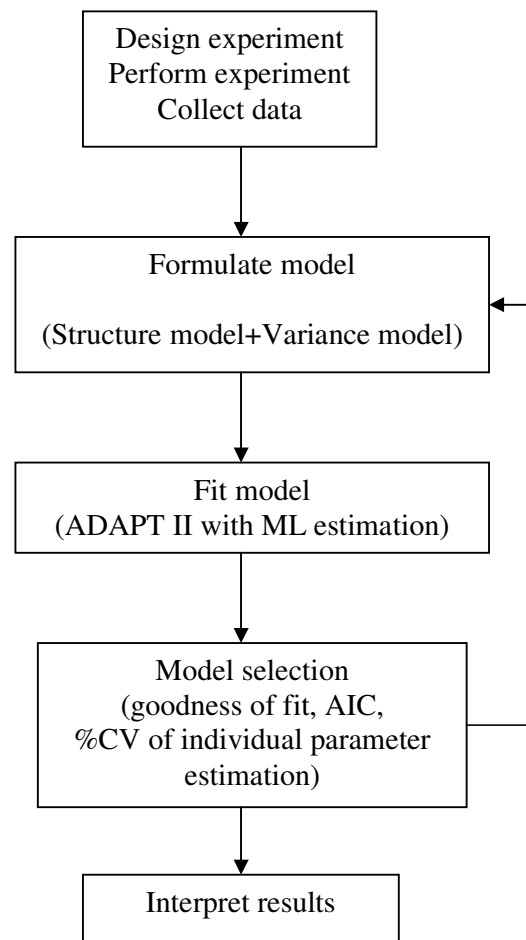


**Figure 3.1** The model development process

#### 3.1. Measurement Model

All measured values usually contained errors; in other words, this can be written as:

$$z(t_i) = y(t_i) + v(t_i) \quad i = 1, \dots, m \quad (3.1)$$

where  $z(t_i)$  denotes the measured value;  $y(t_i)$  denotes output of the structure model;  $v(t_i)$  is the measurement error (or additive error) which represents the deviation between model predicted values and observed values (D'Argenio and Schumitzky, 1997).

Hence, a measurement model usually consists of structure model and variance model (statistical model). The structure model is used to describe the behavior of drug in the system, while the variance model is used to describe the error in the system. If  $y(t)$  denotes the measured concentration in a compartment then  $y(t) = x(t)/V$  where  $x(t)$  is the amount in the compartment and  $V$  is the volume of the compartment.

Many types of variance models have been used in research for PK/PD modeling (Bonate, 2006). To choose an appropriate variance function, we must consider all sources of variation. In present study, we used the residual error variance model of the form.

$$\text{var}\{v(t)\} = (\sigma_{inter} + \sigma_{slope} y(t))^2 \quad (3.2)$$

where  $\sigma_{inter}$  is closely related to the sensitivity of the analytical method and  $\sigma_{slope}$  is closely related to the coefficient of variation.

#### 3.2. Parameter Estimation

To fit the model and estimate model parameters, various estimation methods can be used such as Weighted Least Squares (WLS), Maximum Likelihood (ML), Generalized Least Squares (GLS), Bayesian estimation, etc.

In present study, ML estimation was mainly used. Note that both system and variance model parameters can be estimated by maximizing the likelihood function, when the additive error ( $v(t)$ ) is normally distributed.

#### 3.3. Model Selection

##### *Goodness of fit criteria*

Goodness of fit criteria can be assessed by either visual examination or the coefficient of determination ( $R^2$ ).

$$R^2 = 1 - \frac{\sum_{i=1}^n (Y_i - \hat{Y}_i)^2}{\sum_{i=1}^n (Y_i - \bar{Y})^2} \quad (3.3)$$

$\bar{Y}$  is the mean of the observed  $Y$  value;  $\hat{Y}$  is the model predicted data vector.

$R^2$  refers to the proportion of variation explained by the model. It ranges from 0 to 1 with 1 being a perfect fit to data. In present study, we used a  $R^2$  threshold of 0.8.

##### *Model discrimination criteria*

Using ADAPT II program with ML estimation, Akaike Information Criteria (AIC) is automatically calculated. These criteria were used to select a model during model development. The model with a lower value of AIC is better. Note that AIC value tells nothing about how good the model is. The exact value is meaningless; it is worth only for comparing AIC between different models using the same data set and the same error structure.

##### *The uncertainty of parameter estimation*

The approximate coefficients of variation of individual parameter estimates (CV) represent imprecision of parameter estimation. In present study, we used a CV threshold of < 50%.

## 4. Amiodarone

### 4.1. Background

Amiodarone, which is a thyroid hormone analogue, was firstly introduced as an antianginal drug because of its coronary and systemic vasodilator properties (Charlier et al., 1968). Presently, the drug is widely used for antiarrhythmic treatment in spite of wide range of side effects and long term toxicity. Amiodarone possesses properties of all four classes of antiarrhythmic drugs and is indicated for a wide range of arrhythmias. Amiodarone inhibits sodium channels, L-type calcium channels, several types of potassium channels, and the sodium-calcium exchanger, and is a noncompetitive blocker of  $\alpha$ - and  $\beta$ - adrenoceptors. Because of its efficacy and safety, amiodarone is currently one of the most used antiarrhythmic agents (Connolly, 1999).

Amiodarone is a highly lipophilic basic drug ( $\log P = 5.95$  and  $pK_a = 8.7$  at  $37^\circ\text{C}$  (Chatelain et al., 1986)) and is almost insoluble in water or aqueous buffer solution. Because of this, the use of different type of vehicles (dimethyl sulfoxide, ethanol, albumin, Polysorbate 80 or blood) has been reported for dissolving the drug (Kodama et al., 1997). Amiodarone has an unusual pharmacokinetics such as extremely long and variable half-life (8 to 107 days) due to an unusually large volume of distribution of amiodarone. Its unusual pharmacokinetics makes predictions of drug accumulation following multiple dosing difficult (Latini et al., 1984) Thus, it has been shown that classical pharmacokinetic models fail to describe time course of plasma concentration during long-term treatment (Weiss, 1999). Acute pharmacokinetic processes, on the other hand, are particularly important in view of the use of intravenous amiodarone for the treatment of life-threatening arrhythmias (Desai et al., 1997). However, limited quantitative information is available on the uptake kinetics of amiodarone into the myocardium (Beder et al., 1998). We, therefore, used a PK/PD modeling approach to evaluate the initial distribution of amiodarone in Langendorff-perfused rat hearts together with the resulting negative inotropic effect. Thus, the aim of this study was to estimate PK parameters describing the uptake of amiodarone by the heart together with the PD parameters of a maximum effect model characterizing the negative inotropic effect.

## 4.2. Materials and Methods

### 4.2.1. Drugs and Chemicals

Amiodarone hydrochloride, triflupromazine hydrochloride and dimethyl sulfoxide (DMSO) were purchased from Sigma-Aldrich Chemie (Steinheim, Germany), Sigma-Aldrich Laborchemikalien (Seelze, Germany) and Carl Roth (Karlsruhe, Germany), respectively. Methanol, acetonitrile tetrahydrofuran and triethylamine were HPLC grade from Carl Roth (Karlsruhe, Germany). All other chemicals and solvents were of highest grade available.

### 4.2.2. Experimental Protocol

#### *Working Solution Preparation*

A concentrated amiodarone stock solution (10 mM) was firstly prepared by dissolving the drug in DMSO. Then, it was diluted to 2 mM amiodarone in DMSO. Finally, the working solution (10  $\mu$ M amiodarone) was freshly prepared by adding 5 ml of 2 mM amiodarone in 1 l modified Krebs-Henseleit buffer. The final concentration of DMSO was  $\leq 0.5$  %v/v, at which DMSO had no significant inotropic effect.

#### *Study Design*

Six hearts were obtained by the method mentioned above in section 2.3. After the heart was attached to the Langendorff system, it was allowed for 20-min equilibrium. Then, 10  $\mu$ M amiodarone in modified Krebs-Henseleit buffer, instead of modified Krebs-Henseleit buffer, were perfused to the heart by a gear pump. The solution was perfused for 15 min and outflow samples were collected every 30 s for 20.5 min and every 1 min for the next 26 min. The samples were frozen at  $-20^{\circ}\text{C}$  until analysis. The HPLC analysis was conducted within 3 months after collecting samples. During experiment, LVDP, CVR and HR were continuously monitored.

In order to determine vehicle effect, 3 hearts were tested by perfusing 5%v/v of DMSO in modified Krebs-Henseleit buffer for 15 min.

Due to high lipophilicity of amiodarone we have to account for the possibility of drug adsorption in the perfusion system, e.g., plastic tube, gear pump component, etc. (Peters and Hayball, 1990 ). Thus, the time course of outflow concentration was, additionally, evaluated in the absence of hearts in the Langendorff apparatus. The average concentrations of three control experiments (outflow without heart) were used as time course of input concentration to the heart in estimating model parameters.

### 4.2.3. Quantification of Amiodarone

Concentration of amiodarone in buffer was determined by high-pressure liquid chromatography (HPLC). The method was modified from the previous published procedure (Jun and Brocks, 2001) with the following condition:

#### *HPLC condition*

Column: reversed-phase column C 18, 4  $\mu\text{m}$  particle, 25 cm length, 4 mm internal diameter (Lichrospher 100 RP)

Mobile phase: methanol: acetonitrile: water: tetrahydrofuran: triethylamine (55:38:14:8.4:0.05 v/v)

Internal standard: trifluorpromazine HCl 10  $\mu\text{g}/\text{ml}$

Flow rate: 1.5 ml/min

Injection volume: 100  $\mu\text{l}$

Detection wavelength: 242 nm

Temperature: room temperature (25°C)

#### *Sample Preparation for HPLC*

The sample, amiodarone in the buffer (250  $\mu\text{l}$ ), was added with 50  $\mu\text{l}$  of internal standard solution (10  $\mu\text{g}/\text{ml}$ ). Acetonitrile (500  $\mu\text{l}$ ) was added for protein precipitation. Then, the sample was centrifuged at 3000  $\times g$  for 2 min and the supernatant was extracted by 4 ml of hexane. The sample was strongly vortexed for 1 min, and subsequently centrifuged at 3000  $\times g$  for 5 min. The organic solvent layer was transferred to new tube and evaporated to dryness. The residue was reconstituted by 250  $\mu\text{l}$  of mobile phase. The 100  $\mu\text{l}$  of aliquot was injected to HPLC column.

The amiodarone calibration curve was linear over the range of 0.1 to 10  $\mu\text{M}$  (linear regression coefficient  $\geq 0.995$ ). The method showed good accuracy ( $> 85\%$ ) and precision (coefficients of variation  $< 18\%$ ) at 3 different amiodarone concentrations (5, 1, and 0.25  $\mu\text{M}$ ) for both inter-day and intra-day assay.

#### 4.2.4. PK/PD Model and Data Analysis

The PK/PD model describing cardiac uptake and inotropic response of amiodarone is shown in Fig. 4.1. Perfusate flow (flow rate  $Q$ ) and drug input (rate  $QC_{in}$ ) as well as drug outflow (rate constant  $Q/V_{vas}$ ) occur in vascular compartment (distribution volume  $V_{vas}$ ). In fitting the outflow data,  $V_{vas}$  was fixed to the value 0.06 ml/g, taken from anatomic data (Dobson and Cieslar, 1997). Transport to extravascular compartment and back is governed by first-order rate constants  $k_{in}$  and  $k_{out}$ , respectively.

The corresponding differential equations that describe changes in the amounts of amiodarone ( $x_i$ ) in each compartment  $i$  are given by Eqs. (4.1) and (4.2):

$$\frac{dx_{vas}(t)}{dt} = -\left(\frac{Q}{V_{vas}} + k_{in}\right)x_{vas}(t) + k_{out}x_T(t) + QC_{in} \quad (4.1)$$

$$\frac{dx_T(t)}{dt} = k_{in}x_{vas}(t) - k_{out}x_T(t) \quad (4.2)$$

The concentration of amiodarone in the biophase or effect site  $C_e(t)$  is assumed to be delayed with respect to the concentration in vascular compartment,  $C_{vas}(t) = x_{vas}(t)/V_{vas}$ , with time constant  $\tau$ .

$$\frac{dC_e(t)}{dt} = \frac{1}{\tau}[C_{vas}(t) - C_e(t)] \quad (4.3)$$

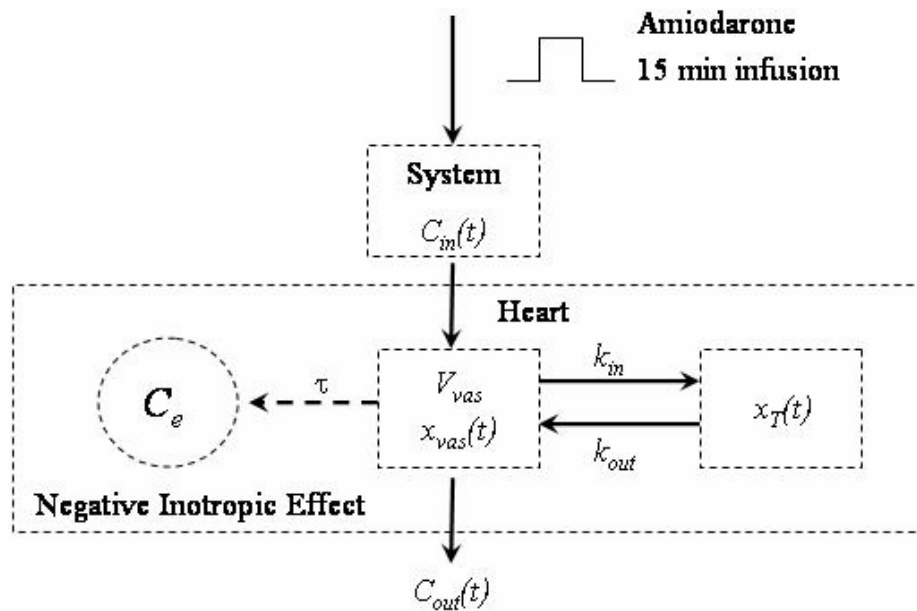


**Figure 4.1** Kinetic model of cardiac amiodarone uptake and inotropic response in the perfused rat heart. The input concentration to the heart ( $C_{in}$ ) is the outflow of the Langendorff apparatus (without heart) for a 15 min perfusion with  $10 \mu\text{M}$  amiodarone in perfusate. The negative inotropic effect (decrease in *LVD*P) is delayed (time constant  $\tau$ ) with respect to  $C_{out}(t) = x_{vas}(t)/V_{vas}$ . ( $V_{vas}$ ,  $x_{vas}$ ,  $x_T$ ,  $k_{in}$  and  $k_{out}$  denote the intravascular volume, drug amounts in vascular compartment, drug amounts in tissue compartment (or cardiac cell) and first order distribution rate constants, respectively.)

For the relationship between  $C_e(t)$  and the inotropic effect  $E(t)$  the  $E_{\max}$  - model was assumed:

$$E(t) = \frac{E_{\max} C_e(t)}{EC_{50} + C_e(t)} \quad (4.4)$$

where  $E_{\max}$ , and  $EC_{50}$  are the maximal response, and the concentration required to produce 50% maximal response, respectively. As a measure of inotropic response  $E(t)$ , we used the fractional change of left ventricular developed pressure  $LVDP(t)$ , i.e., the increase in  $LVDP$  with respect to the baseline (predrug) value  $LVDP_0$ ,

$$E(t) = \frac{LVDP_0 - LVDP(t)}{LVDP_0} \quad (4.5)$$

Differential equations [Eqs. (4.1)-(4.3)] were solved numerically and outflow concentration  $C_{out}(t) = C_{vas}(t) = x_{vas}(t)/V_{vas}$  and time course of the negative inotropic effect [Eq. (4.5)] were fitted to the data using ADAPT II, release 4 (D'Argenio and Schumitzky, 1997). First, the outflow concentration data were fitted in order to estimate the PK parameters. Thereby, the time course of the actual input concentration  $C_{in}(t)$  to the heart [Eq. (4.1)] produced by our amiodarone perfusate concentration of 10  $\mu\text{M}$  infused over 15 minutes, which had been measured in separate experiments, was approximated by linear interpolation between concentration values. Second, the PK parameters were held fixed in fitting Eq. (4.4) to the  $E(t)$  data [Eq. (4.5)].

The maximum likelihood estimator using Eq. (3.2) as variance model was used in both cases. The approximate coefficients of variation of individual parameter estimates ( $CV$ ) represent the uncertainty in parameter estimates (imprecision). As criteria for evaluating the numerical identifiability of estimates, we used  $CV < 50\%$  and a correlation coefficient threshold of 0.8.

The following secondary parameters were derived to characterize distribution of amiodarone in the rat heart. The distribution clearance or permeation clearance  $CL_P = V_{vas}k_{in}$  that characterizes cardiac uptake kinetics. The partition coefficient and the volume of distribution at steady state are given by  $K_p = k_{in}/k_{out}$  and  $V_{ss} = V_{vas}(1 + K_p)$ ,

respectively. The mean transit time ( $MTT$ ) determined by  $V_{ss}$  and  $Q$  according to  $MTT = V_{ss}/Q$ . Due to the apparent one-compartment behavior ( $V_{vas} \ll V_{ss}$ ), the half-life for the washout phase is given by 0.693  $MTT$ .

The recovery of amiodarone was calculated from the inflow and outflow concentration versus time data using a numerical integration method as the amount recovered at the end of experiment ( $t_{last} = 45.5$  min):

$$\text{Recovery} = \frac{\int_0^{45.5} C_{out}(t) dt}{\int_0^{45.5} C_{in}(t) dt} \quad (4.6)$$

Note that  $C_{in}(t) = 10 \mu\text{M}$  in experiments without heart to evaluate the effect of adsorption in the system using  $C_{out,system}(t)$  and  $C_{in}(t) = C_{out,system}(t)$  to estimate the single-pass extraction across the heart.

### 4.3. Results

Figure 4.2 shows the average outflow concentration-time profiles obtained for the 15 min infusion of 10  $\mu\text{M}$  amiodarone in the presence and absence of hearts in the Langendorff apparatus. The data of the control experiment (outflow without heart) served as input concentration  $C_{in}(t)$  in fitting the PK model (Eq. (4.1)) to the concentration-time data determined in the outflow from the heart  $C_{out}(t)$ . Plateau concentrations were  $\sim 5.5$  and  $\sim 2$   $\mu\text{M}$  for the experiments without and with hearts, respectively. From the amiodarone amount infused in the control experiment, 64 % recovered from the system and acted as input to the heart, i.e., the single pass extraction by the system alone (tubings, etc.) was 36 %. The single-pass extraction of amiodarone by the heart was  $63.2 \pm 0.6$  %, i.e., only 36.8 % of input amount to heart recovered within 45.5 min after start of the 15 min infusion.

Typical fits of the model to the  $C_{out}(t)$  and  $E(t)$  data are depicted in Fig. 4.3. It is apparent that the compartment model fitted the data reasonably well. The mean values and standard deviations of estimated model parameters are listed in Table 4.1 together with the approximate coefficients of variations ( $CV$ ) obtained in individual fits. Note that the relative low  $CV$  values ( $< 50\%$ ) suggest that the parameters were estimated with reasonable precision.

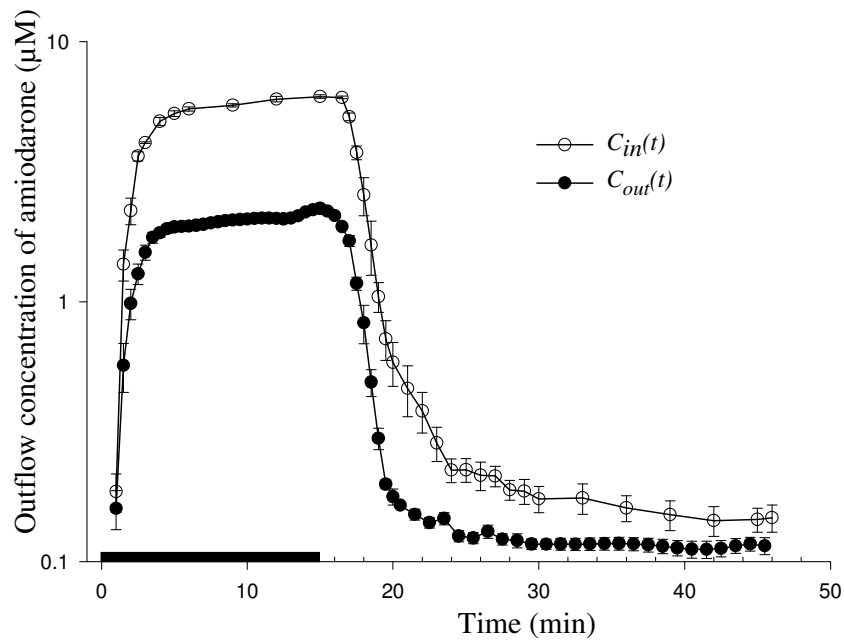


**Figure 4.2** Average outflow concentration-time profiles (mean  $\pm$  SEM,  $n = 6$ ) of the Langendorff apparatus as measured without heart [ $C_{in}(t)$ ] and the outflow concentration of the heart [ $C_{out}(t)$ ] for a 15 min perfusion with 10  $\mu$ M amiodarone in perfusate. Note that  $C_{in}(t)$  is used as input concentration in fitting the model to the  $C_{out}(t)$  data.

**Table 4.1** Parameter estimates from sequential fitting of amiodarone outflow and negative inotropic response data after 15 min infusion of amiodarone in rat hearts (n = 6).

Parameter	Mean (SD)	
	Estimate	CV <sup>a</sup> (%)
<b>Pharmacokinetics</b>		
$k_{in}$ (min <sup>-1</sup> )	519.0 ± 40.9	2.4 ± 1.2
$k_{out}$ (min <sup>-1</sup> )	0.0030 ± 0.0008	17.5 ± 4.8
<b>Pharmacodynamics</b>		
$\tau$ (min)	11.1 ± 8	4.9 ± 1.7
$E_{max}$ (%)	37.0 ± 5.8	3.3 ± 1.7
$EC_{50}$ (μM)	0.53 ± 0.34	9.3 ± 3.4

<sup>a</sup> Approximate coefficients of variations of individual fits (imprecision)

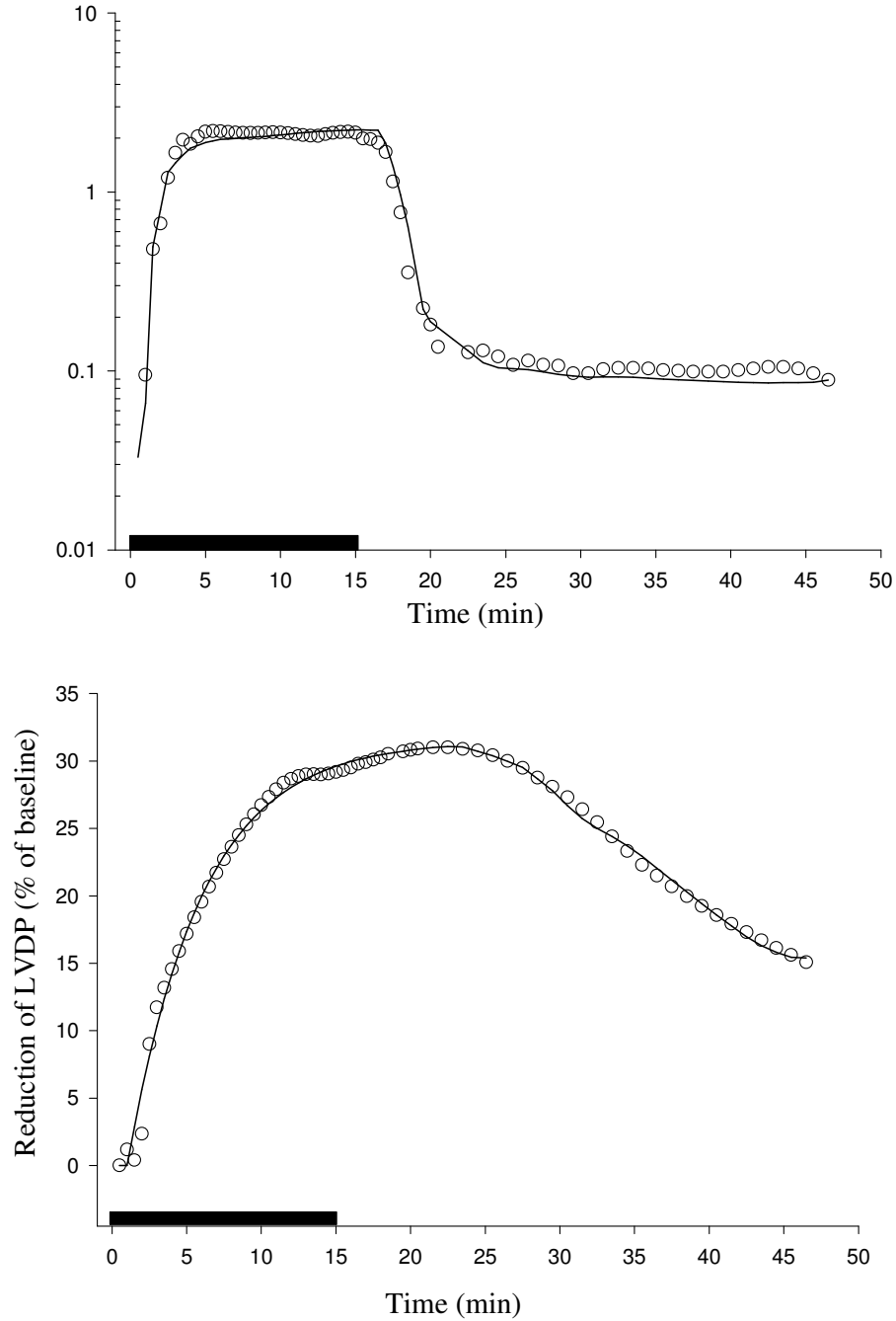


**Figure 4.3** Representative fit of the PK/PD model to experimental data obtained in one heart: amiodarone outflow concentration (upper panel) and negative inotropic effect (lower panel).

The rate constant  $k_{in}$  of  $519.1 \pm 40.0 \text{ min}^{-1}$  accounts for the extremely rapid cardiac uptake of amiodarone. Together with the low value of  $k_{out} = 0.003 \pm 0.0008 \text{ min}^{-1}$ , it leads to quasi-irreversible accumulation in the myocardium, characterized by a partition coefficient of  $K_p = 180,508 \pm 38,374$ . The average time courses of the cardiac amount of amiodarone,  $x_T(t)$ , predicted by the model are shown in Fig. 4.4. The volume of distribution  $V_{ss}$  was  $10,830 \pm 2,302 \text{ ml}$  leading to a washout half-life ( $0.69 \text{ MTT}$ ) of  $13 \pm 3 \text{ h}$  which was not much different from the value of  $16.5 \text{ h}$  estimated from the washout curve (Fig. 4.4) simulated on the basis of the mean parameter estimates. The estimate of uptake clearance  $CL_p = 31.1 \pm 2.5 \text{ ml/min}$  exceeded flow rate, indicating perfusion limited distribution. Thus, our estimate is only a lower bound of the real  $CL_p$ .

Amiodarone decreased myocardial contractility with a maximum effect of  $29 \pm 4 \%$  at the end of the 15-min infusion period, i.e., the LVDP was decreased to  $\sim 70 \%$  of baseline level and mostly did not recover within 30 min (Fig. 4.5). The response was described adequately by the  $E_{max}$  model with an  $E_{max}$  of  $37.0 \pm 5.8\%$ , an  $EC_{50}$  of  $0.53 \pm 0.34 \mu\text{M}$  (Fig. 4.6) and an equilibration time constant  $\tau$  of  $11.1 \pm 8 \text{ min}$  between vascular amiodarone concentration and effect. Heart rate and perfusion pressure were decreased by  $12.54 \pm 3.65 \%$  and  $9.35 \pm 4.85 \%$ , respectively, at the end of infusion.

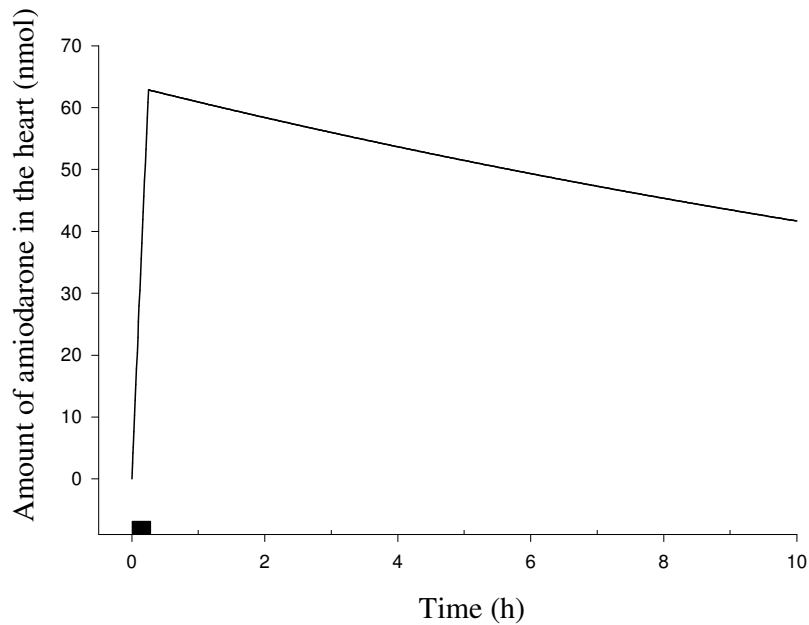


**Figure 4.4** Model simulation of the time course of total amount of amiodarone in the heart (based on the mean values of PK parameter estimates).

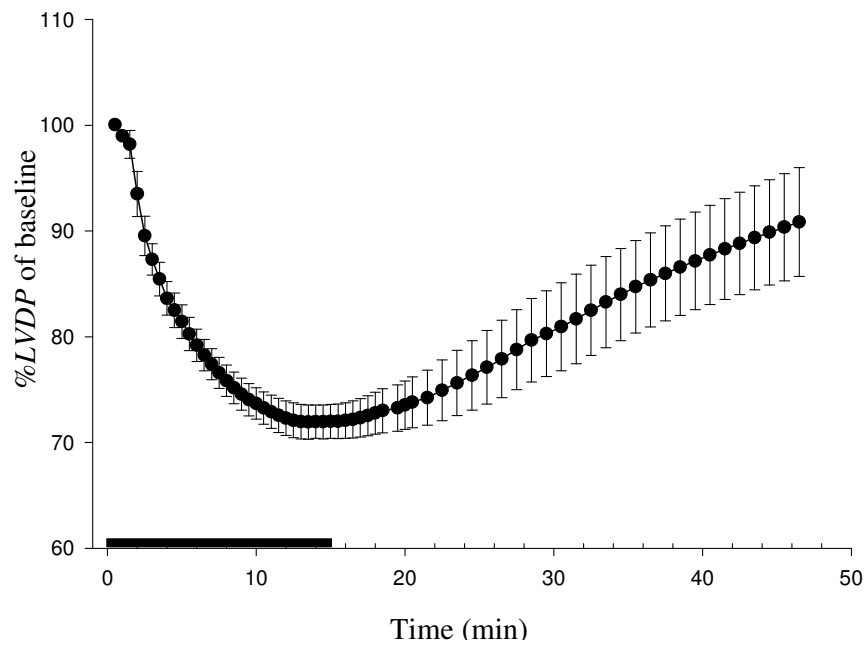


**Figure 4.5** Average time course (mean  $\pm$  SEM) of negative inotropic response to the input concentration-time profile shown in Fig. 4.2 (15 min perfusion with 10  $\mu$ M amiodarone).

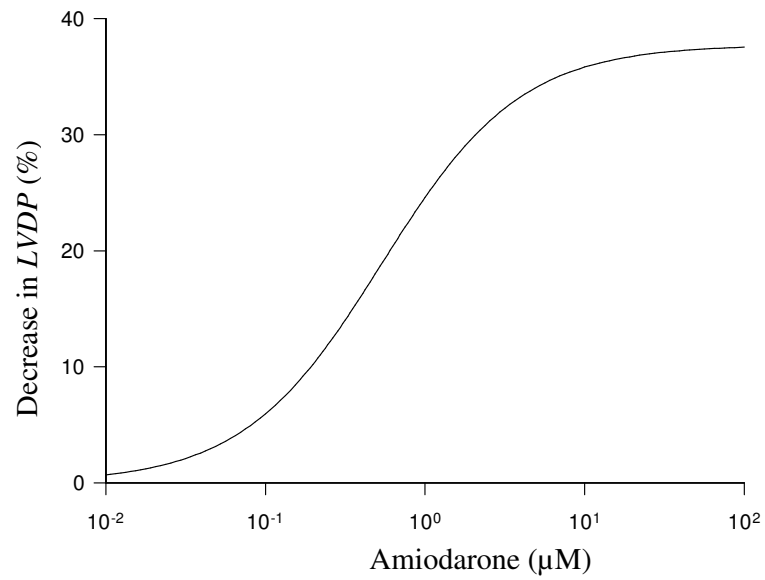


**Figure 4.6** Concentration-response curve of the negative inotropic effect of amiodarone in rat heart predicted by the model from the mean values of  $E_{max}$  and  $EC_{50}$  (Table 4.1).

#### 4.4. Discussion

This study shows that amiodarone was rapidly taken up by the isolated perfused heart. The distribution clearance of 31 ml/min exceeded perfusate flow rate suggesting that uptake is flow-limited. This is in accordance with results obtained in experiments with pigs that showed a rapid uptake of amiodarone by the myocardium within 5 minutes after a single intravenous dose (Beder et al., 1998). In order to compare the extremely high partition coefficient of 180,508 with that obtained from serum and myocardial concentration values measured under in vivo conditions in animals and humans, the protein binding of amiodarone has to be taken into account. If the partition coefficient  $K_p$  is determined in whole body experiments as ratio of tissue concentration ( $C_T$ ) to the corresponding plasma concentration at steady state ( $C_P$ ), we have  $K_p = (C_T / C_P) = f_u K_{pu}$ , where  $f_u$  is free fraction in plasma and  $K_{pu}$  the partition coefficient related to unbound drug concentration (Rodgers et al., 2005). Thus, for an unbound fraction of 0.085 % measured in rats (Shayeganpour et al., 2005) the partition coefficient or volume of distribution of amiodarone estimated for the perfused heart has to be multiplied by a factor ( $f_u$  value) of 0.00085. (Note that the 0.1 % albumin in perfusate has no significant effect.) The resulting myocardial partition coefficient of 153 is well in accordance with the ratio of myocardial to serum concentration of 128 measured in rats 16 h after intravenous injection (Riva et al., 1982). Also the washout half-life of 17 h calculated from our model parameters in the perfused rat heart is in the same order of magnitude as the myocardial half-life of 26.8 h (Najjar, 2001) measured in rats.

The  $EC_{50}$  of 0.53  $\mu\text{M}$  for the negative inotropic effect of amiodarone in the isolated rat heart estimated here using PK/PD modeling is somewhat lower than that of 1.7  $\mu\text{M}$  in electrically stimulated rabbit right ventricular strips (Lubic et al., 1994). In isolated guinea pig hearts, an amiodarone concentration of 1  $\mu\text{M}$  induced a ~ 30 % decrease in contractility (Bicer et al., 2002). An intravenous administration of 3.0 mg/kg (~ 1.5  $\mu\text{M}$  after 10 min) exerted ~ 25 % decrease in inotropy in anesthetized dogs (Sugiyama et al., 2001). Several lines of evidence support the suggestion that the negative inotropic effect of amiodarone is mediated by its calcium channel blocking action, including the observations that L-type calcium channels are blocked with an dissociation constant of 0.36  $\mu\text{M}$  in the activated state (Nishimura et al., 1989)

and that the specific binding of [<sup>3</sup>H]nitrendipine is inhibited with a  $K_i$  of  $\sim 0.3 \mu\text{M}$  (Lubic et al., 1994). While our estimate of  $EC_{50}$  for the negative inotropic effect of amiodarone is in the same order of magnitude as those in other in vitro experiments, correction for the free fractions in plasma would result in plasma concentrations that are much higher ( $> 100 \mu\text{M}$ ) than those observed in vivo, e.g., the above mentioned value of  $\sim 1.5 \mu\text{M}$  in dogs. This could suggest that for the extremely hydrophobic drug amiodarone concentration at or near the site of action (e.g., membrane), due to a possible lack of equilibrium between biophase and receptor, may not be linearly related to free concentration in plasma in the transient state (Rhodes et al., 1992). Interestingly, in all previous papers where in vitro results were compared with therapeutic plasma concentrations of amiodarone ( $0.1 - 10 \mu\text{M}$ ), the effect of the extremely low free fraction  $f_u$  was not discussed (Lubic et al., 1994; Gray et al., 1998; Watanabe and Kimura, 2000; Bicer et al., 2002). Thus, it remains an open question as to whether for amiodarone free plasma concentration at steady state may be representative for concentration at the site of action and the in vivo drug effect. In addition, it is not clear which process determines the temporal delay of 11 min between vascular concentration and effect. Although the rationale of the present model is a delay due to the transport to the site of action, the involvement of postreceptor events cannot be excluded. However, the predictions of an alternative model assuming only time-dependent signal transduction (Mager and Jusko, 2001) was not in accordance with the data.

Finally, it should be recalled that apart from the modeling results discussed above, the amiodarone extraction by the heart of  $63.2 \pm 0.6 \%$  and the maximum decrease in myocardial contractility of  $29 \pm 4 \%$  were estimated by model-independent methods.

In conclusion, the PK/PD analysis of cardiac uptake and negative inotropic response of amiodarone in the isolated perfused rat heart may improve our understanding of the factors that control the onset of pharmacologic response after intravenous amiodarone in clinical practice.

## 5. Verapamil

### 5.1. Background

Verapamil causes vasodilation and depresses myocardial contractility and electrical activity in the atrioventricular and sinoatrial nodes through inhibition of the L-type calcium channels (Catterall and Striessnig, 1992; Bodi et al., 2005). Calcium antagonists are used in the treatment of stroke, hypertension, cardiac arrhythmias and angina pectoris (Eisenberg et al., 2004). Although the use of verapamil may be limited by its direct negative inotropic effect, less is known on its cardiac uptake kinetics in relation to the time course of the negative inotropic action and factors which affect these processes (Powell, 1990; Huang et al., 1998).

Verapamil is also a standard substrate of P-glycoprotein (Pgp); however, in contrast to the brain (e.g., (Sasongko et al., 2005)), the functional role of this transporter for drug uptake into the myocardium is not well established (for review see (Couture et al., 2006)). In the heart, Pgp is expressed in endothelial cells of capillaries (Meissner et al., 2002) but not in cardiomyocytes (Lazarowski et al., 2005). However, the level is far below those detected in the liver, kidneys, and brain (Wang et al., 2005). An increased cardiac accumulation of doxorubicin has been reported in *mdr1a* Pgp deficient mice (van Asperen et al., 1999). Previously, Weiss and Kang (2002) interpreted the substantial increase in myocardial uptake of the Pgp substrate idarubicin in the presence of verapamil or amiodarone in terms of an impairment of Pgp-mediated influx hindrance; however, this hypothesis remains open to debate in view of alternative explanations in terms of physico-chemical properties of these drugs (Speelmans et al., 1995), including the membrane transport of idarubicin by a flip-flop mechanism (Regev et al., 2005). Since cardiac Pgp pumps may alter intracardiac concentrations and hence the efficacy and toxicity of cardioactive drugs, an understanding of their role in myocardial drug uptake merits further investigations (Couture et al., 2006). Therefore, the objectives of this experiment were:

- 1) to analyze uptake and inotropic response of verapamil in the perfused rat heart using a PK/PD modeling approach that accounts acute tolerance to the negative inotropic verapamil effect, and

2) to evaluate the effect of the Pgp inhibitor amiodarone (Stein, 1997) on the cardiac uptake kinetics and negative inotropic response of verapamil.

Additionally, another aim of the present study was also to assess the influence of endotoxemia on negative inotropic and vasodilator action of verapamil in isolated perfused rat hearts using the information provided by the outflow concentration-time profile and the time courses of pharmacological effects.

Experimental and human septic shock can alter both the kinetics and dynamics of drugs (De Paepe et al., 2002). Intravenous endotoxin (lipopolysaccharide, LPS) administration causes systemic inflammatory response syndrome or multiple organ failure and is used as an experimental model of sepsis (Muller-Werdan et al., 1996). Here we investigated the effect of LPS-induced endotoxemia on cardiac uptake and actions of verapamil. This is interesting for the following reasons: First, endotoxemia diminishes the expression of L-type calcium-channels (Lew et al., 1996). A reduced calcium influx (Zhong et al., 1997; Abi-Gerges et al., 1999) and/or abnormalities in intramyocyte calcium accumulation (Thompson et al., 2000) might contribute to depression of myocardial contractility. The significantly attenuated dromotropic effect of verapamil observed in arthritic patients (Mayo et al., 2000) and rats (Sattari et al., 2003) was attributed to a downregulation of calcium channels by inflammatory cytokines. Second, since coronary vasoconstriction may play a role in the development of cardiac depression in LPS-treated rats (Tu et al., 2004), the vasodilator action of verapamil may be beneficial (Buwalda and Ince, 2002). It should be noted, however, that protective effects of calcium channel antagonists in endotoxin shock have been reported (Bosson et al., 1985; Lee and Lum, 1986; Hotchkiss et al., 1995; Mustafa and Olson, 1999; Wu et al., 1999) Simagul et al., 2006, Li et al., 2006).

## 5.2. Materials and Methods

### 5.2.1. Drugs and Chemicals

Verapamil hydrochloride, [N-methyl <sup>3</sup>H]verapamil hydrochloride (80 Ci/mmol), amiodarone hydrochloride and dimethyl sulfoxide were purchased from MP Biomedicals (Eschwege, Germany), American radiolabeled chemicals (St. Louis, USA), Sigma-Aldrich Chemie (Steinheim, Germany) and Carl Roth (Karlsruhe, Germany), respectively. Lipopolysaccharide (from *Escherichia coli*: serotype 055:B5) were purchased from Sigma-Aldrich Chemie (Steinheim, Germany). Lumasafe Plus was obtained from Lumac\*LSC B.V. (Groningen, The Netherlands). All other chemicals and solvents were of highest grade available.

### 5.2.2. Experimental Protocol

#### 1) Working Solution Preparation

The verapamil solution (1.5  $\mu$ M) was firstly prepared by adding 15  $\mu$ l concentrated stock solution in water (2.5 mM) to a final volume of 25 ml perfusate buffer. Then, 3 ml of 1.5  $\mu$ M verapamil was mixed with 2  $\mu$ l labeled verapamil (1 mCi/ml). The 1.5  $\mu$ M labeled verapamil was, finally, infused into the aortic cannula directly above the heart.

The perfusate containing 1  $\mu$ M amiodarone was prepared by diluting a concentrated 2 mM amiodarone in DMSO solution. The final concentration of DMSO was  $\leq 0.05\%$ . This concentration had no significant inotropic effect.

#### 2) Study design

In order to fulfill our objectives, the following 5 study designs were performed. The isolated perfused rat hearts were prepared following the method in section 2.3. Meanwhile, *LVDP*, *HR* and *CVR* were continuously monitored.

### ***Single Dose Experiment***

Eight hearts were obtained from the Wistar rats. After a 20-min equilibration period, the labeled 1.5 nmol verapamil was infused for 1 min and outflow samples were collected every 5 s for 3 min, every 10 s for next 7 min, every 30 s for next 10 min, and every 1 min for the next 5 min.

### ***Double Dose Experiment***

The double dosing experiment (8 hearts) was conducted by infusing the two doses of labeled 0.75 nmol verapamil for 1 min at time 0 and 10. The time 0 was defined as 20 minutes after the start of experiment. After the first dose, outflow samples were collected every 5 s for 3 min, and every 10 s for next 7 min. At tenth-minutes, the second dose was performed and the samples were collected every 5 s for 3 min, and every 10 s for next 7 min, every 30 s for next 10 min, and every 1 min for the next 5 min.

### ***Single Dose Experiment in Presence of Amiodarone***

In another series of single dose experiments (4 hearts), the same procedure was conducted in presence of amiodarone (1  $\mu$ M) in perfusate.

### ***Single dose experiment: Endotoxemia Condition***

In endotoxemia experiments, lipopolysaccharide (LPS) was injected intraperitoneally at a dose of 4 mg/kg. If after 3.5 h the rectal temperature was still below 38°C, an additional dose of 2 mg/kg was injected. Control animals (sham group) received an equivalent volume of sterile saline (0.9% NaCl). Hearts were removed from endotoxemic and control animals 5.5 h after injection of the first dose for isolated perfused heart experiments as described below. Before excision, rectal temperature was measured using a digital thermometer.

Six sterile saline-treated rats and eight LPS-treated rats were used for control and endotoxemia experiments, respectively. They were undergoing the same procedure as the single dose experiment.

### ***Steady State Experiment***

In order to construct dose-response curve, cumulative infusions of verapamil with input concentrations of 7.4, 14.9, 22.3, 29.7, 49.6, 74.3, 99.0, and 247.9 nM (each infusion for 15 min) were performed in four hearts.

### **5.2.3. Quantification of Verapamil**

The sample analysis was conducted within 3 days after collecting samples. The samples (250  $\mu$ M) were mixed with 2 ml Lumasafe Plus used as cocktail solution, and were analyzed using a liquid scintillation counter (Perkin Elmer Instruments, Shelton, CT). To determine the drug concentrations, calibration curves in the range of 0.5-100 nM verapamil were established.

### **5.2.4. PK/PD Model and Data Analysis**

The model of cardiac PK of verapamil (Fig. 5.1) describes drug uptake from the vascular space ( $V_{vas}$ ) into the tissue compartment with an uptake rate  $k_{in}$ , where  $k_{in}=CL_p/V_{vas}$  and  $CL_p$  is the permeation clearance or permeability-surface product. In fitting the outflow data, this parameter was fixed to the value  $V_{vas} = 0.06$  ml/g, taken from anatomic data (Dobson and Cieslar, 1997). Note that perfusate flow (flow rate  $Q$ ) and drug input (rate  $QC_{in}$ ) as well as drug outflow (rate constant  $Q/V_{vas}$ ) occur in this vascular compartment. An additional compartment with volume  $V_0$  (in series with the vascular compartment) was introduced (not shown in Fig. 5.1) to account for the mixing in nonexchanging elements of the system. Tissue distribution is characterized by the distribution volume accounting for reversible quasi-instantaneous myocardial binding  $V_c=(k_{in}/k_{out})V_{vas}$ . The rate constant  $k_{ir}$  describes irreversible tissue binding (during the time course of experiment) and/or metabolism of verapamil. Neglecting this effect of quasi-irreversible binding, the total (or steady-state) distribution volume of the heart is then given by

$$V_{ss} = V_{vas} (1 + k_{in}/k_{out}) \quad (5.1)$$

and the equilibrium cardiac tissue/perfusate partition coefficient of verapamil is obtained as  $K_{pu} = V_{ss,vera}/V_{ss,water}$ , where  $V_{ss,water}$  denotes the water distribution volume of the rat heart.

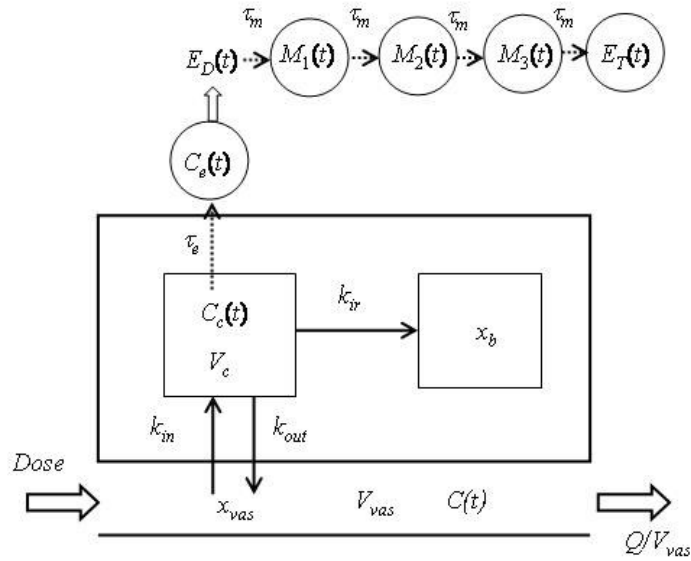


**Figure 5.1** Model of verapamil pharmacokinetics and pharmacodynamics in the perfused rat heart. The rate constants,  $k_{in}$  and  $k_{out}$ , describe uptake from the vascular space ( $V_{vas}$ ) into the heart (permeation clearance,  $CL_p = k_{in}V_{vas}$ ) where tissue concentration  $C_c(t)$  is governed by the distribution volume  $V_c$ . The direct negative inotropic effect  $E_D(t)$  (decrease in  $LVDP$ ) is related to the delayed (time constant  $\tau_e$ ) effect site concentration  $C_e(t)$  by a sigmoidal  $E_{max}$  model, and causes a compensatory positive inotropic tolerance effect  $gE_T(t)$  ( $0 < g < 1$ ) that is delayed with respect to  $E_D(t)$  by a mean delay time  $4\tau_m$  Eq.(5.10). The net effect is given by  $E(t) = E_0 - E_D(t) + gE_T(t)$  Eq(5.6).

The changes in drug amounts ( $x_i$ ) in compartments  $i$  after input (dosing) rate  $I$  are described by the following differential equations

$$\frac{dx_0(t)}{dt} = -\frac{Q}{V_0}x_0(t) + I \quad (5.2)$$

$$\frac{dx_{vas}(t)}{dt} = \frac{Q}{V_0}x_0(t) + k_{out}x_c(t) - k_{in}x_{vas}(t) - \frac{Q}{V_{vas}}x_{vas}(t) \quad (5.3)$$

$$\frac{dx_c(t)}{dt} = k_{in}x_{vas}(t) - k_{out}x_c(t) - k_{ir}x_c(t) \quad (5.4)$$

$$\frac{dx_b(t)}{dt} = k_{ir}x_c(t) \quad (5.5)$$

Note that the measured outflow concentration  $C_{out}(t) = x_{vas}(t)/V_{vas}$  is the concentration in the vascular compartment. Since the inotropic effect rebounded to levels above the original baseline after the verapamil infusion was stopped (Fig. 5.2, lower panel), the cardiac PK/PD model previously used for amiodarone in Chapter III was extended to account for the tolerance development. Analogous to the tolerance model (Mandema and Wada, 1995), the observed effect was regarded as the sum of the baseline effect  $E_0$  (average pre-dose value), the “direct” negative inotropic effect  $E_D(t)$ , and a compensatory positive inotropic effect  $E_T(t)$  (Fig. 5.1)

$$E(t) = E_0 - E_D(t) + gE_T(t) \quad (5.6)$$

where the constant  $g$  determines the extent of tolerance development. Like in the normal link model without tolerance,  $E_D(t)$  is related to the effect site (myocardial) concentration  $C_e(t)$  via a sigmoid  $E_{max}$  model (Hill equation)

$$E_D(t) = \frac{E_{max}C_e^N(t)}{EC_{50}^N + C_e^N(t)} \quad (5.7)$$

where  $EC_{50}$  is the effect concentration that corresponds to 50% of the maximum effect ( $E_{max}$ ) and  $N$  is the Hill coefficient that determines the sigmoidicity of the curve. The effect site concentration  $C_e(t)$  in Eq. (5.7) is delayed (time constant  $\tau_e$ ) relative to the myocardial concentration  $C_c(t)$

$$\frac{dC_e(t)}{dt} = \frac{1}{\tau_e} [C_c(t) - C_e(t)] \quad (5.8)$$

We assumed that the negative inotropic effect of verapamil  $E_D(t)$  triggers a counter-regulation, i.e., the delayed positive inotropic response  $E_T(t)$ . This delay time of the tolerance effect  $E_T(t)$  with respect to  $E_D(t)$  was not simply due to a first-order process as in previously used tolerance models (Mandema and Wada, 1995), but could be well approximated by a gamma distribution with  $n = 4$ , i.e., a series of transit compartments (Sun and Jusko, 1998)

$$\frac{dM_i(t)}{dt} = \frac{1}{\tau_m} [M_{i-1}(t) - M_i(t)] \quad \text{for } i = 1 \dots 4 \quad (5.9)$$

where  $M_0(t) = E_0 - E_D(t)$  and  $M_4(t) = E_T(t)$ . Note that the mean delay time of the tolerance effect  $MTT_{tol}$  (i.e., the mean transit time of the gamma distribution) is given by

$$MTT_{tol} = n\tau_m = 4 \tau_m \quad (5.10)$$

and  $1/MTT_{tol}$  characterizes the rate of tolerance development. At steady-state, we obtain from Eqs. (5.6) and (5.9)

$$\Delta E_{ss} / E_{ss, non-tolerance} = g \quad (5.11)$$

Thus, tolerance development attenuates the negative inotropic effect by the fraction  $g$  and it becomes clear that  $0 < g < 1$ . As a measure of inotropic response  $E(t)$ , we used the time course of left ventricular developed pressure  $LVDP(t)$ , i.e.,  $E_0$  is identical to the baseline (predrug) contractility  $LVDP_0$ .

Equations (5.2) to (5.9) were solved numerically and fitted to the data using ADAPT II Version 4 (D'Argenio and Schumitzky, 1997). First the outflow concentration data were fitted to estimate the PK parameters. These parameter values were then held fixed in fitting Eqs. (5.6), (5.7) and (5.9) to the  $E(t)$  data. Using maximum likelihood estimation, we assumed that the measurement error or variance model has a standard deviation which is a linear function of the measured quantity as previously shown in Eq. (3.2). The 'goodness of fit' was judged by visual examination of the distribution of residuals and Akaike information criterion (AIC value);

additionally, the  $R^2$  value of the fits was reported. The reliability of parameter estimation was assessed by the asymptotic coefficients of variation ( $CV$ ) of individual parameter estimates.

The cumulative infusion data relating inflow concentration of verapamil to inotropic effect measured after 15 min were directly fitted by Eq. (5.7) to estimate the PD parameters.

The recovery of verapamil was calculated from the outflow concentration versus time data using a numerical integration method as the amount recovered at the end of experiment ( $t_{\text{last}} = 25$  min):

$$\text{Recovery} = \frac{\int_0^{25} C_{\text{out}}(t) dt}{\text{Dose}} \quad (5.12)$$

The results are expressed as mean  $\pm$   $SD$  of all parameters estimated. Kruskal-Wallis ANOVA on ranks and Dunn all-pairwise comparison test were used to evaluate differences of group means between the control single-dose ( $n = 8$ ), control double-dose ( $n = 8$ ) and amiodarone ( $n = 4$ ) groups, respectively. A  $p$ -value of less than 0.05 was considered statistically significant.

For endotoxemia experiment, Student's  $t$ -test and Mann-Whitney Rank Sum test (when the normality test was violated) were used to evaluate differences of group means between the sham group ( $n = 6$ ), and LPS ( $n = 8$ ) groups. A  $p$ -value of less than 0.05 was considered statistically significant.

### 5.3. Results and Discussion

#### 5.3.1. Effect of Amiodarone on PK/PD Modeling of Verapamil

##### *Results*

The upper panel of Fig. 5.2 shows the mean outflow concentration-time profiles for the 1-min infusion of 1.5 nmol verapamil in absence (control) and presence of amiodarone (1  $\mu$ M) in the perfusate. The recovery of verapamil in the perfusate (up to 25 min) for control and amiodarone group amounted to  $89.2 \pm 8.3$  % and  $94.1 \pm 12.2$  %, respectively. There were no statistical significant differences between both groups. The corresponding time course of negative inotropic effect is presented in Fig. 5.2 (lower panel). Compared with the respective baseline values, the maximum negative inotropic effect of verapamil was  $42.6 \pm 3.1$ % and  $28.1 \pm 3.0$ % for control and amiodarone group, respectively ( $p < 0.001$ ). There was a tendency towards a baseline reduction in the presence of amiodarone. Compared to the baseline before amiodarone infusion, inotropy was reduced by  $14.3 \pm 5.3$ %. The maximum effect was achieved at  $\sim 2$  min after infusion in both groups, and the negative inotropic effect recovered to baseline after  $\sim 10$  min. This was followed by a positive inotropic rebound effect in the control group that was nearly abolished in the amiodarone group. The coronary vascular resistance (CVR) of  $4.67 \pm 0.83$  mmHg min/ml under control conditions was reduced by 42 % to  $2.73 \pm 0.22$  mmHg min/ml in the presence of amiodarone in perfusate ( $p < 0.001$ ). Verapamil infusion induced a coronary vasodilation with a  $17.9 \pm 6.1$  % decrease in CVR ( $p < 0.01$ ). Under vasodilation with amiodarone, only a  $4.3 \pm 1.6$  % further decrease in CVR was observed ( $p < 0.01$ ).

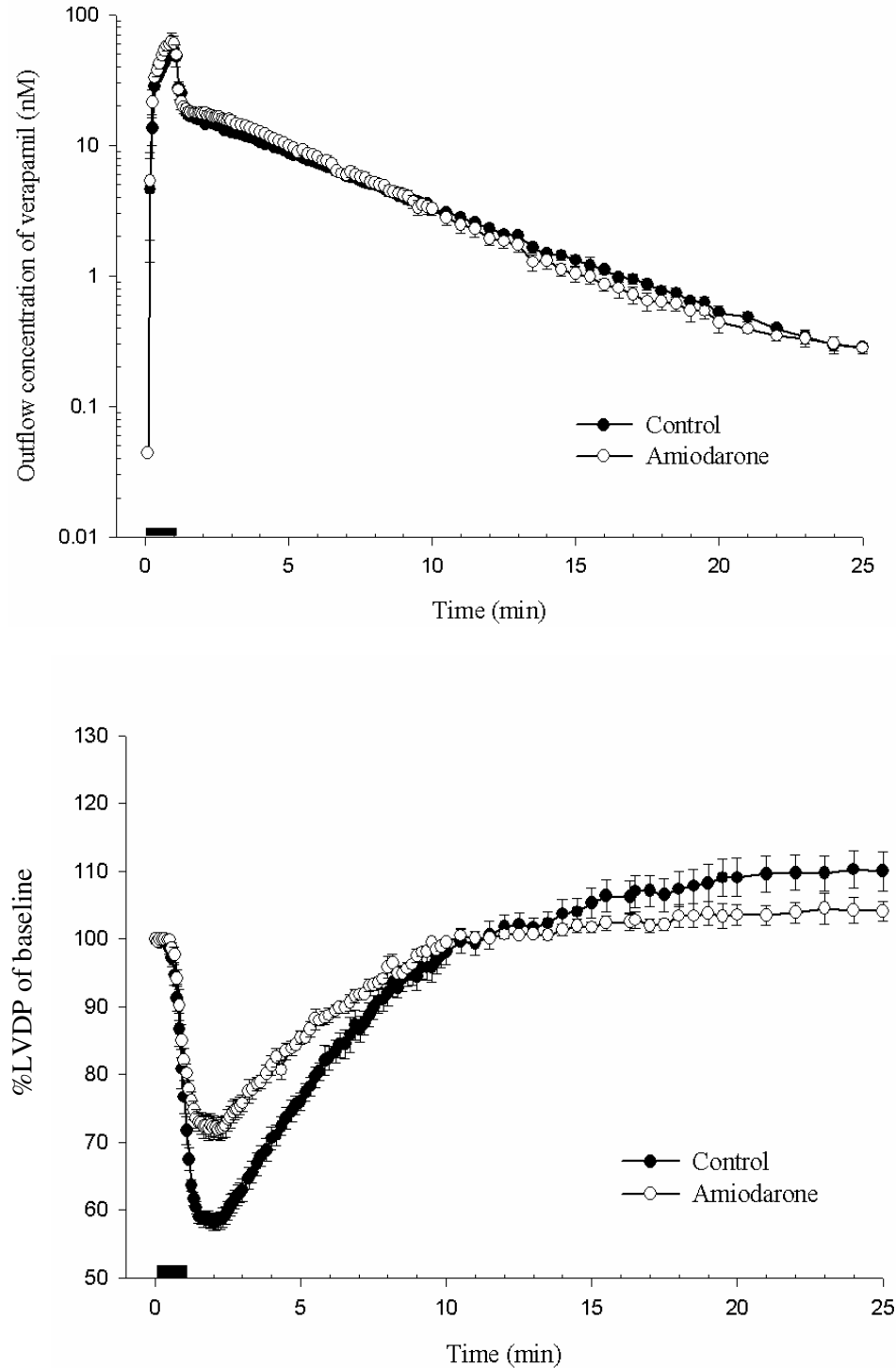


**Figure 5.2** Outflow concentration-time profiles (upper panel) and negative inotropic effect of verapamil (lower panel) in rat hearts for a 1-min infusion 1.5 nmol of verapamil, measured in control experiments (●) and in the presence of 1  $\mu$ M amiodarone in perfusate (○) (mean  $\pm$  SEM). Error bars that fall within the symbols are not shown.

The fit of the PK/PD model to outflow concentration and inotropic response data of verapamil after a single dose are exemplified in Fig. 5.3. Note that ‘representative fits’ means that an experiment (heart) with an AIC value which was closest to group median value was selected.

The model well described the biphasic inotropic response: the negative inotropic effect followed by a rebound increase in contractility. The mean  $R^2$ , a measure of goodness of fit of the model, were 0.953 and 0.991 for PK and PD data, respectively. A comparable good fit and similar parameter estimates were obtained from the data of the double dose experiment where 10 min after the 1-min infusion of 0.75 nmol verapamil a second dose was given (Fig. 5.4). Also the single dose response in the presence of amiodarone in perfusate was well described by the PK/PD tolerance model (Fig. 5.5). The averaged model parameters and estimation errors (as coefficients of variation obtained in individual fits) are listed in Table 5.1. Most parameters were estimated with sufficient precision, i.e., with relatively low asymptotic coefficients of variation. Exceptions are the parameters of the tolerance model ( $\tau_m$  and  $g$ ) in single dose experiments.

The uptake or permeation clearance of verapamil ( $CL_p = 38.1 \pm 11.0$  ml/min) was higher than perfusate flow (9.7 ml/min) indicating flow-limited uptake. The steady-state distribution volume of  $51.2 \pm 11.6$  l corresponds to an equilibrium tissue/perfusate partition coefficient  $K_{pu}$  of  $64.0 \pm 14.5$ .

The “direct” negative inotropic action of verapamil following a single dose was characterized by  $EC_{50} = 16.4 \pm 4.1$  nM,  $E_{max} = 50.5 \pm 18.9$  mmHg and a delay relative to the free myocardial concentration  $C_c(t)$  of  $\tau_e = 0.34 \pm 0.15$  min. Extent and delay of tolerance development were described by parameters  $g = 0.27$  and  $MTT_{tol} = 25$  min. These parameters were estimated with higher precision in double dose experiments ( $g = 0.16$  and  $MTT_{tol} = 12$  min). Although according to average effect-time curves (Fig. 5.2, lower panel) the rebound positive inotropic response appears to be nearly abolished in the presence of amiodarone, the tolerance model provided a better fit than normal PK/PD link model [ $g = 0$  in Eq. (5.6)]. There was a tendency toward a reduced tolerance development (decrease in  $g$  and increase in  $MTT_{tol}$ ) as well as a reduction in  $E_0$  and  $E_{max}$  but the differences between groups were not significant.

The parameter estimates obtained by fitting Eq. (5.7) to the negative inotropic response following stepwise verapamil infusion were  $EC_{50} = 31.6 \pm 14.2$  nM ,  $E_{max} = 73.2 \pm 11.2$  % reduction, and  $N = 1.2 \pm 0.5$ . The asymptotic coefficients of variation (CV) of individual parameter estimates were less than 13 %.

**Table 5.1** Parameter estimates (SD in parenthesis) from fitting of verapamil outflow and negative inotropic response data for a 1-min infusion 1.5 nmol of verapamil in rat hearts under control conditions and in the presence of 1  $\mu$ M amiodarone.

Parameter	Mean (SD)		
	Control Single Dose (n=8)	Control Double Dose (n=8)	Amiodarone Single Dose (n=4)
<b>Pharmacokinetics</b>			
$k_{in}$ ( $\text{min}^{-1}$ )	<b>635.0 (184.0)</b>	<b>679.0 (167.0)</b>	<b>587.0 (197.4)</b>
$CV^a$ (%)	6.4 (1.3)	4.6 (0.7)	7.6 (2.8)
$k_{out}$ ( $\text{min}^{-1}$ )	<b>0.740 (0.078)</b>	<b>0.739 (0.187)</b>	<b>0.865 (0.162)</b>
$CV$ (%)	5.2 (1.0)	3.9 (0.8)	6.3 (2.0)
$k_{ir}$ ( $\text{min}^{-1}$ )	<b>0.035 (0.029)</b>	<b>0.035 (0.027)</b>	<b>0.024 (0.029)</b>
%CV	13.6 (11.5)	4.9(4.1)	8.9 (7.1)
$V_{ss}$ (ml)	<b>51.2 (11.6)</b>	<b>56.4 (12.6)</b>	<b>40.3 (8.8)</b>
$CV$ (%)	2.8 (0.6)	2.3 (0.5)	3.3 (1.2)
<b>Pharmacodynamics</b>			
$E_{max}$ (mmHg)	<b>50.5 (18.9)</b>	<b>42.7 (18.3)</b>	<b>38.8 (23.0)</b>
$CV$ (%)	13.1 (6.6)	28.5 (26.32)	48.4 (11.8)
$EC_{50}$ (pmol/ml)	<b>16.4 (4.1)</b>	<b>12.8 (6.9)</b>	<b>21.1 (7.7)</b>
$CV$ (%)	12.9 (8.3)	29.7 (40.8)	32.6 (42.3)
$N$	<b>2.1 (0.6)</b>	<b>2.3 (1.2)</b>	<b>2.3 (0.7)</b>
$CV$ (%)	8.6 (2.1)	11.9 (7.4)	9.6 (9.1)
$\tau_e$ (min)	<b>0.34 (0.15)</b>	<b>0.36 (0.10)</b>	<b>0.46 (0.05)</b>
$CV$ (%)	8.8 (12.5)	6.3 (4.3)	4.2 (0.03)
$g$	<b>0.27 (0.22)</b>	<b>0.16 (0.11)</b>	<b>0.10 (0.09)</b>
$CV$ (%)	60.4 (67.2)	6.7 (5.0)	369 (434)
$\tau_m$ (min)	<b>6.25 (4.86)</b>	<b>2.98 (1.25)</b>	<b>16.9* (13.2)</b>
$CV$ (%)	81.0 (171.3)	8.0 (7.7)	165 (169)
$E_o$ (mmHg)	<b>71.1 (18.6)</b>	<b>71.6 (15.8)</b>	<b>65.8 (4.9)</b>
$CV$ (%)	0.7 (0.2)	0.7 (0.5)	0.8 (0.1)

The results obtained in double-dose experiments (0.75 nmol verapamil at  $t = 0$  and 10 min) under Control Conditions are also shown.

<sup>a</sup> Approximate coefficients of variations of individual fits (imprecision).

\* $p < 0.05$  vs control (double-dose).

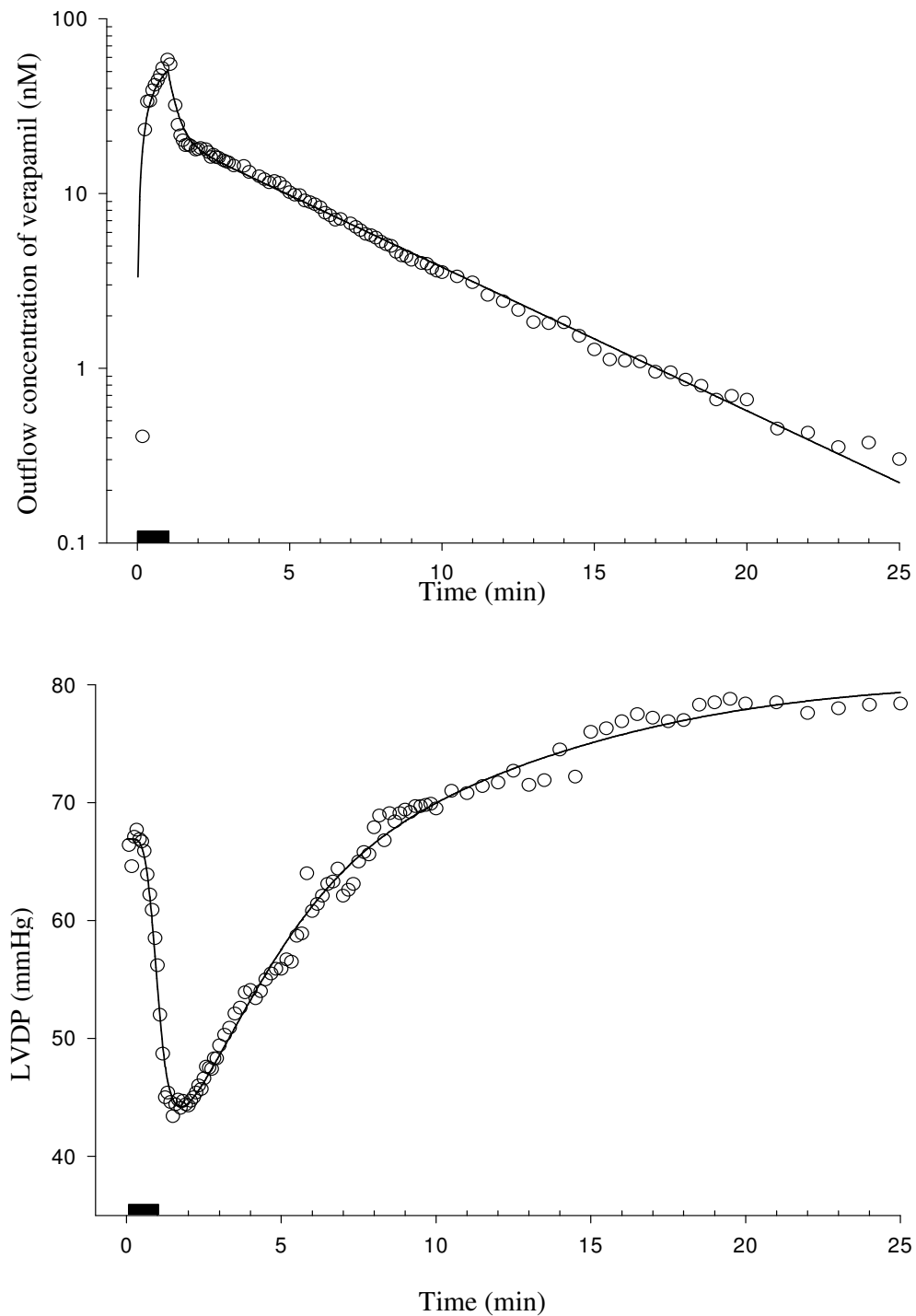


**Figure 5.3** Representative fit of the PK/PD tolerance model to experimental data obtained in one heart for a 1-min infusion 1.5 nmol of verapamil: outflow concentration (upper panel) and negative inotropic effect (lower panel).

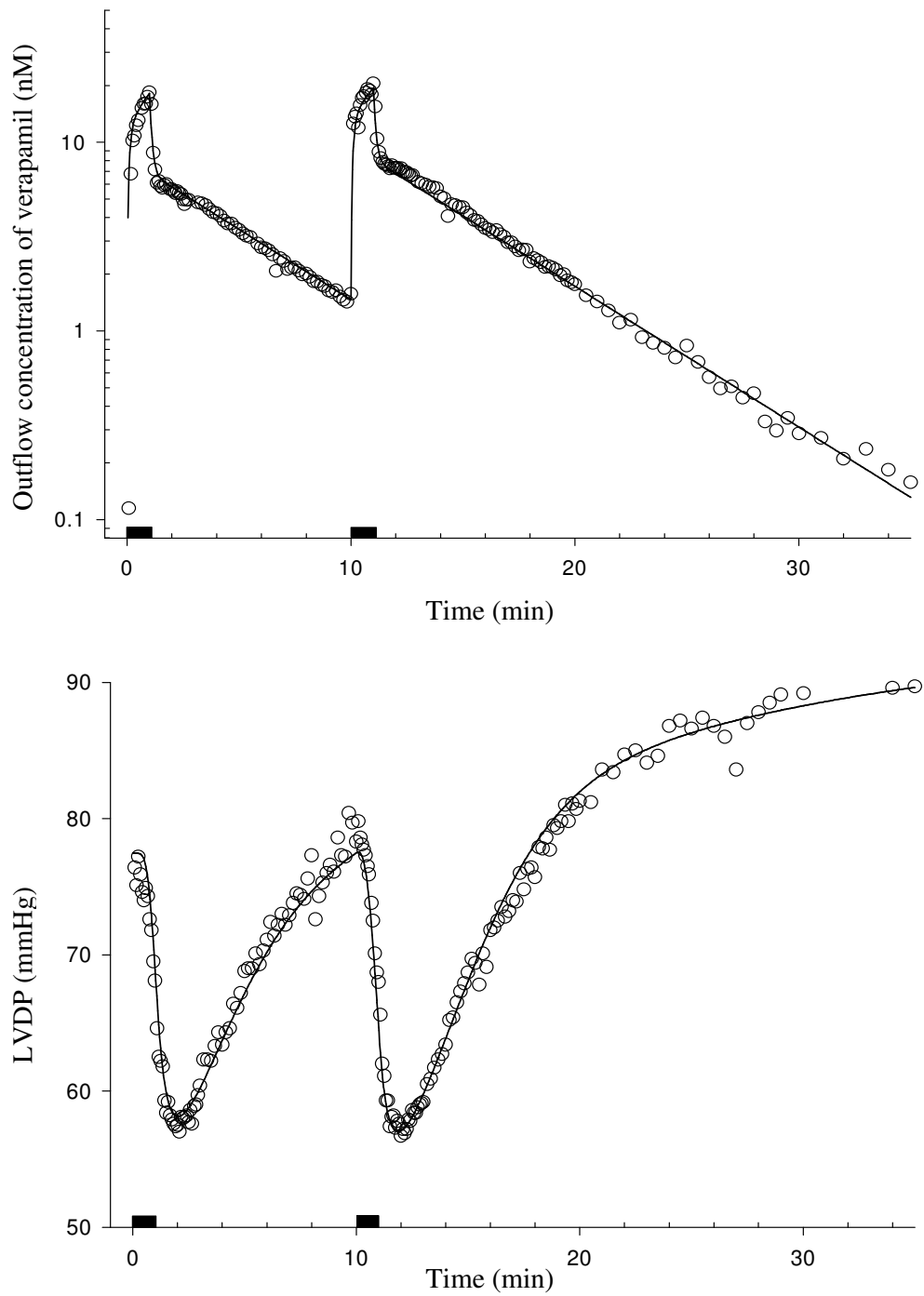


**Figure 5.4** Representative fits of outflow concentration (upper panel) and negative inotropic effect (lower panel) after two 0.75 nmol doses of verapamil in one heart.

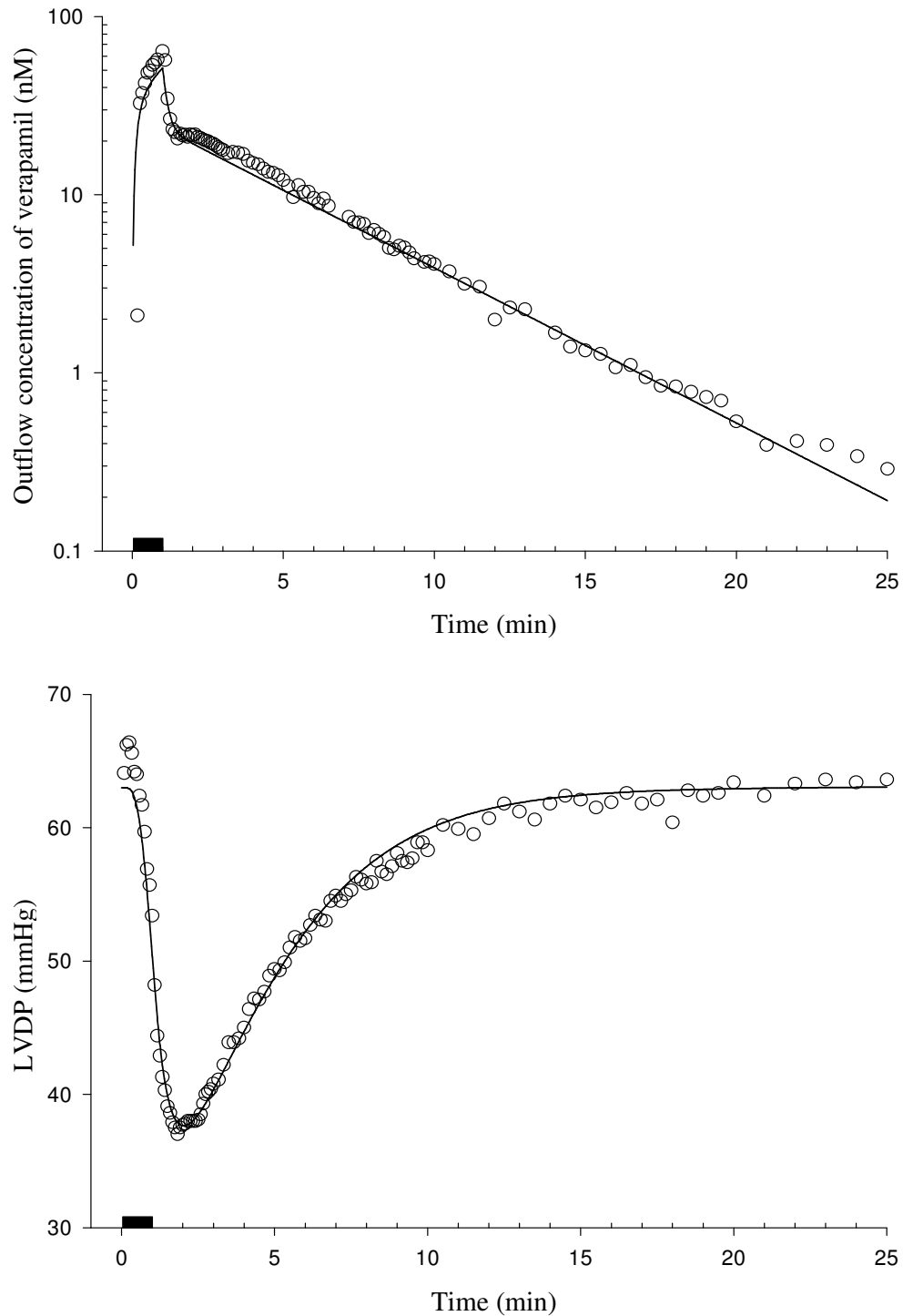


**Figure 5.5** Representative fits of outflow concentration (upper panel) and negative inotropic effect (lower panel) in one heart for a 1-min infusion 1.5 nmol of verapamil in the presence of amiodarone ( $1\mu\text{M}$ ) in perfusate.

### ***Discussion***

Although verapamil, as most drugs, exerts its effects not within the plasma compartment but at receptors in target tissues, this distribution process to the site of action has not got much attention in the past. Here we analyzed the cardiac PK of verapamil and its relationship to negative inotropic response in perfused rat hearts under control conditions and in the presence of amiodarone. The latter was used in a concentration that significantly increased the cardiac uptake of idarubicin (Weiss and Kang, 2002).

### ***Pharmacokinetics***

The lipophilic drug verapamil distributed rapidly into the rat heart with a permeation clearance  $CL_p$  (effective permeability-surface product) that is  $\sim 5$ -fold higher than that of digoxin or the hydrophilic solute sucrose (Weiss et al., 2004). Note, however, that under in vivo conditions the degree of plasma protein binding has to be taken into account. Plasma protein binding of 90% (Keefe et al., 1981) reduces  $CL_p$  to 10% of the estimated 38 ml/min. The equilibrium tissue/perfusate partition coefficient  $K_{pu}$  of 64 is in good agreement with  $K_p$  values of 5.1 (Huang et al., 1998) and 6.2 (Keefe and Kates, 1982) measured in dogs for a free fraction in plasma  $f_u = 0.1$  (since  $K_p = f_u K_{pu}$ ). In order to elucidate the underlying cardiac binding sites, it appears especially interesting that  $K_{pu}$  values of 94.8 and 66.2 were theoretically predicted for rat heart using a mechanistic equation that takes partitioning into neutral lipids and phospholipids as well as binding to acidic phospholipids into account (Rodgers et al., 2005). Although it appears hardly possible to identify uniquely different classes of binding sites on the basis of these data, one may speculate that slow binding ( $k_{ir} = 0.04 \text{ min}^{-1}$ ) is due to electrostatic interaction with tissue acidic phospholipids (Mason et al., 1989). That we found an apparent irreversible myocardial binding may be due to the experimental design, i.e., the limited observation time determined by the sensitivity of the analytical method; a model with reversible binding was not identifiable. In principle, cardiac metabolism of verapamil could be considered as an alternative explanation (Walles et al., 2001; Borlak et al., 2003); however, no data on the resulting extraction of verapamil in the perfused rat

heart are yet available and extrapolating the in vitro data, one would expect a value of less than 1%.

It appears most interesting, however, that the Pgp inhibitor amiodarone neither increased the cardiac uptake rate nor the equilibrium partition coefficient of the Pgp substrate verapamil. In the presence of amiodarone at the same concentration, cardiac uptake of idarubicin, in contrast, nearly doubled (Weiss and Kang, 2002). In the light of the results obtained here for verapamil, it is open for discussion whether this increase in idarubicin uptake can be attributed to Pgp inhibition. Alternative explanations that could account for the increase in myocardial uptake of idarubicin in the presence of Pgp inhibitors have been based on drug-lipid interactions (Speelmans et al., 1995), e.g., an increase in membrane fluidity that leads to increased membrane permeability (Drori et al., 1995). Recently, it was shown that idarubicin is transported across membranes by a fast flip-flop process that is less influenced by Pgp (Regev et al., 2005). Note further that in contrast to verapamil, the cardiac uptake of idarubicin was saturable and could be inhibited by doxorubicin (Weiss and Kang, 2002; Kang and Weiss, 2003). This unexpected lack of an increased cardiac uptake of the Pgp substrate verapamil in the presence of amiodarone puts new questions to the functional consequences of cardiac Pgp expression (Couture et al., 2006).

### *Pharmacodynamics*

The time course of the negative inotropic effect and positive inotropic "rebound" upon cessation of 1-min verapamil infusion is quite well described by our model (Fig. 5.3, lower panel). The validity of the tolerance model is further supported by its usefulness in fitting the response to double dosing, where half of the single dose was administered at  $t = 0$  and 10 min (Fig. 5.4, lower panel) and the fact that the PD parameters estimated in these hearts were similar (not statistically different) from those obtained in the single dose group. As expected, the parameters describing the delay and extent of tolerance development ( $\tau_m$ ,  $g$ ) were estimated with much less precision in single dose experiments, where the observation time was shorter relative to  $MTT_{tol}$ , than in double dose experiments. Thus, we think that a mean delay time of 12 min and a  $g$  value of 0.16, corresponding to a 16% reduction of the negative inotropic effect at steady-state, represent the relevant parameters of tolerance

development. However, the possibility of a dependency of tolerance development on drug input rate should be also taken into account. The high *SD* of  $\tau_m$  and  $g$  estimates (*CV* in the order of 80%) suggests that there is a high interindividual variability in tolerance development. Note that it can be excluded that the observed rebound phenomenon is caused by a baseline shift since in separate experiments no significant change in baseline value of LVDP could be detected over an observation time of 40 min ( $n = 5$ , data not shown) and, if at all, then such a shift would be expected in the opposite direction. In developing the model, we tested all relevant models of acute tolerance reviewed by Gardmark et al. (1999); however, none of these models could predict both the rebound effect and the steady-state behavior of the system. The present approach is the most parsimonious model for tolerance and rebound phenomena that could be found for verapamil. With respect to the compensatory feedback mechanism, our model is similar to the “direct moderator model” (Mandema and Wada, 1995; Gardmark et al., 1999) characterized by an additive reduction of the effect. However, as Gardmark et al. (1999) pointed out, all available tolerance models are empirical since, first, a mechanistic model would be too complex and, second, the underlying mechanisms are unknown. This also applies here but the following possibilities could be considered, for example: a compensatory feedback release of endothelium-derived substances (Brutsaert, 2003) or counter-regulation at the level of cellular  $\text{Ca}^{2+}$  transport, e.g., the participation of reverse mode  $\text{Na}^+/\text{Ca}^{2+}$  exchanger. In view of the latter, it may be interesting to note that amiodarone inhibits the  $\text{Na}^+/\text{Ca}^{2+}$  exchanger (Watanabe and Kimura, 2000). That to our knowledge such a rebound effect was not previously reported for verapamil is not surprising in view of the fact that only apparent steady-state data (after stepwise infusion) but no single dose response data in the perfused heart were published so far (Hess et al., 1975; Kolar et al., 1990).

The  $EC_{50}$  of 16.4 nM (verapamil concentration causing half the maximum negative inotropic response) estimated from the response to 1-min verapamil infusion of 1.5 nmol using PK/PD modeling was lower than that of 31.6 nM estimated in the traditional way from cumulative drug infusion experiments. Using the latter method in rat hearts, values of 50 nM and 79 nM were reported by Hess et al. (1975) and Kolar et al. (1990). Since there is no proof that steady-state was attained in these stepwise infusion experiments, these estimates should be regarded with caution. It is important

to note, however, that the response data observed in our stepwise infusion experiments (mean values) are in reasonable agreement with those simulated with the model (using the mean parameter estimates of the double dose experiment). Assuming plasma protein binding of 90%, the  $EC_{50}$  determined in sheep for (-) verapamil by Huang et al. (1998) using single dose experiments corresponds to a free concentration of 12 nM, which is in reasonable agreement with our estimate. Note that the human therapeutic concentration of 41 nM free drug is in the order of the  $EC_{25}$  of the negative inotropic effect of verapamil measured in isolated human papillary muscle strips (Schwinger et al., 1990). Verapamil suppresses L-type  $Ca^{2+}$  channels (and myocardial contractility) by binding at a site accessible from the inside of the cell (Hockerman et al., 1997). Thus, the temporal delay between negative inotropic effect and unbound concentration in cardiac tissue, characterized by the time constant  $\tau_e$  of 19 s, could be caused by membrane transport, binding to receptors and the cellular effectuation process. Interestingly, a time constant  $\tau_{step}$  of  $\sim 10$  s and an equilibrium dissociation constant  $K_d$  of 58 nM were obtained from the kinetic constants of verapamil binding to cardiac membrane vesicles (Garcia et al., 1984). The kinetics of block by verapamil of L-type calcium current in rat myocytes led to a time constant of the same order of magnitude (Nawrath and Wegener, 1997). Note that under in vivo conditions, the arterial input concentration profile changes slowly relative to the step input in the present case, which leads to a loss of kinetic information on cardiac uptake rate of verapamil (Powell, 1990; Huang et al., 1998). Note further that the mean transit time,  $V_{ss}/Q$  ( $\sim 5$  min), is the counterpart of the equilibration time ( $1/k_{eo}$ ) between arterial and effect site concentration estimated in vivo using the traditional link model. Our estimate is in reasonable agreement with the estimates obtained in vivo (Huang et al., 1998). As expected for flow limited myocardial equilibration, the delay due to other transport and effectuation processes is negligible.

In the presence of amiodarone, only the maximum negative inotropic effect was significantly reduced if expressed as percent change from initial (pre-drug) values (Fig. 5.2). Because of the negative inotropic action of amiodarone a baseline reduction was expected. However, the intra-individual difference of 14% was not significant, and as expected this change is even less obvious in comparing the groups, where a non-significant ( $\sim 8\%$ ) reduction of  $E_0$  was observed. An additivity of the negative inotropic effects of amiodarone and verapamil (Campbell and Williams,

1998) would be in accordance with the fact that the negative inotropic effect of amiodarone is mainly mediated by its calcium channel blocking action (Sugiyama et al., 2001). The small reduction in *CVR* by verapamil in the presence of amiodarone (only 4 % decrease) may be due to limitation to maximal response since amiodarone already reduced the baseline of *CVR* by 42 %. This coronary vasodilating effect of amiodarone is well established and recently shown to be mediated primarily by the nitric oxide pathway (Guiraudou et al., 2004).

In summary, the present results suggest that cardiac uptake of verapamil is rapid and unaffected by amiodarone. A PK/PD model that accounts for acute tolerance has been successfully applied to the negative inotropic verapamil effect. Amiodarone tended to suppress tolerance development. It will be important to further investigate the effects of Pgp inhibition on cardiac uptake of Pgp substrates in view of a potential role in drug-drug interactions (Balayssac et al., 2005; Couture et al., 2006).

### 5.3.2. Effect of Endotoxemia on PK/PD Modeling of Verapamil

#### *Results*

At the time of heart isolation, rats of the LPS group were lethargic and body temperature was significantly increased to  $38.2 \pm 0.4^\circ\text{C}$  compared to  $36.9 \pm 0.4^\circ\text{C}$  in the control group ( $p < 0.001$ ). No deaths occurred in any group over the treatment period. Baseline coronary vascular resistance of Langendorff perfused hearts was doubled in heart of the LPS treated rats ( $8.1 \pm 3.8$  vs.  $4.1 \pm 0.6$  mmHg,  $p < 0.05$ ). Although the difference in baseline contractility ( $LVDP_0$ ) between control group ( $65.3 \pm 8.8$  mmHg) and LPS group ( $55.3 \pm 10.0$  mmHg) did not reach significance, the reduction in LPS treated hearts was significantly correlated with the increase in body temperature ( $p < 0.01$ ).

The mean time profiles of outflow concentration and negative inotropic response for the 1-min infusion of 1.5 nmol verapamil in the control and LPS group are shown in Fig. 5.6. The maximal response to verapamil was markedly reduced in hearts of LPS treated rats ( $\Delta LVDP/LVDP_0 = 32.16 \pm 7.81\%$ ) compared with control ( $\Delta LVDP/LVDP_0 = 49.78 \pm 9.08\%$ ) ( $p < 0.001$ ). After achieving the maximum effect (at  $\sim 2.5$  min), the negative inotropic effect recovered to baseline after  $\sim 10$  min and was followed by a positive inotropic rebound effect. Verapamil infusion induced a coronary vasodilation with a maximal decrease in *CVR* of  $15.18 \pm 6.66\%$  and  $25.81 \pm 15.11\%$  in hearts of saline and LPS treated rats, respectively.

As shown in Fig. 5.7, the PK/PD model fitted the verapamil outflow concentration-time curves (upper panel) and the negative inotropic response data (lower panel) reasonably well. (The same quality of fit was obtained in endotoxemic hearts.) The parameter estimates and their estimated asymptotic coefficients of variation (*CV*) of individual fits are summarized in Table 5.2. The relatively low *CV* values ( $< 10\%$ ) indicate that all parameters, except those describing irreversible binding ( $k_{ir}$ ) and tolerance development group ( $g$ ,  $\tau_m$ ) could be estimated with high precision.

The significant decrease of uptake or permeation clearance of verapamil  $CL_p$  from  $35.4 \pm 3.9$  ml/min to  $27.7 \pm 5.0$  ml/min ( $p < 0.01$ ) in endotoxemic hearts is reflected in a significantly higher maximal concentration (Fig. 5.6). The time course of the inotropic effect of verapamil is characterized by the “direct” negative inotropic action with parameters  $EC_{50} = 14.5 \pm 2.7$  nM,  $E_{max} = 54.4 \pm 11.6$  mmHg and a delay relative to the free myocardial concentration  $C_c(t)$  of  $\tau_e = 0.55 \pm 0.19$  min, as well as the extent and delay of tolerance development with parameters  $g = 0.12 \pm 0.11$  and  $MTT_{tol} = 23.2 \pm 19.7$  min. Endotoxemia led to a significant reduction in  $E_{max}$  to  $30.1 \pm 15.5$  mmHg ( $p < 0.01$ ); all other PD parameters remained unchanged.

**Table 5.2** Parameter estimates (means  $\pm$  SD) from fitting of verapamil outflow and negative inotropic response data in rat hearts of control and endotoxin groups

Parameter	Means (SD)	
	Control (n=6)	Endotoxin(n=8)
<b>Pharmacokinetics</b>		
$k_{in}$ (min <sup>-1</sup> )	589.6 (65.6)	461.0 (82.8)*
$k_{out}$ (min <sup>-1</sup> )	0.800 (0.147)	0.546 (0.100)*
$k_{ir}$ (min <sup>-1</sup> )	0.004 (0.007)	0.012 (0.015)
$CL_p$ (ml/min)	35.4 (3.9)	27.7 (5.0)*
$V_{ss}$ (ml)	45.0 (5.5)	52.9 (10.1)
<b>Pharmacodynamics</b>		
$E_{max}$ (%)	54.4 (11.6)	30.1 (15.5)*
$EC_{50}$ (pmol/ml)	14.5 (2.7)	10.0 (5.2)
$N$	1.9 (0.3)	2.2 (0.6)
$\tau_e$ (min)	0.55 (0.19)	0.92 (0.73)

\*  $p < 0.01$  vs. control rats

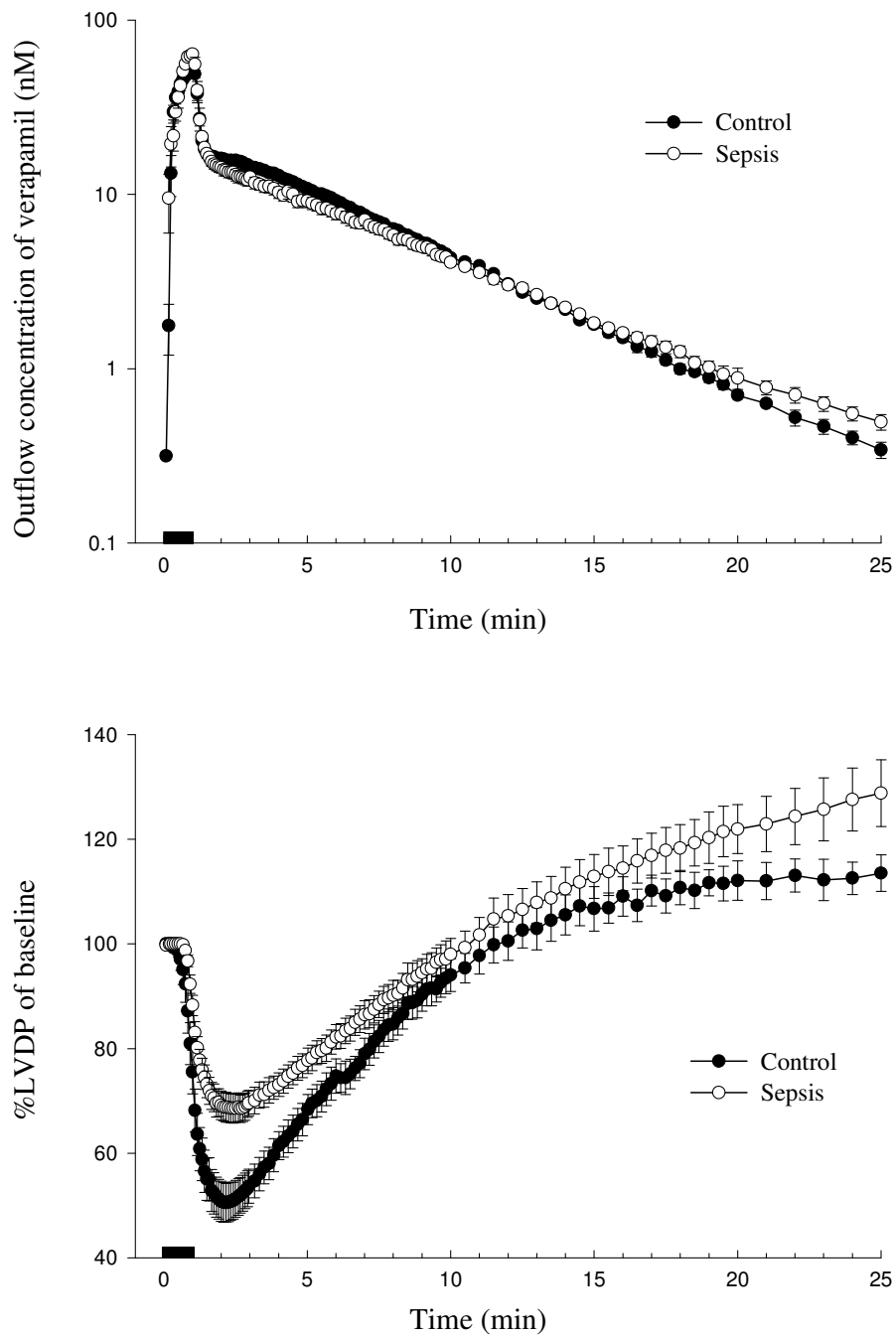


**Figure 5.6** Average verapamil outflow concentration (upper panel) and percent change in left ventricular developed pressure (*LVDP*) (lower panel) as observed for a 1-min infusion 1.5 nmol of verapamil in hearts of sham-treated (●) and endotoxemic rats (○), respectively (mean  $\pm$  SEM). Error bars that fall within the symbols are not shown.

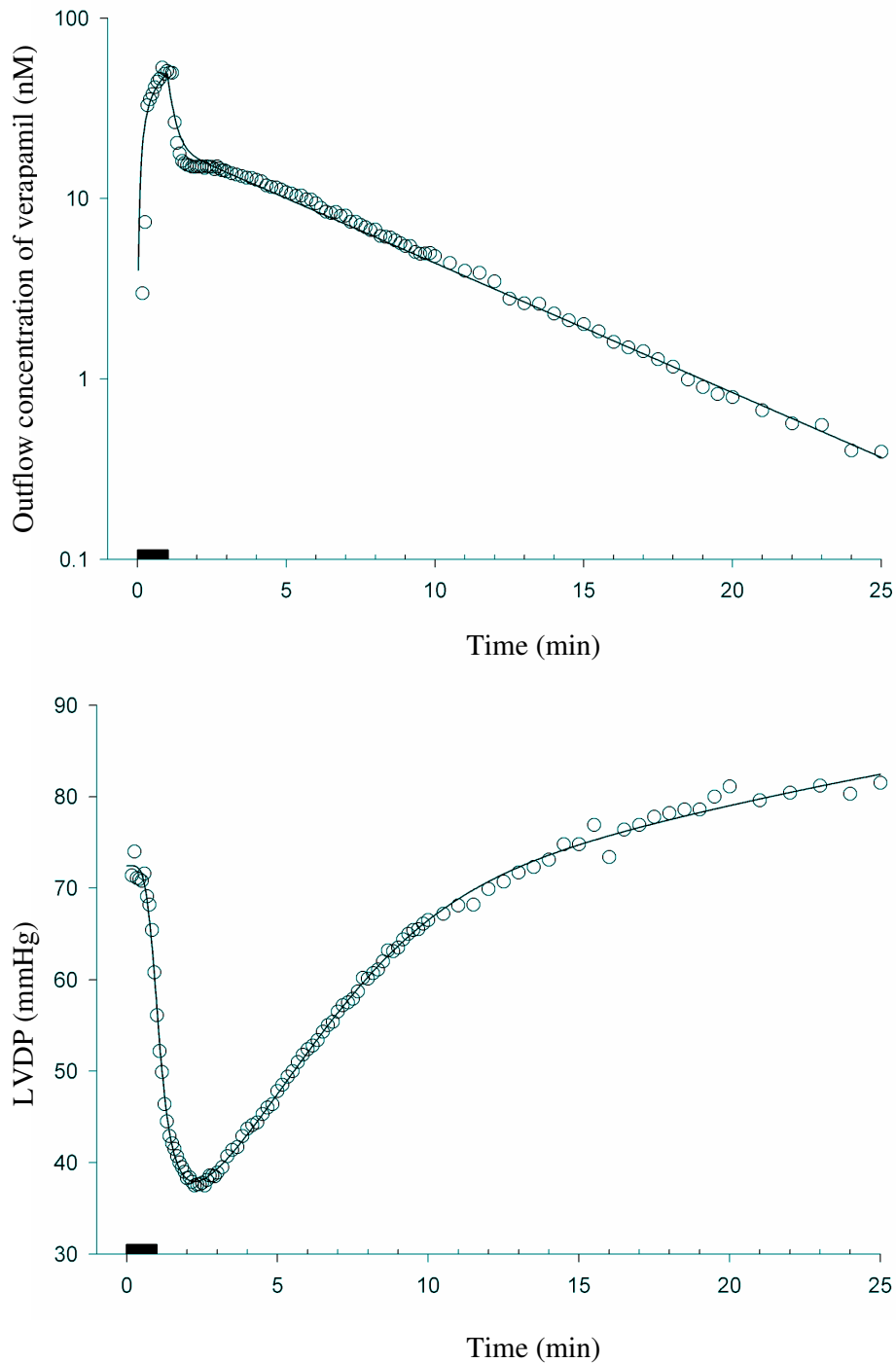


**Figure 5.7** Representative fits of the PK/PD tolerance model to experimental data obtained in one heart for a 1-min infusion 1.5 nmol of verapamil: outflow concentration (upper panel) and negative inotropic effect (lower panel).

### ***Discussion***

Little information exists about the effect of endotoxemia on cardiac kinetics and dynamics of drugs and no studies have examined verapamil in this disease model. While it is of general interest to study the effect of endotoxemia on pharmacokinetics (in this case cardiac uptake), the specific question was whether changes in pharmacodynamics could be explained by a downregulation of calcium channels. Since, a protective action of calcium channel blockers in LPS-induced septic shock has been discussed (Bosson et al., 1985; Lee and Lum, 1986; Hotchkiss et al., 1995; Mustafa and Olson, 1999; Wu et al., 1999; Li et al., 2006; Sirmagul et al., 2006), our results may also shed some light on potential cardiac effects of verapamil in this case. The present study shows that endotoxin shock attenuates the negative inotropic effect of verapamil without affecting its vasodilator action in Langendorff perfused rat hearts. These changes are independent of the observed decreased cardiac uptake rate of verapamil. All parameter estimates obtained in the control group are in accordance with the results of normal hearts which were previously discussed in section 3.1 of this chapter.

Since the uptake clearance of verapamil ( $CL_p$ ) is identical to the effective permeability-surface product  $PS$ , the significant decrease by  $\sim 22\%$  of  $CL_p$  may reflect the decrease in the functional area ( $S$ ) available for transcapillary uptake due to the  $\sim 100\%$  increase in  $CVR$ . Such a derecruitment of microvascular surface area accompanies, for example, the pulmonary vasoconstrictor response (Parker and Townsley, 2004). Coronary vasoconstriction was previously observed in endotoxin-treated rats by use of a Langendorff heart preparation (Hohlfeld et al., 1995; McLean et al., 1999; Bogle et al., 2000; Tessier et al., 2003; Tu et al., 2004) and was discussed in terms of increased endothelin production (Hohlfeld et al., 1995; Wanecek et al., 2001; Tu et al., 2004). Contradictory reports on coronary vasodilation may be due to differences in experimental design [e.g., (Avontuur et al., 1995)]. Note that the proportional decrease in  $k_{out}$  simply reflects the fact that the distribution volumes (or the equilibrium tissue /perfusate partition coefficient) remained unchanged.

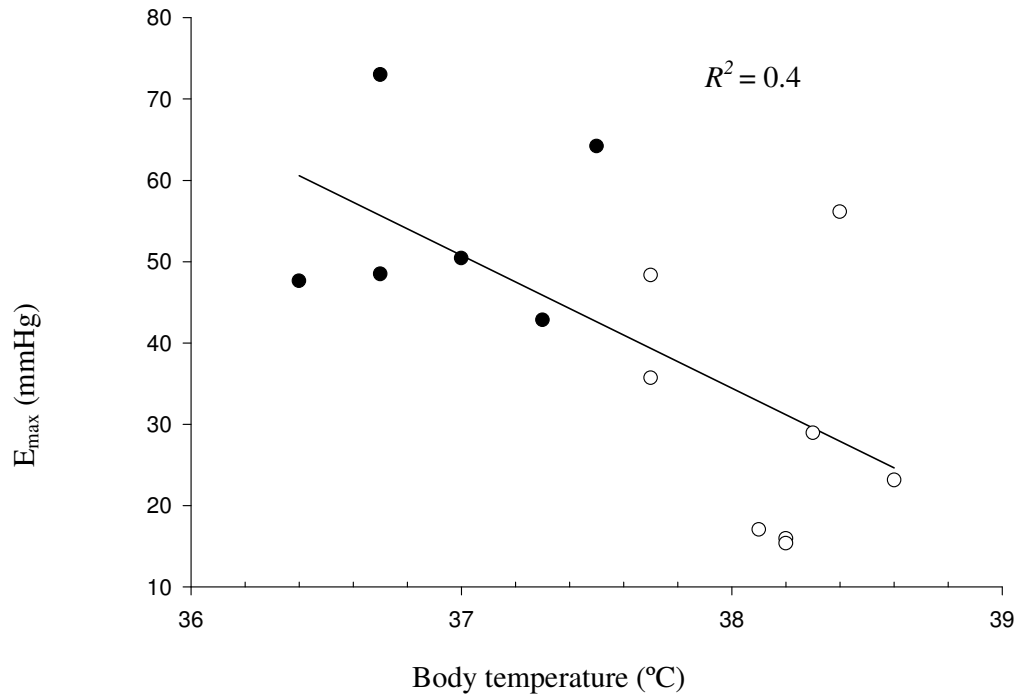


**Figure 5.8** The  $E_{max}$  estimate of the inotropic verapamil effect was negatively correlated with the LPS-induced rise in body temperature (slope = -0.16,  $R^2 = 0.4$ ,  $p < 0.01$ ). The sham-treated and endotoxemic rats are denoted by (●) and (○), respectively.

That the  $E_{max}$  of negative inotropic effect of verapamil was significantly smaller in LPS-treated rats than in control rats (55% of that under control conditions) could be explained by a decreased number of L-type calcium channels (Lew et al., 1996; Sattari et al., 2003), where the same degree of reduction was observed. Altered calcium transporter expression was also accompanied with burn-induced myocardial contractile dysfunction (Ballard-Croft et al., 2004). Due to the low specific binding of verapamil (relative to unspecific binding), we cannot differentiate between effects elicited at the receptor and postreceptor level (in contrast to a similar study with digoxin (Baek and Weiss, 2005)). Interestingly, the reduction in maximal response  $E_{max}$  [Eq. (5.7)] was significantly correlated with the LPS-induced rise in body temperature (Fig. 5.8), indicating that the latter may act as a measure of the degree of endotoxemia. An analogous correlation was found for the inotropic responsiveness to digoxin (Baek and Weiss, 2005). This suggests that the LPS-induced changes in drug action and body temperature could be caused by a circulating mediator, such as interleukin-6 (Rummel et al., 2006), possibly due to an indirect effect. While the inherent variability in the degree of endotoxemia-induced suppression in baseline contractility prevented a significant difference between LPS and control group the correlation with increase in body temperature was significant. In contrast to inotropy, endotoxemia did not affect the vasodilator response to verapamil. This is in accordance with the observation reported for the calcium channel blocker nicardipine (Bogle et al., 2000).

In summary, the present study demonstrates for verapamil and the heart that endotoxemia is associated with organ-related changes in pharmacokinetics and pharmacodynamics. Our data show for the first time that the negative inotropic response to verapamil is reduced in LPS-treated rats. This reduction is independent of the observed decrease in myocardial uptake rate of verapamil, which may be explained by the increase in coronary resistance.

## 6. $\alpha_1$ -Adrenergic Agents

### 6.1. Background

$\alpha_1$ -Adrenoceptors are essential for a normal cardiac contraction (McCloskey et al., 2003). Acute stimulation of  $\alpha_1$ -adrenoceptors lead to a positive inotropic effect in most mammalian species including rats and humans, and this  $\alpha_1$ -adrenoceptors mediated response increase in the failing heart when  $\beta$ -adrenoceptors are downregulated (Skomedal et al., 1997; Sjaastad et al., 2003). Furthermore, recent results suggest a possible role for  $\alpha_1$ -signaling myocardial preconditioning and cardiac adaption (O'Connell et al., 2006; Xiao et al., 2006). A variety of changes of receptor number, affinity and intrinsic efficacy can be associated with disease states (Xiao et al., 2006). Interactions between cardiac  $\alpha_1$ -adrenoceptors and agonists (or antagonists) have traditionally been studied using pharmacological steady-state methods such as dose-response curves and receptor binding studies; methods that do not allow a direct evaluation of receptor kinetics and the stimulus-response relationship. Other potential shortcomings of equilibrium models based on consecutive cumulative dosing experiments have been pointed out recently (Corsi and Kenakin, 2000; Shea et al., 2000; Vauquelin et al., 2002).

For a better understanding of the functional role of  $\alpha_1$ -adrenoceptors, it appears important to get further insights into the relationship between ligand-receptor binding kinetics, cellular signaling and transient inotropic response in the intact heart. Mathematical models provides the basis for such an integrated dynamic approach (Christopoulos, 2001; Weiss et al., 2004). In the Langendorff-perfused heart, one necessary condition (and the main difficulty of the approach) is that the effect of receptor binding can be detected in the ligand outflow concentration. This cannot be expected to hold for the  $\alpha_1$ -adrenoceptor agonist phenylephrine (PE) due to the dominating influence of uptake into vesicles of sympathetic nerve terminals (Raffel and Wieland, 1999). The high degree of specific binding of the selective  $\alpha_1$ -adrenoceptor antagonist prazosin (PRZ), however, appears promising (Edwards et al., 1988). Thus, we thought it worth attempting to develop a method that uses the measurement of PRZ outflow concentration-time profile following after short-term

injection of PRZ in the presence of PE together with the time course of PRZ induced reduction of inotropy. The approach is based on modeling the kinetics of the competition of receptor binding between PRZ and PE. Such a real-time approach, that combines the kinetics of cardiac uptake and ligand–receptor binding with response dynamics, has not been used before in pharmacology to analyze cardiac receptor function, except for digoxin binding to sodium pumps (Kang and Weiss, 2002; Weiss et al., 2004; Baek and Weiss, 2005).

Therefore, the goal of this study was 1) to investigate whether binding of PRZ to cardiac  $\alpha_1$ -adrenoceptors in the perfused rat heart is high enough to be measured in the outflow concentration; 2) to develop a mathematical model that describes transcapillary transport of PRZ, its competitive receptor binding leading to a transient decrease in  $\alpha_1$ -adrenoceptor occupation by PE and the induced inotropic response dynamics and 3) to find an experimental design that enables the estimation of binding rate parameters of PRZ and PE together with  $\alpha_1$ -adrenoceptor concentration.

To our knowledge, the usefulness of receptor occupation kinetics to predict  $\alpha_1$ -adrenoceptor mediated inotropic response dynamics has never been rigorously tested. Here we show that this approach, the kinetic version of the equilibrium 'operational model of drug action, is in accordance with experimental data. It allows the quantification of receptor concentration and ligand binding rate constants, together with the stimulus-response relationship (as a drug- independent property of the system) and may improve our understanding of the mechanism of  $\alpha_1$ -adrenoceptor mediated inotropic response.

## 6.2. Materials and Methods

### 6.2.1. Drugs and Chemicals

Prazosin hydrochloride and phenylephrine hydrochloride were obtained from Sigma-Aldrich chemie (Steinheim, Germany), [7-methoxy- $^3\text{H}$ ]Prazosin (85 Ci/mmol) from PerkinElmer (Boston, USA), and Dimethyl sulfoxide (DMSO) from Carl Roth (Karlsruhe, Germany). All other chemicals and solvents were of highest grade available.

### 6.2.2. Experimental Protocol

#### *Working Solution Preparations*

A concentrated PRZ stock solution was prepared by dissolving 2 mg PRZ in 1 ml DMSO. Then, a 1.4- $\mu\text{M}$  PRZ solution was prepared by adding 15  $\mu\text{l}$  of the stock solution to the perfusate buffer, and adjusting final volume to 50 ml. Finally, 3 ml of 1.4- $\mu\text{M}$  PRZ were mixed with 5  $\mu\text{l}$  [7-methoxy- $^3\text{H}$ ] PRZ. This labeled PRZ (1.4  $\mu\text{M}$ ) was later infused into the heart.

In order to prepare 12.3 and 6.1  $\mu\text{M}$  phenylephrine in the perfusate buffer, 12 mg/ml phenylephrine in water was prepared, and then 200 and 100  $\mu\text{l}$  of the solution were added in the perfusate buffer and adjusted to 1 l.

#### *Study Design*

This experiment was designed for observing the effect of PRZ in the presence of 12.3 and 6.1  $\mu\text{M}$  phenylephrine. Firstly, in presence of 12.3  $\mu\text{M}$ , 1.27 nmol of the labeled PRZ was infused within 1 min into the aortic cannula directly above the isolated heart that was prepared following the method in section 2.3. Then, outflow samples were collected every 5 s for 1.5 min, every 10 s for next 1.5 min, and every 30 s for next 7 min. The heart was allowed 5 min to recover to baseline.

Secondly, in presence of 6.1  $\mu\text{M}$  phenylephrine, the same dose of labeled PRZ was infused and the samples were collected as the same procedure as the first dose. The collected samples were kept in -20  $^{\circ}\text{C}$  until sample analysis. Note that both

infusions of PRZ were conducted after 15-min perfusion of each phenylephrine concentration.

### 6.2.3. Quantification of Prazosin

The sample concentrations were determined within 3 days after collecting samples using a liquid scintillation counter (Perkin Elmer Instruments, Shelton, CT). Calibration curve concentrations (0.5-140 nM) were prepared by firstly diluting one-tenth of 1.4- $\mu$ M labeled PRZ, and then the solution was serially half diluted.

The samples (250  $\mu$ M) were mixed with 2 ml Lumasafe Plus used as cocktail solution, and were analyzed using Liquid Scintillation Analyzer.

### 6.2.4. Cumulative Dose-Response Curve of Phenylephrine

A stepwise cumulative infusion with 15-min time interval of phenylephrine in perfusate buffer was conducted in five perfused hearts. The input concentrations of phenylephrine were 0.0125, 0.05, 0.1, 0.3, 0.5, 2, and 40  $\mu$ M. The drug effect, LVDP, was measured at the end of each infusion time interval.

### 6.2.5. PK/PD Model and Data Analysis

The PK/PD model of competitive  $\alpha_1$ -adrenergic agents has been developed as shown in Fig. 6.1. It consists of cardiac uptake and competitive receptor binding between agonist (PE) and antagonist (PRZ) which link to cellular process (inotropic response). Note that the cardiac uptake of PE is not determined since steady state concentration of PE is assumed.

#### *Cardiac uptake and receptor binding kinetics*

The competitive interaction between agonist PE ( $A$ ), antagonist PRZ ( $D$ ) and receptor ( $R$ ) can be written as:



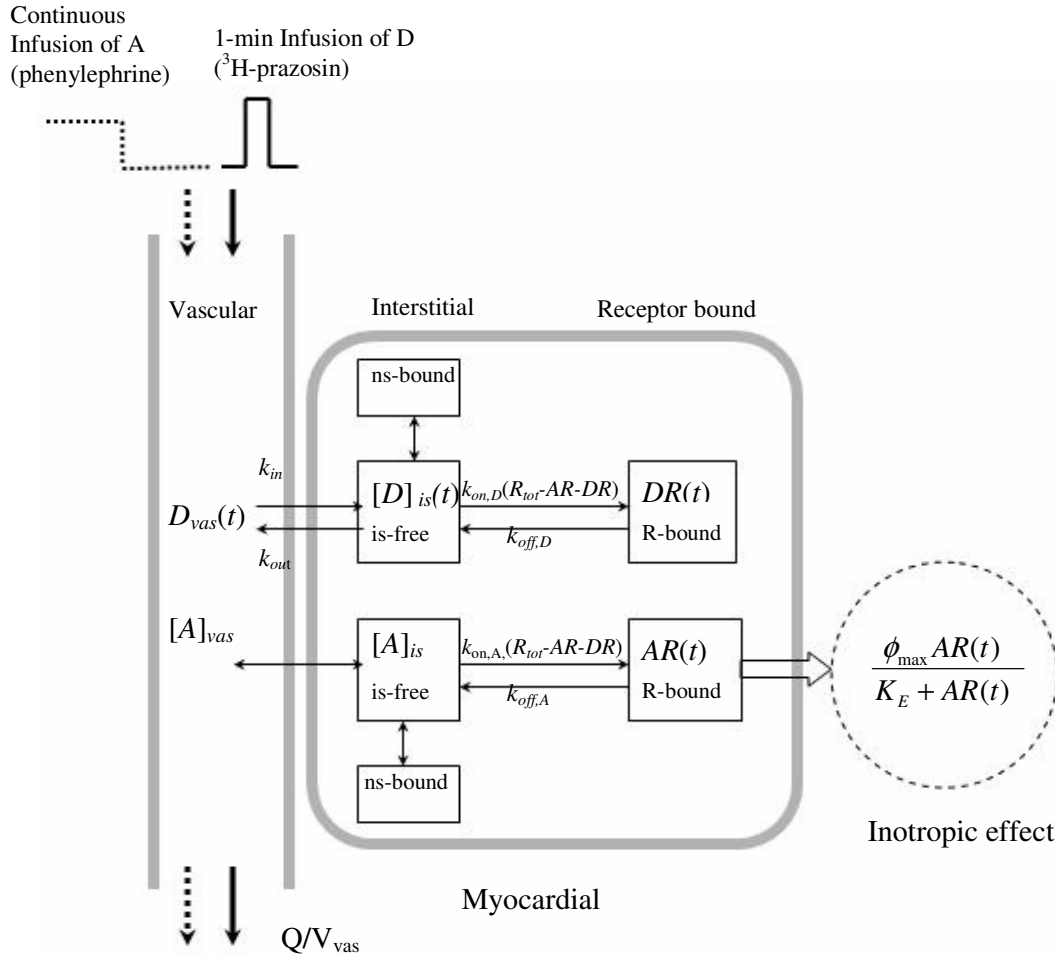


**Figure 6.1** Model of  $\alpha_1$ -adrenergic mediated inotropic response in the perfused rat heart. Model input is governed by stepwise infusion of PE (A) and 1-min infusion of 1.27 nmol  $\text{H}^3$ -PRZ (D). The inotropic effect is related to receptor occupation of the agonist PE ( $AR(t)$ ), and a hyperbolic function for the transduction of  $AR(t)$  into response. ( $k_{in}$  and  $k_{out}$ : first order distribution rate constants between vascular and interstitial space;  $k_{on,D}$  and  $k_{off,D}$ : the association rate constant and the dissociation rate constant for PRZ;  $k_{on,A}$  and  $k_{off,A}$ : the association rate constant and the dissociation rate constant for PE;  $[D]_{is}$  and  $[A]_{is}$ : concentration of PRZ and PE, respectively, in interstitial space where the drugs are in free form (is-free) and/or bind with nonspecific binding (ns-bound))

where  $k_{on}$  and  $k_{off}$  are the association and dissociation rate constants, respectively. In the present experimental design, the agonist is infused at constant rate and it is assumed that binding  $AR$  or agonist receptor occupancy is at steady state when the antagonist is injected at  $t = X$ :

$$AR_{ss} = \frac{R_{tot}[A]}{[A] + K_A}, \quad DR(X) = 0 \quad (6.2)$$

where  $[A]$  denotes the concentration,  $R_{tot}$  is the amount of receptor sites available for binding,

$$R_{tot} = AR + DR + R \quad (6.3)$$

and  $K_A$  the equilibrium dissociation constant (ratio of the dissociation rate constant  $k_{off,A}$  to the association rate constant  $k_{on,A}$ ).

Since  $\alpha_1$ -adrenoceptors are located at the cell surface,  $A_{is}$  and  $D_{is}$  are the drug amounts in the interstitial space, and we need a kinetic model that describes transport of the ligands from the perfusate to this free ligand compartment (transcapillary uptake) to predict the time course of receptor binding after drug infusion in the single-pass perfused heart. For PE we have a steady-state situation, i.e., the interstitial concentration  $[A]_{is}$  is identical to the vascular concentration  $[A]_{vas}$ , while for the kinetics of PRZ we need a compartmental model, describing changes in the amounts of PRZ in the mixing, capillary, and interstitial space as shown in Fig. 6.1.

Perfusate flow ( $Q$ ) (including drug) first passes the mixing volume  $V_0$  (tubing and large vessels where no exchange with tissue occurs) before it enters the vascular space (distribution volume  $V_{vas}$ ) where transcapillary transport of the unbound drug between vascular and interstitial space is described by rate constants  $k_{in}$  and  $k_{out}$ , respectively, and the apparent permeability surface-area or permeation clearance  $CL_P = k_{in}V_{vas}$  is determined by  $k_{in}$  and  $V_{vas}$ . Assuming passive transport processes, we have  $k_{in}V_{vas} = k_{out}V_{app,is}$  where  $V_{app,is}$  denotes the apparent volume that governs initial distribution of PRZ in the interstitial space. The value of  $V_{app,is}$  might exceed the distribution space  $V_{is}$  due to quasi-instantaneous nonspecific tissue binding. The free concentration in the interstitial space that governs receptor binding is then given by

$[D]_{is}(t) = D_{is}(t)/V_{app,is}$ , with  $V_{app,is} = (k_{in}/k_{out})V_{vas}$ . The time-dependent fractional binding rates of PRZ and PE to free membrane receptors are given by  $k_{on,D}(R_{tot}-AR(t)-DR(t))$  and  $k_{on,A}(R_{tot}-AR(t)-DR(t))$ , respectively, where  $AR(t)$  and  $DR(t)$  are the amounts of PE and PRZ, respectively, bound at time  $t$  to receptor  $R$  (receptor occupancy).

This integrated model of drug uptake and receptor binding (Fig. 6.1) is described by the following differential equations:

$$\frac{dD_0(t)}{dt} = -\left(\frac{Q}{V_0}\right)D_0(t) + I_D(t) \quad (6.4)$$

$$\frac{dD_{vas}(t)}{dt} = -\left(\frac{Q}{V_{vas}} + k_{in}\right)D_{vas}(t) + k_{out}D_{is}(t) + \left(\frac{Q}{V_0}\right)D_0(t) \quad (6.5)$$

$$\frac{dD_{is}(t)}{dt} = k_{in}D_{vas}(t) - k_{out}D_{is}(t) - k_{on,D}(R_{tot} - AR(t) - DR(t))C_{D,is} + k_{off,D}DR(t) \quad (6.6)$$

$$\frac{dDR(t)}{dt} = k_{on,D}(R_{tot} - AR(t) - DR(t))C_{D,is} - k_{off,D}DR(t) \quad (6.7)$$

$$\frac{dAR(t)}{dt} = k_{on,A}(R_{tot} - AR(t) - DR(t))C_{A,is} - k_{off,A}AR(t) \quad (6.8)$$

where  $I_D(t)$  denotes the input rate of PRZ (1 min infusion). For the sake of clarity,  $C_{D,is} = [D]_{is}$  and  $C_{A,is} = [A]_{is}$  have been used to denote the unbound ligand concentrations in the interstitial space. As the steady state is assumed for PE, the PE concentration,  $C_{A,is}(t)$ , is equal to the input concentration of PE which is constant before and after the stepwise reduction from 12.3 to 6.1  $\mu\text{M}$  at  $t = 30$  min. Since a receptor occupation by endogenous ligands cannot be excluded, the only nonzero initial condition in Eqs. (6.4)-(6.8) is the receptor occupation before PE infusion ( $t = 0$ )

$$AR(0) = AR_0 \quad (6.9)$$

By solving Eqs. (6.4)-(6.8) numerically one obtains the time course of PRZ outflow concentration,  $C_D(t) = [D]_{vas}(t) = D_{vas}(t)/V_{vas}$ , and the receptor occupation by the agonist PE,  $AR(t)$ .

***Cellular effectuation and dose-response relationship***

The relationship between agonist receptor occupation  $AR(t)$  and the positive inotropic effect is described by the stimulus-response relationship  $\Delta E(t) = \phi AR(t)$ , where  $\phi$  refers to the chain of cellular processes which convert the stimulus into response (Kenakin, 1993). According to the operational model of receptor agonism (Black and Leff, 1983; Kenakin, 1993), we use a hyperbolic function for the transduction of receptor occupancy into response

$$E(t) = E_B + \frac{\phi_{\max} AR(t)}{K_E + AR(t)} \quad (6.10)$$

where  $E_B$  is the baseline effect when  $AR = 0$  and the  $K_E$  denotes AR producing 50% of  $\phi_{\max}$ . With decreasing  $K_E$ , the response sensitivity increases. The  $LVD P(t)$  data were used as a measure of inotropic effect,  $E(t) = LVD P(t)$ .

According to Eq. (6.8) and (6.10), the temporal displacement of agonist from the receptor [decrease in  $AR(t)$ ] by the competitor PRZ leads to a transient decrease in  $LVD P(t)$ . Note that the observed baseline ( $E_0$ ) is the result from the summation between the inotropic effect before PE infusion results of the (unknown) inotropy without receptor stimulation ( $E_B$ ) and a possible effect of an endogenous ligand ( $\phi AR_0$ ):  $E_0 = E_B + \phi AR_0$ .

The steady-state concentration-response curve for the positive inotropic effect induced by cumulative infusion of PE is obtained by substituting  $AR(t) = AR_{ss}$ , into Eq. (6.10), whereby  $AR_{ss}$  is given by Eq. (6.2) with  $[A] = C_A$ :

$$E_{ss} = E_B + \frac{\phi_{\max} R_{tot} C_A}{K_E K_A + (K_E + R_{tot}) C_A} \quad (6.11)$$

This is the basic equation of the operational model of drug action (Kenakin, 1993).

Corresponding to the effect at steady-state,  $E_{ss}$  [Eq. (6.11)] we have:

$$E_{\max} = \frac{\phi_{\max} R_{tot}}{K_E + R_{tot}} \quad (6.12)$$

$$EC_{50} = \frac{K_E K_A}{K_E + R_{tot}} \quad (6.13)$$

Where  $E_{\max}$  is maximum effect;  $EC_{50}$  is the concentration that corresponds to 50% of  $E_{\max}$ .  $E_{\max}$  can be calculated as secondary parameters, and used to compare with the results obtained from dose-response curve of PE.

Using ADAPT II Version 4 (D'Argenio & Schumitzky, 1997) with maximum likelihood estimator, Eqs. (6.4)-(6.8) and Eq. (6.10) were solved and fitted simultaneously to  $C_D(t)$  and  $E(t)$  data. However,  $CV$  of individual fits of the parameter estimation could not be estimated. It means the estimate was unreliable or the set of parameters was not unique. In order to improve the estimation,  $K_E$  [in Eq. (6.10)] was written in form of  $EC_{50}$  [Eq. (6.14)], and the  $EC_{50}$  was fixed at the values obtained from the dose-response curve of PE using Eq. (6.15). Then, the model fitting process was repeated again. Note that Eq. (3.2) was used as variance model.

Equation (6.13) can be rewritten as:

$$K_E = \frac{EC_{50} R_{tot}}{K_A - EC_{50}} \quad (6.14)$$

The following equation demonstrates the  $E_{\max}$ -model with observed baseline ( $E_0$ ) used to determine  $E_{\max}$  and  $EC_{50}$  from cumulative dose-response curve of PE.

$$E_{ss} = E_0 + \frac{E_{\max} C_A}{EC_{50} + C_A} \quad (6.15)$$

Using a model independent method, the recovery of PRZ was calculated from outflow concentration versus time data using a numerical integration method as the amount recovered at 10 min after PRZ infusion:

$$\text{Recovery} = \frac{\int_0^{10} C_{out}(t) dt}{Dose} \quad (6.16)$$

The quality of the model was judged by the goodness of fit  $R^2$  and AIC. The reliability of parameter estimation was assessed by the asymptotic coefficients of variation (CV) of individual parameter estimates.

The results are reported as mean  $\pm$  *SD*. Pair *t-test* and one-way *t-test* were used to test differences between group means. A *p*-value of less than 0.05 considered statistically significant.

### 6.3. Results

After 15-min equilibrium time, averages ( $n=5$ ) of *LVDP*, *HR* and *CVR* at baseline were  $96.3 \pm 16.4$  mmHg,  $256 \pm 18$   $\text{min}^{-1}$  and  $4.42 \pm 1.25$  mmHg·min/ml, respectively. Figure 6.2 shows the average PRZ outflow concentration and PRZ induced negative inotropic response data ( $n = 5$  in each group) following two consecutive 1.27 nmol doses of PRZ in the presence of 12.3  $\mu\text{M}$  and 6.1  $\mu\text{M}$  PE, respectively. Note that the 15-min infusion of 12.3  $\mu\text{M}$  PE increased *LVDP* by  $22.3 \pm 9.5$  % ( $p < 0.01$ ). The reduction in agonist (PE) concentration led to an increased transient negative inotropic response to the antagonist PRZ, with maximum values of  $22.6 \pm 2.1$  % vs.  $14.1 \pm 1.1$  % ( $p < 0.001$ ). The recoveries of PRZ in the perfusate up to 10 min were  $100.5 \pm 3.5$  % and  $104.0 \pm 4.7$  %, respectively, for the two doses. PE infusion (12.3  $\mu\text{M}$ ) increased heart rate by  $11 \pm 11$ % and decreased *CVR* by  $20.5 \pm 13.4$ %, but the changes showed no significant difference to the baseline values. While no change in heart rate was observed following the PRZ doses, *CVR* significantly decreased by  $11.0 \pm 3.7$ % and  $6.6 \pm 4.6$  % for the first and second dose, respectively ( $p < 0.05$ ).

The observed and predicted PRZ outflow,  $C_D(t)$ , and the inotropic response curves,  $LVDP(t)$ , are depicted in Fig. 6.3 for one heart as an illustrative example. The model (Fig. 6.1) fitted the data well. The mean  $R^2$ , a measure of goodness of fit of the model, were 0.983 and 0.949 for  $C_D(t)$  and  $LVDP(t)$  data, respectively. For the double PRZ dose experiment in the presence of two different PE concentrations, the model was identifiable and parameters were estimated with reasonable precision except the parameters describing the dissociation rate constant of PE ( $k_{off, A}$ ). The reason might be that only steady state concentrations of PE were not enough to estimate the parameter precisely. The averaged model parameters and estimation errors, as a percentage of related parameter estimates, are listed in Table 6.1.

**Table 6.1** The mean (*SD* in parenthesis) of estimated parameters from fitting of PRZ outflow concentration and inotropic response data following two consecutive 1.27 nmol doses of PRZ in the presence of 12.3  $\mu\text{M}$  and 6.1  $\mu\text{M}$  PE, respectively.

Parameters	Mean ( <i>SD</i> )	% <i>CV</i> <sup>a</sup>
<b>Distribution</b>		
$k_{vi}$ ( $\text{min}^{-1}$ )	223.6 (29.8)	7.2 (2.3)
$k_{iv}$ ( $\text{min}^{-1}$ )	1.21 (0.14)	6.3 (1.9)
<b>Binding</b>		
$K_{A,D}$ (nM)	0.084 (0.029)	36.6 (9.8)
$k_{off,D}$ ( $\text{min}^{-1}$ )	0.35 (0.20)	19.4 (6.2)
$R_{tot}$ (pmol)	49.6 (11.2)	27.0 (19.9)
$K_{A,A}$ (nM)	98.6 (31.4)	28.0 (5.9)
$k_{off,A}$ ( $\text{min}^{-1}$ )	3.12 (5.33)	82.8 (124.5)
<b>Response</b>		
$\phi_{max}$ (mmHg)	98.7 (25.1)	28.4 (7.4)
$KE$ (pmol)	22.9 (9.2)	53.2 (17.4)
$E_B$ (mmHg)	51.1 (21.2)	44.2 (39.2)
$AR(0)$ (pmol)	21.0 (13.7)	47.9 (16.8)
$E_{max}$ (mmHg)	61.8 (15.4)	34.1 (17.4)
$EC_{50}$ (nM)	28.7(Fix)	

<sup>a</sup> Approximate coefficients of variations of individual fits (imprecision).

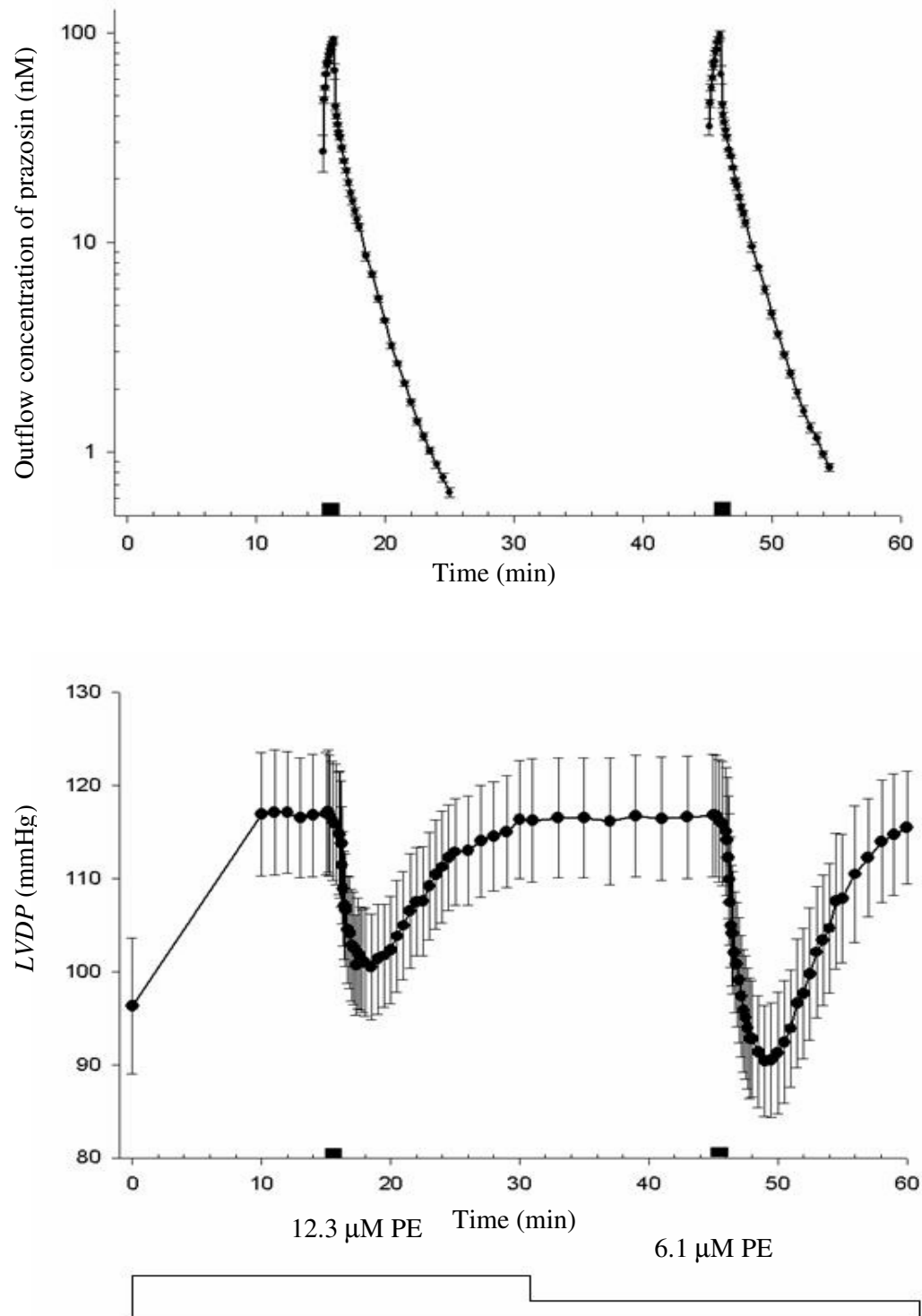


**Figure 6.2** Average (mean  $\pm$  SEM, n=5) PRZ outflow concentration (upper panel) and left ventricular developed pressure (LVDP) (lower panel) as observed for a 1-min infusion of two consecutive 1.27 nmol doses of PRZ in the presence of 12.3  $\mu$ M and 6.1  $\mu$ M PE, respectively. Error bars that fall within the symbols are not shown.

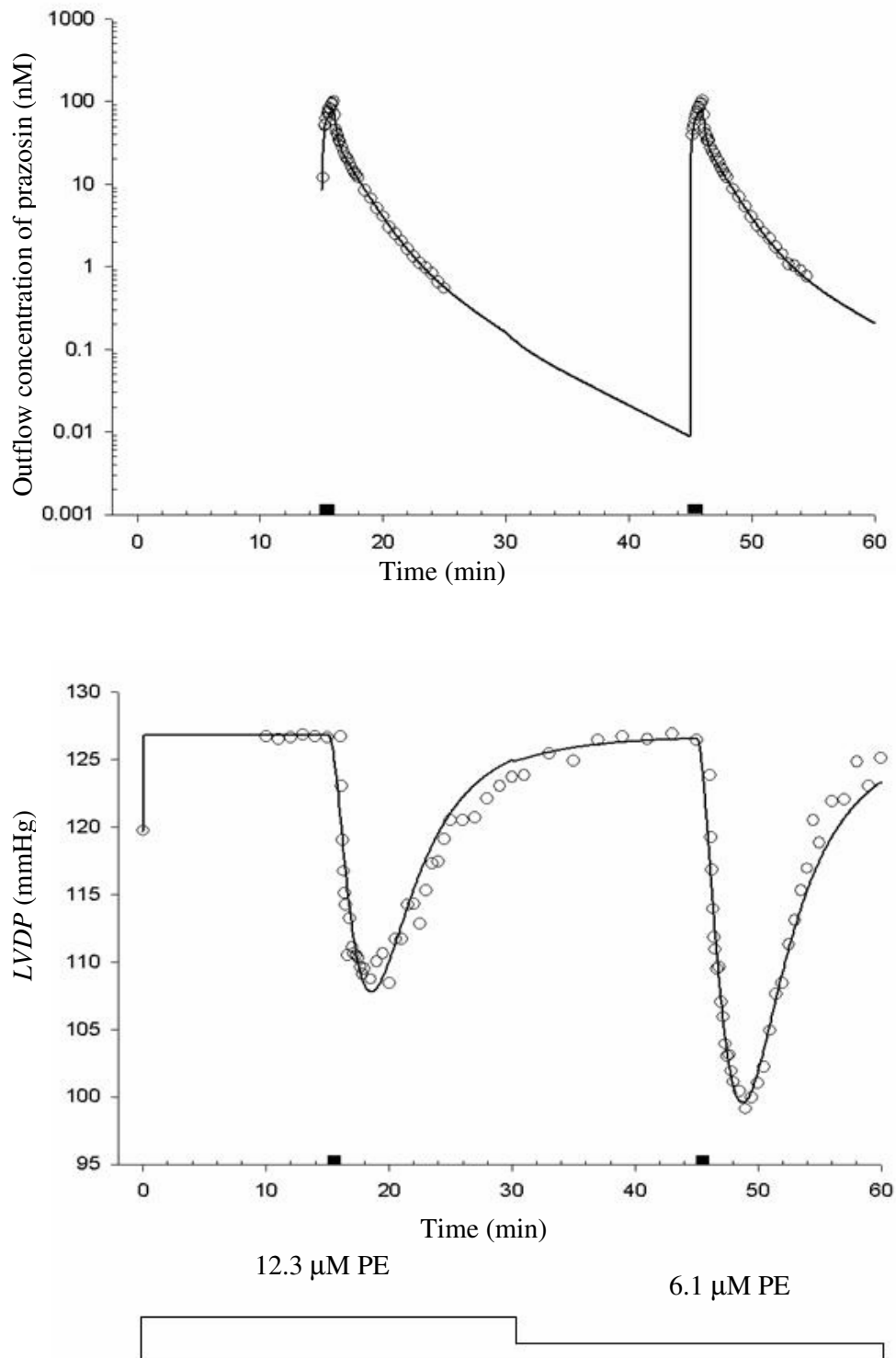


**Figure 6.3** Representative fits of the PK/PD model to experimental data obtained in one heart for a 1-min infusion of two consecutive 1.27 nmol doses of PRZ in the presence of 12.3  $\mu$ M and 6.1  $\mu$ M PE, respectively.

***Cumulative dose-response curve of PE***

The mean concentration response curve obtained by cumulative infusion of PE is shown in Fig. 6.4. The parameter estimates obtained by fitting Eq. (6.15) to the steady state concentration-response data were  $EC_{50} = 28.7 \pm 19.8$  nM,  $E_{max} = 43.8 \pm 14.4$  mmHg, and  $E_0 = 88.7 \pm 15.8$  mmHg. The asymptotic coefficients of variation (CV) of individual parameter estimates were less than 40 %, and the mean  $R^2$  was 0.954.

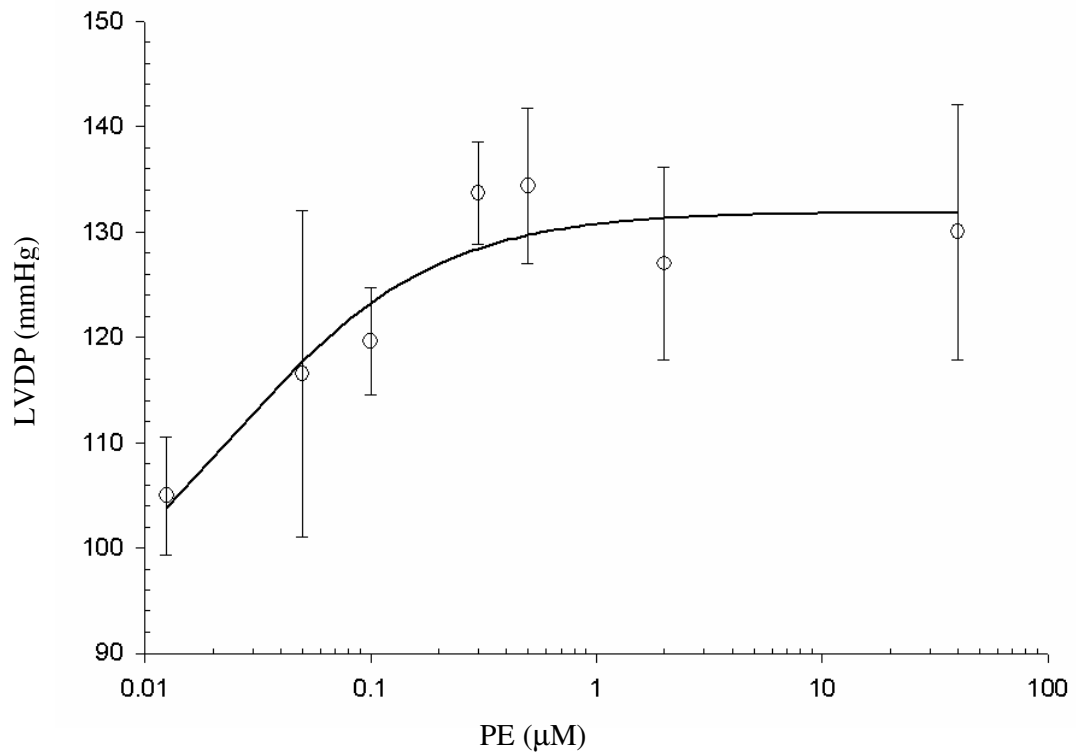


**Figure 6.4** Representative fit of mean  $\pm$  SEM of cumulative dose-response curve of PE using Eq. (6.15) ( $n=5$ ).

#### 6.4. Discussion

PE induces an  $\alpha_1$ -adrenoceptor-mediated inotropic response that can be antagonized by PRZ. Surprisingly, our results showed that PRZ did not only antagonize the effect of PE, but also decreased LVDP below the observed baseline at equilibrium time. Based on our model, this can be explained by the competitive binding of PRZ to endogenous catecholamines.

High concentration of PE has been reported to stimulate both  $\alpha_1$ - and  $\beta$ -adrenoceptors; thus,  $\beta$ -adrenergic antagonist (propranolol) was usually used to block the  $\beta$ -adrenergic effect in some  $\alpha_1$ -adrenergic studies. However, the concentration of PE using in our experiment was not enough to stimulate  $\beta$ -adrenoceptors since no significant change of *HR* after PE infusion was observed. Moreover, this was supported by the fact that PRZ can antagonize all the positive inotropic effect mediated by PE (Fig. 6.2). Additionally, using propranolol together with PE would complicate the situation since an interaction between  $\alpha_1$ - and  $\beta$ -adrenoceptor signaling could be expected (Xiao et al., 2006).

Transcapillary uptake clearance of PRZ ( $CL_p = 13$  ml/min) is close to those of sucrose and digoxin (Weiss et al., 2004) indicating passive transport of PRZ through interendothelial gaps. Cardiac kinetics of PRZ was then characterized by the passive transport and specific binding to  $\alpha_1$ -adrenoceptors. About 100 percent of PRZ was recovered in the outflow perfusate.

The affinity of prazosin ( $K_{A,D}$  0.084 nM) is comparable with the values obtained by other radioligand binding studies [0.025-0.41 nM (Yamada et al., 1980; Edwards et al., 1988; Gross et al., 1988; Fedida et al., 1993)]. However, in some vitro binding experiments, the values (2.9 nM and 5.84 nM) are much higher. The high variation of the reported  $K_A$  values for PRZ might be because of the difference of sample preparation and experiment conditions (Edwards et al., 1988). Edwards et al. (1988) have suggested that the tissue manipulation for in vitro binding study (e.g., sarcolemma isolation) may alter receptor properties, and recommended the perfused heart as an appropriate model system in which to study the relationship between receptor occupancy and biological response. Compared with PE, PRZ ( $K_{A,D}$  0.084

nM) has higher affinity to  $\alpha_1$  adrenoceptors than PE ( $K_{A,A}$  98.6 nM); however, there is no previous report of the equilibrium dissociation constant of PE ( $K_{A,A}$ ) for comparison with our result.

PRZ dissociates from  $\alpha_1$ -adrenoceptors with a  $t_{1/2}$  of 1.98 min; this suggests reversible binding to the receptor. This result is different from some previous reports where the dissociation  $t_{1/2}$  was about 40 min indicating a pseudo-irreversible binding to the receptor (Amitai et al., 1984; Edwards et al., 1988). In our point of view, the pseudo-irreversible binding of PRZ is unlikely, since our results showed that the reduction of PRZ recovered to the baseline within 15 min suggesting reversible binding with the dissociation  $t_{1/2}$  less than 15 min. Moreover, our result is in agreement with experiments in rat aorta (Agrawal and Daniel, 1985; Tanaka et al., 2004) that suggest reversible binding of the drug with the dissociation  $t_{1/2}$  in the range of 0.4-8.9 min. Note that drugs that possess a long dissociation  $t_{1/2}$ , usually act as pseudo-noncompetitive antagonists by reducing the maximal effect (Sakamoto et al., 1994; Vauquelin et al., 2002).

The estimated  $\alpha_1$ -receptor concentration ( $R_{tot}$ ) of 50 pmol/g wet weight corresponds to ~ 333-840 fmol/mg protein (assuming 59.8-150 mg protein/mg wet weight (Edwards et al., 1988; Gengo et al., 1988)). This result is in the same range as the value of 13.2 pmol/g wet weight measured by equilibrium radioligand binding assay in perfused rat heart (Edwards et al., 1988), the value of 12.2 pmol/g wet weight measured by Positron Emission Tomography (PET) (Law et al., 2000), and 448 fmol/mg protein assessed in vitro binding study (Gengo et al., 1988). However, the results from homogenate-binding studies (5.9-167 fmol/mg (Fedida et al., 1993)) were much less than our estimated value. This might be explained by a substantial loss of receptor due to a low yield of receptor-bearing membranes after homogenization and fractionation (Colucci et al., 1984; Faber et al., 2001; Tanaka et al., 2004).

It is important to note that the estimation of  $R_{tot}$  in our model is based on the inotropic activity, thus, the model could not estimate the receptor binding in nonmyocytes such as intramyocardial vessels, mast cells, endothelial cell, etc. This could possibly lead to underestimate the parameter. However, the receptor binding sites in nonmyocytes represent only a small portion relative to the binding by ventricular myocytes (Skomedal et al., 1984; Fedida et al., 1993).

In summary, the PK/PD modeling of  $\alpha_1$ -adrenergic agents, which was established from outflowed concentration together with inotropic effect of competitive interaction between agonist PE and antagonist PRZ, has many advantages. Firstly, capillary permeation, drug receptor interaction and stimulus-response relationship can be evaluated in one experiment. Secondly, based on competitive interaction concept, agonist parameters can be estimated using antagonist outflow concentration. Thirdly, the model can discriminate the effects of receptor occupation from signal transduction in response generation. Moreover, in contrast to in vitro binding studies, the binding parameters can be estimated without influence of tissue manipulations. Finally, our model which is based on understanding of signal transduction systems can be used to predict transient response characteristics.

## 7. Summary

For whole body pharmacokinetic/pharmacodynamic (PK/PD) models based on plasma concentration- and response-time data, the information on the underlying processes of drug transport to the effect site and effectuation is limited. More complex mechanistic models that include transcapillary drug exchange and the dynamics of drug-receptor interaction, can be analyzed after complexity reduction; i.e., the decomposition of the system into subsystems which can be identified separately. Studies in the isolated perfused heart offer an efficient possibility to develop more detailed PK/PD models that provide insight into processes underlying the action of cardioactive drugs. In the present thesis, the cardiac uptake and response kinetics of amiodarone, verapamil, and  $\alpha_1$ -adrenergic agents phenylephrine and prazosin were investigated. While for amiodarone and verapamil due to their low specific binding, only empirical PD models were applied, a mechanism-based model based on receptor-binding kinetics was developed to describe the interaction between prazosin and phenylephrine.

The results obtained for amiodarone indicated a rapid cardiac uptake, a high equilibrium tissue/perfusate partition coefficient, and long washout half-life of 17 h. The negative inotropic effect was related to the vascular concentration with delay time of 11 min.

For verapamil after rapid uptake, the negative inotropic effect is directly linked to cellular concentration with short delay time of 19 s. The negative inotropic effect caused a positive inotropic rebound effect. This tolerance development lead to a reduction in the predicted steady-state effect (16 %). Coadministration of the Pgp inhibitor amiodarone did not influence the cardiac kinetic of verapamil. In endotoxemic hearts, the negative inotropic of verapamil was significantly decreased, which may be explained by a reduction number of L-type calcium channels.

With the mechanism-based model for  $\alpha_1$ -adrenergic agents it was possible to estimate cardiac  $\alpha_1$ -AR concentration, association and dissociation constants of receptor ligands, simultaneously with the stimulus-response relationship by studying the interaction of the  $\alpha_1$ -AR agonist phenylephrine with the selective  $\alpha_1$ -AR blocker

## 7. Summary

---

prazosin. The PK/PD model accounted for cardiac uptake and receptor binding kinetics of prazosin, assuming that the competitive displacement of phenylephrine reduced the receptor occupation by the agonist and consequently contractility. The approach allowed, for the first time, a differentiation between effects elicited at the  $\alpha_1$ -adrenergic receptor and postreceptor level.

## 8. Zusammenfassung

Für die klassischen pharmakokinetischen/ pharmakodynamischen (PK/PD) Modelle, die auf Plasmakonzentrations- und Effektdaten beruhen, sind die Informationen über die zugrunde liegenden Prozesse des Pharmakontransportes zum Wirkungsort und den Mechanismus der Signaltransduktion begrenzt. Komplexere mechanistische Modelle, die den transkapillären Transport und die Dynamik der Pharmakon-Rezeptor-Wechselwirkungen berücksichtigen, erfordern eine Aufteilung des Systems in Subsysteme, die einzeln identifiziert werden können. Untersuchungen am isoliert-perfundierten Herzen geben die Möglichkeit, detailliertere PK/PD-Modelle für herzwirksame Arzneimittel zu entwickeln.

In der vorliegenden Arbeit werden der kardiale Transport und die Effektkinetik von Amiodaron, Verapamil und der  $\alpha_1$ -adrenergen Pharmaka Phenylephrin und Prazosin untersucht. Während für Amiodaron und Verapamil wegen ihrer geringen spezifischen Bindung nur empirische PD-Modelle angewendet wurden, konnte die Interaktion zwischen Prazosin und Phenylephrin mit einem mechanistischem Modell der Rezeptorbindungskinetik beschrieben werden. Die Ergebnisse für Amiodaron zeigen eine schnelle kardiale Aufnahme, einen hohen Gleichgewichts-Gewebe/Perfusat-Verteilungskoeffizienten und eine lange Auswaschzeit von 17 h. Der negativ-inotrope Effekt korrelierte mit dem Zeitverlauf der vaskulären Konzentration bei einer Verzögerungszeit von 11 min.

Für Verapamil war nach schneller Aufnahme der negativ-inotrope Effekt eine Funktion der zellulären Konzentration mit einer kurzen Verzögerungszeit von 19 s. Der negativ-inotrope Effekt erzeugte einen positiv-inotropen Reboundeffekt. Diese Toleranzentwicklung führte zu einer Reduktion des vorausgesagten steady-state Effektes (16%). Die gleichzeitige Gabe des Pgp Hemmers Amiodaron hatte keinen Einfluss auf die kardiale Kinetik von Verapamil. In endotoxemischen Herzen war der negativ-inotrope Effekt von Verapamil signifikant vermindert, was durch eine Reduktion der Anzahl der L-type Kalzium Kanäle erklärt werden kann.

Mit dem mechanistischen Modell für die  $\alpha_1$ -adrenergen Pharmaka war es möglich, die kardiale  $\alpha_1$ -AR Konzentration, die Assoziations- und Dissoziationskonstanten der Rezeptorliganden zusammen mit der stimulus-response Beziehung zu bestimmen, indem die Interaktion des  $\alpha_1$ -AR Agonisten Phenylephrin mit dem selektiven  $\alpha_1$ -AR Blocker Prazosin untersucht wurde.

Das PK/PD-Modell beschrieb den kardialen Transport und die Rezeptorbindungskinetik von Prazosin unter der Annahme, dass die kompetitive Verdrängung von Phenylephrin die Rezeptorbesetzung des Agonisten und damit die Kontraktilität reduzierte. Diese Methode erlaubte erstmalig eine Unterscheidung zwischen Effekten am  $\alpha_1$ -adrenergen Rezeptor und postreceptor Mechanismen.

## 9. References

- Abi-Gerges N, Tavernier B, Mebazaa A, Faivre V, Paqueron X, Payen D, Fischmeister R and Mèry P (1999) Sequential changes in autonomic regulation of cardiac myocytes after in vivo endotoxin injection in rat. *Am. J. Respir. Crit. Care Med.* **160**:1196-1204.
- Agrawal DK and Daniel EE (1985) Two distinct populations of [3H]prazosin and [3H]yohimbine binding sites in the plasma membranes of rat mesenteric artery. *J. Pharmacol. Exp. Ther.* **233**:195-203.
- Amitai G, Brown RD and Taylor P (1984) The relationship between alpha 1-adrenergic receptor occupation and the mobilization of intracellular calcium. *J. Biol. Chem.* **259**:12519-12527.
- Avontuur JAM, Bruining HA and Ince C (1995) Inhibition of Nitric Oxide Synthesis Causes Myocardial Ischemia in Endotoxemic Rats. *Circ. Res.* **76**:418-425.
- Baek M and Weiss M (2005) Mechanism-based modeling of reduced inotropic responsiveness to digoxin in endotoxemic rat hearts. *Eur. J. Pharmacol.* **514**:43-51.
- Balaysac D, Authier N, Cayre A and Coudore F (2005) Does inhibition of P-glycoprotein lead to drug-drug interactions. *Toxicol. Lett.* **156**:319-329.
- Ballard-Croft C, Carlson D, Maass DL and Horton JW (2004) Burn trauma alters calcium transporter protein expression in the heart. *J. Appl. Physiol.* **97**:1470-1476.
- Beder SD, Cohen MH and BenShachar G (1998) Time course of myocardial amiodarone uptake in the piglet heart using a chronic animal model. *Pediatr. Cardiol.* **19**:204-211.
- Bicer S, Patchell JS, Hamlin DM and Hamlin RL (2002) Acute effects of escalating doses of amiodarone in isolated guinea pig hearts. *J. Vet. Pharmacol. Ther.* **25**:221-226.
- Bodi I, Mikala G, Koch SE, Akhter SA and Schwartz A (2005) The L-type calcium channel in the heart: the beat goes on. *J. Clin. Invest.* **115**:3306-3317
- Bogle RG, McLean PG, Ahluwalia A and Vallance P (2000) Impaired vascular sensitivity to nitric oxide in the coronary microvasculature after endotoxaemia. *Br. J. Pharmacol.* **130**:118-124.
- Bonate PL (2006) *Pharmacokinetic-Pharmacodynamic modeling and simulation*. Springer Science&Business Media, Inc., New York, USA.
- Borlak J, Walles M, Levsen K and Thum T (2003) Verapamil: metabolism in cultures of primary human coronary arterial endothelial cells. *Drug Metab. Dispos.* **31**:888-891.
- Bosson S, Kuenzig M and Schwartz SI (1985) Verapamil improves cardiac function and increases survival in canine E. coli endotoxin shock. *Circ. Shock* **16**:307-316.
- Brodde O-E and Michel MC (1999) Adrenergic and muscarinic receptors in the human heart. *Pharmacol. Rev.* **51**:651-690.
- Brutsaert DL (2003) Cardiac endothelial-myocardial signaling: its role in cardiac growth, contractile performance, and rhythmicity. *Physiol. Rev.* **83**:59-115.

## 9. References

---

- Buwalda M and Ince C (2002) Opening the microcirculation: can vasodilators be useful in sepsis. *Intensive Care Med.* **28**:1208-1217.
- Campbell TJ and Williams KM (1998) Therapeutic drug monitoring: antiarrhythmic drugs. *Br. J. Clin. Pharmacol.* **46**:307-319.
- Catterall WA and Striessnig J (1992) Receptor sites for Ca<sup>2+</sup> channel antagonists. *Trends Pharmacol. Sci.* **13**:256-262.
- Charlier R, Deltour G, Baudine A and Chaillet F (1968) Pharmacology of amiodarone, an antianginal drug with a new biological profile. *Arzneim. Forsch.* **18**:1408-1417.
- Chatelain P, Ferreira J, Laruel R and Ruyschaert J (1986) Amiodarone-induced modifications of the phospholipid physical state. A fluorescence polarization study. *Biochem. Pharmacol.* **35**:3007-3013.
- Christopoulos A (2001) Annual Scientific Meeting of ASCEPT, 1999 from 'captive' agonism to insurmountable antagonism: demonstrating the power of analytical pharmacology. *Clin Exp Pharmacol Physiol* **28**:223-229.
- Cleton A, Ödman J, Graff PHVd, Ghijsen W, Voskuyl R and Canhof M (2004) Mechanism-based modeling of functional adaptation upon chronic treatment with midazolam. *Pharm. Res.* **3**:321-327.
- Colucci WS, Gimbrone MA, Jr. and Alexander RW (1984) Regulation of myocardial and vascular alpha-adrenergic receptor affinity. Effects of guanine nucleotides, cations, estrogen, and catecholamine depletion. *Circ. Res.* **55**:78-88.
- Connolly SJ (1999) Evidence-based analysis of amiodarone efficacy and safety. *Circulation* **100**:2025-2034.
- Corsi M and Kenakin T (2000) The relative importance of the time-course of receptor occupancy and response decay on apparent antagonist potency in dynamic assays. *J Auton Pharmacol* **20**:221-227.
- Couture L, Nash JA and Turgeon J (2006) The ATP-binding cassette transporters and their implication in drug disposition: a special look at the heart. *Pharmacol. Rev.* **58**:244-258.
- D'Argenio DZ and Schumitzky A (1997) *ADAPT II user's guide: pharmacokinetic/ pharmacodynamic systems analysis software* Simulations Resource, Los Angeles.
- De Paepe P, Belpaire FM and Buylaert WA (2002) Pharmacokinetic and pharmacodynamic considerations when treating patients with sepsis and septic shock. *Clin. Pharmacokinet.* **41**:1135-1151.
- Desai AD, Chun S and Sung RJ (1997) The role of intravenous amiodarone in the management of cardiac arrhythmias. *Ann. Intern. Med.* **127**:294-303.
- Dhein S (2005) The Langendorff heart, in *Practical methods in cardiovascular research* (Dhein S, Mohr FW and Delmar M eds) pp 155-172, Springer-Verlag, Berlin.
- Dobson GP and Cieslar JH (1997) Intracellular, interstitial and plasma spaces in the rat myocardium in vivo. *J. Mol. Cell Cardiol.* **29**:3357-3363.

## 9. References

---

- Drori S, Eytan GD and Assaraf YG (1995) Potentiation of anticancer-drug cytotoxicity by multidrug-resistance chemosensitizers involves alterations in membrane fluidity leading to increased membrane permeability. *Eur. J. Biochem.* **228**:1020-1029.
- Edwards SJ, Rattigan S, Colquhoun EQ, Woodcock EA and Clark MG (1988) Characterization of alpha 1-adrenergic receptors in perfused rat heart. *J Mol Cell Cardiol* **20**:1025-1034.
- Eisenberg MJ, Brox A and Bestawros AN (2004) Calcium channel blockers: an update. *Am. J. Med.* **116**:35-43
- Epstein MAF (1994) Winds of change: Current focus of the modeling in physiology department. *Am. J. Physio.* **267**:E628.
- Faber JE, Yang N and Xin XH (2001) Expression of  $\alpha$ -adrenoceptor subtypes by smooth muscle cell and adventitial fibroblast in rat aorta and in cell culture. *J. Pharmacol. Exp. Ther.* **298**:441-452.
- Fedida D, Braun AP and Giles WR (1993) Alpha 1-adrenoceptors in myocardium: functional aspects and transmembrane signaling mechanisms. *Physiol. Rev.* **73**:469-487.
- Fuller SJ, C.J. G, Hatchett RJ and DSugden PH (1991) Acute  $\alpha_1$ -adrenergic stimulation of cardiac protein synthesis may involve increased intracellular pH and protein kinase activity. *Biochem. J.* **273**:347-353.
- Garcia ML, Trumble MJ, Reuben JP and Kaczorowski GJ (1984) Characterization of verapamil binding sites in cardiac membrane vesicles. *J. Biol. Chem.* **259**:15013-15016.
- Gardmark M, Brynne L, Hammarlund-Udenaes M and Karlsson MO (1999) Interchangeability and predictive performance of empirical tolerance models. *Clin. Pharmacokinet.* **36**:145-167.
- Gengo PJ, Bowling N, Wyss VL and Hayes JS (1988) Effects of prolonged phenylephrine infusion on cardiac adrenoceptors and calcium channels. *J. Pharmacol. Exp. Ther.* **244**:100-105.
- Gray DF, Mihailidou AS, Hansen PS, Buhagiar KA, Bewick NL, Rasmussen HH and Whalley DW (1998) Amiodarone inhibits the Na<sup>+</sup>-K<sup>+</sup> pump in rabbit cardiac myocytes after acute and chronic treatment. *J. Pharmacol. Exp. Ther.* **284**:75-82.
- Gross G, Hanft G and Rugevics CU (1988)  $\alpha_1$ -adrenoceptors of rat myocardium: comparison of agonist binding and positive inotropic response. *Naunyn. Schmiedebergs Arch. Pharmacol.* **338**:582-588.
- Guiraudou P, Pucheu SC, Gayraud R, Gautier P, Roccon A, Herbert JM and Nisato D (2004) Involvement of nitric oxide in amiodarone- and dronedarone-induced coronary vasodilation in guinea pig heart. *Eur. J. Pharmacol.* **496**:119-127.
- Henningsson A, Karlsson MO, Vigano L, Gianni L, Verweij J and Sparreboom A (2001) Mechanism-based pharmacokinetic model for paclitaxel. *J. Clin. Oncol.* **19**:4065-4073.
- Hess ME, Shanfeld J and Levine NR (1975) Metabolic and inotropic effects of verapamil in perfused rat heart. *Recent Adv. Stud. Cardiac Struct. Metab.* **10**:81-88.
- Hockerman GH, Peterson BZ, Johnson aBD and Catterall WA (1997) Molecular determinants of drug binding and action on L-type calcium channels. *Ann. Rev. Pharmacol. Toxicol.* **37**:361-396.

## 9. References

---

- Hohlfeld T, Klemm P, Thiernemann C, Warner TD, Schror K and Vane JR (1995) The contribution of tumour necrosis factor-alpha and endothelin-1 to the increase of coronary resistance in hearts from rats treated with endotoxin. *Br. J. Pharmacol.* **116**:3309-3315.
- Holford N and Sheiner L (1981) Pharmacokinetic and pharmacodynamic modeling in vivo. *CRC Crit. Rev. Bioeng.* **5**:273-322.
- Hotchkiss RS, Osborne DF, Lappas GD and Karl IE (1995) Calcium antagonists decrease plasma and tissue concentrations of tumor necrosis factor-alpha, interleukin-1 beta, and interleukin-1 alpha in a mouse model of endotoxin. *Shock* **3**:337-342.
- Huang YF, Upton RN, Zheng D, McLean C, Gray EC and Grant C (1998) The enantiomer-specific kinetics and dynamics of verapamil after rapid intravenous administration to sheep: physiological analysis and modeling. *J. Pharmacol. Exp. Ther.* **284**:1048-1057.
- Jun AS and Brocks DR (2001) High-performance liquid chromatographic assay of amiodarone in rat plasma. *J. Pharm. Pharmaceut. Sci.* **4**:263-268.
- Kang W and Weiss M (2002) Digoxin uptake, receptor heterogeneity, and inotropic response in the isolated rat heart: A comprehensive kinetic model. *J. Pharmacol. Exp. Ther.* **302**:577-583.
- Kang W and Weiss M (2003) Kinetic analysis of saturable myocardial uptake of idarubicin in rat heart. Effect of doxorubicin and hypothermia. *Pharm. Res.* **20**:58-63.
- Keefe DL and Kates RE (1982) Myocardial disposition and cardiac pharmacodynamics of verapamil in the dog. *J. Pharmacol. Exp. Ther.* **220**:91-96.
- Keefe DL, Yee YG and Kates RE (1981) Verapamil protein binding in patients and in normal subjects. *Clin. Pharmacol. Ther.* **29**:21-26.
- Kenakin T (1993) *Pharmacologic analysis of drug-receptor interaction*. Raven Press, Ltd., New York, USA.
- Kodama I, Kamiya K and Toyama T (1997) Cellular electropharmacology of amiodarone. *Cardiovasc. Res.* **35**:13-29.
- Kolar F, Ost'adal B and Papousek F (1990) Effect of verapamil on contractile function of the isolated perfused rat heart during postnatal ontogeny. *Basic Res. Cardiol.* **85**:429-434.
- Latini R, Tognoni G and Kates RE (1984 ) Clinical pharmacokinetics of amiodarone. *Clin. Pharmacokinet.* **9**:136-156.
- Law MP, Osman S, Pike VW, Davenport RJ, Cunningham VJ, Rimoldi O, Rhodes CG, Giardina D and Camici PG (2000) Evaluation of [<sup>11</sup>C]GB67, a novel radioligand for imaging myocardial alpha 1-adrenoceptors with positron emission tomography. *Eur. J. Nucl. Med.* **27**:7-17.
- Lazarowski AJ, Garcia Ravello HJ, Vera Janavel GL, Cuniberti LA, Cabeza Meckert PM, Yannarelli GG, Mele A, Crottogini AJ and Laguens RP (2005) Cardiomyocytes of chronically ischemic pig hearts express the MDR-1 gene-encoded P-glycoprotein. *J. Histochem. Cytochem.* **53**:845-850.
- Lee HC and Lum BK (1986) Protective action of calcium entry blockers in endotoxin shock. *Circ. Shock* **18**:193-203.
- Lefkowitz RJ, Hoffman BB and Taylor P (1990) Chapter 5: Neurohumoral transmission: the autonomic and somatic motor nervous systems, in *Goodman & Gilman's The Pharmacological Basis of*

## 9. References

---

- Therapeutics* (Gilman GA, Rall TW, Nies AS and Taylor P eds) pp 221-243, *Pergamon Press, Inc.*, New Yorks.
- Lew W, Yasuda S, Yuan T and Hammond H (1996) Endotoxin- induced cardiac depression is associated with decreased cardiac dihydropyridine receptors in rabbits. *J. Mol. Cell Cardiol.* **28**:1367-1371.
- Li G, Qi XP, Wu XY, Liu FK, Xu Z, Chen C, Yang XD, Sun Z and Li JS (2006) Verapamil modulates LPS-induced cytokine production via inhibition of NF-kappa B activation in the liver. *Inflamm. Res.* **55**:108-113.
- Lubic SP, Nguyen KP, Dave B and Giacomini JC (1994 ) Antiarrhythmic agent amiodarone possesses calcium channel blocker properties. *J. Cardiovasc. Pharmacol.* **24**:707-714.
- Mager DE and Jusko WJ (2001) Pharmacodynamic modeling of time-dependent transduction systems. *Clin. Pharmacol. Ther.* **70**:210-216.
- Mandema JW and Wada DR (1995) Pharmacodynamic model for acute tolerance development to the electroencephalographic effects of alfentanil in the rat. *J. Pharmacol. Exp. Ther.* **275**:1185-1194
- Marks AR and Marx SO (2001) Chapter 2 cardiac contraction and relaxation: molecular and cellular physiology, in *Essential cardiology* (Rosendorff C ed) pp 23-37, W.B. Saunders Company, Pennsylvania.
- Mason RP, Gonye GE, Chester DW and Herbette LG (1989) Partitioning and location of Bay K 8644, 1,4-dihydropyridine calcium channel agonist, in model and biological membranes. *Biophys. J.* **55**:769-778.
- Mayo PR, Skeith K, Russell AS and Fakhreddin J (2000) Decreased dromotropic response to verapamil despite pronounced increased drug concentration in rheumatoid arthritis. *Br. J. Clin. Pharmacol.* **50**:605-613.
- McCloskey DT, Turnbull L, Swigart P, O'Connell TD, Simpson PC and Baker AJ (2003) Abnormal myocardial contraction in [alpha]1A- and [alpha]1B-adrenoceptor double-knockout mice. *J. Mol. Cell Cardiol.* **35**:1207-1216.
- McLean PG, Perretti M and Ahluwalia A (1999) Inducible expression of the kinin B1 receptor in the endotoxemic heart: mechanisms of des-Arg9bradykinin-induced coronary vasodilation. *Br. J. Pharmacol.* **128**:275-282.
- Meissner K, Sperker B, Karsten C, Zu Schwabedissen HM, Seeland U, Bohm M, Bien S, Dazert P, Kunert-Keil C, Vogelgesang S, Warzok R, Siegmund W, Cascorbi I, Wendt M and Kroemer HK (2002) Expression and localization of P-glycoprotein in human heart: effects of cardiomyopathy. *J. Histochem. Cytochem.* **50**:1351-1356.
- Muller-Werdan U, Reithman C and Werdan C (1996) Molecular mechanisms of septic cardiomyopathy, in *Cytokines and the heart* (Landes R ed) pp 21-124, Austin, Texas.
- Mustafa SB and Olson MS (1999) Effects of calcium channel antagonists on LPS-induced hepatic iNOS expression. *Am. J. Physiol. Heart Circ. Physiol.* **G351-60**.
- Najjar TA (2001) Disposition of amiodarone in rats after single and multiple intraperitoneal doses. *Eur. J. Drug Metab. Pharmacokinet.* **26**:65-69.

## 9. References

---

- Nawrath H and Wegener JW (1997) Kinetics and state-dependent effects of verapamil on cardiac L-type calcium channels. *Naunyn Schmiedebergs Arch. Pharmacol.* **355**:79-86.
- Nishimura M, Follmer CH and Singer DH (1989) Amiodarone blocks calcium current in single guinea pig ventricular myocytes. *J. Pharmacol. Exp. Ther.* **251**:650-659.
- O'Connell TD, Swigart PM, Rodrigo MC, Ishizaka S, Joho S, Turnbull L, Tecott LH, Baker AJ, Foster E, Grossman W and Simpson PC (2006)  $\alpha_1$ -Adrenergic receptors prevent a maladaptive cardiac response to pressure overload. *J. Clin. Invest.* **116**:1005-1014.
- Opie LH (1997) *The heart: Physiology, from cell to circulation*
- Parker JC and Townsley MI (2004) Evaluation of lung injury in rats and mice. *Am. J. Physiol. Heart Circ. Physiol.* **286**:L231-246.
- Perez DM, DeYoung MB and Graham RM (1993) Coupling of expressed alpha 1B- and alpha 1D-adrenergic receptor to multiple signaling pathways is both G protein and cell type specific. *Mol. Pharmacol.* **44**:784-795.
- Peters PG and Hayball PJ (1990 ) A comparative analysis of the loss of amiodarone from small and large volume PVC and non-PVC infusion systems. *Anaesth. Intensive Care* **18**:241-245.
- Powell AC, Horowitz, J. D. , Kertes, P. J. , Hasin, Y. , Syrjanen, M. L. , Henry, C. A. , Sartor, D. M. , Louis, W. J. (1990) Determinants of acute hemodynamic and electrophysiologic effects of verapamil in humans: role of myocardial drug uptake. . *J. Cardiovasc. Pharmacol.* **16**:572-583
- Raffel DM and Wieland DM (1999) Influence of vesicular storage and monoamine oxidase activity on [11C]phenylephrine kinetics: studies in isolated rat heart. *J. Nucl. Med.* **40**:323-330.
- Regev R, Yeheskely-Hayon D, Katzir H and Eytan GD (2005) Transport of anthracyclines and mitoxantrone across membranes by a flip-flop mechanism. *Biochem. Pharmacol.* **70**:161-169.
- Rhodes DG, Newton R, Butler R and Herbette L (1992) Equilibrium and kinetic studies of the interactions of salmeterol with membrane bilayers. *Mol. Pharmacol.* **42**:596-602.
- Riva E, Gerna M, Neyroz P and Urso R (1982 ) Pharmacokinetics of amiodarone in rats. *J. Cardiovasc. Pharmacol.* **4**:270-275.
- Riviere JE (1999) *Comparative pharmacokinetics: principles, techniques, and applications*. Iowa State Press, Iowa, USA.
- Rodgers T, Leahy D and Rowland MJ (2005) Physiologically based pharmacokinetic modeling 1: predicting the tissue distribution of moderate-to-strong bases *J. Pharm. Sci.* **94**:1259-1276.
- Rummel C, Sachot C, Poole S and Luheshi GN (2006) Circulating interleukin-6 induces fever through a STAT3-linked activation of COX-2 in the brain. *Am. J. Physiol. Regul. Integr. Comp. Physiol.* **291**:R1316-1326.
- Sakamoto A, Yanagisawa M, Tsujimoto G, Nakao K, Toyooka T and Masaki T (1994) Pseudo-noncompetitive antagonism by BQ123 of intracellular calcium transients mediated by human ETA endothelin receptor. *Biochem. Biophys. Res. Commun.* **200**:679-686.
- Sasongko L, Link JM, Muzi M, Mankoff DA, Yang X, Collier AC, Shoner SC and Unadkat JD (2005) Imaging P-glycoprotein transport activity at the human blood-brain barrier with positron emission tomography. *Clin. Pharmacol. Ther.* **77**:503-514

## 9. References

---

- Sattari S, Dryden WF, Eliot LA and Jamali F (2003) Despite increased plasma concentration, inflammation reduces potency of calcium channel antagonists due to lower binding to the rat heart. *Br. J. Pharmacol.* **139**:945-954.
- Schwinger RH, Bohm M and Erdmann E (1990) Negative inotropic properties of isradipine, nifedipine, diltiazem, and verapamil in diseased human myocardial tissue. *J. Cardiovasc. Pharmacol.* **15**:892-899.
- Shayeganpour A, Jun AS and Brocks DR (2005) Pharmacokinetics of amiodarone in hyperlipidemic and simulated high fat-meal rat models. *Biopharm. Drug Dispos.* **26**:249-257.
- Shea LD, Neubig RR and Linderman JJ (2000) Timing is everything: The role of kinetics in G protein activation. *Life Sciences* **68**:647-658.
- Sheiner LB, Stanski D, Vozeh S, Miller R and Ham J (1979) Simultaneous modeling of pharmacokinetics and pharmacodynamics: Application to *d*-tubocurarine. *Clin. Exp. Pharmacol. Physiol.* **25**:358-357.
- Sirmagul B, Kilic FS, Tunc O, Yildirim E and Erol K (2006) Effects of verapamil and nifedipine on different parameters in lipopolysaccharide-induced septic shock. *Heart Vessels* **21**:162-168.
- Sjaastad I, Schiander I, Sjetnan A, Qvigstad E, Bokenes J, Sandnes D, Osnes JB, Sejersted OM and Skomedal T (2003) Increased contribution of  $\alpha_1$ - vs.  $\beta$ -adrenoceptor-mediated inotropic response in rats with congestive heart failure. *Acta. Physiol. Scand.* **177**:449-458.
- Skomedal T, Aass H and Osnes J-B (1984) Specific binding of [3H]prazosin to myocardial cells isolated from adult rats. *Biochem. Pharmacol.* **33**:1897-1906.
- Skomedal T, Borthne K, Aass H, Geiran O and Osnes J-B (1997) Comparison between Alpha-1 Adrenoceptor-Mediated and Beta Adrenoceptor-Mediated Inotropic Components Elicited by Norepinephrine in Failing Human Ventricular Muscle. *J. Pharmacol. Exp. Ther.* **280**:721-729.
- Speelmans G, Staffhorst RW, De Wolf FA and De Kruijff B (1995) Verapamil competes with doxorubicin for binding to anionic phospholipids resulting in increased internal concentrations and rates of passive transport of doxorubicin. *Biochim. Biophys. Acta* **1238**:137-146.
- Stein WD (1997) Kinetics of the multidrug transporter (P-glycoprotein) and its reversal. *Physiol. Rev.* **77**:545-590.
- Sugiyama A, Satoh Y and Hashimoto K (2001) Acute electropharmacological effects of intravenously administered amiodarone assessed in the in vivo canine model. *Jpn. J. Pharmacol.* **87**:74-82.
- Sun YN and Jusko WJ (1998) Transit compartments versus gamma distribution function to model signal transduction processes in pharmacodynamics. *J. Pharm. Sci.* **87**:732-737.
- Tanaka T, Zhang L, Suzuki F and Muramatsu I (2004) Alpha-1 adrenoceptors: evaluation of receptor subtype-binding kinetics in intact arterial tissues and comparison with membrane binding. *Br. J. Pharmacol.* **141**:468-476.
- Tessier JP, Thurner B, Jungling E, Luckhoff A and Fischer Y (2003) Impairment of glucose metabolism in hearts from rats treated with endotoxin. *Cardiovasc. Res.* **60**:119-130.
- Thompson M, Kliewer A, Maass D, Becker L, White DJ, Bryant D, Arteaga G, Horton J and Giroir BP (2000) Increased cardiomyocyte intracellular calcium during endotoxin-induced cardiac dysfunction in guinea pigs. *Pediatr. Res.* **47**:669-676.

## 9. References

---

- Tu J, Shan Q, Jin H, Bourreau JP and Xia Q (2004) Endothelin-1-mediated coronary vasoconstriction deteriorates myocardial depression in hearts isolated from lipopolysaccharide-treated rats: interaction with nitric oxide. *Clin. Exp. Pharmacol. Physiol.* **28**:1208-1217.
- van Asperen J, van Tellingen O, Tijssen F, Schinkel AH and Beijnen JH (1999) Increased accumulation of doxorubicin and doxorubicinol in cardiac tissue of mice lacking mdr1a P-glycoprotein. *Br. J. Cancer* **79**:108-113.
- Van Zwieten PA (1994) Alpha-adrenoceptors and their subtypes: Pharmacological aspects, in *Pharmacodynamics and drug development perspectives in clinical pharmacology* (Cutler NR, Sramek, J.J., Narang, P.K. ed) pp 409-434, John Wiley & Sons Ltd., West Sussex.
- Vauquelin G, Van Liefde I and Vanderheyden P (2002) Models and methods for studying insurmountable antagonism. *Trends Pharmacol. Sci.* **23**:514-518.
- Walles M, Thum T, Levsen K and Borlak J (2001) Verapamil metabolism in distinct regions of the heart and in cultures of cardiomyocytes of adult rats. *Drug Metab. Dispos.* **29**:761-768.
- Wanecek M, Weitzberg E, Alving K, Rudehill A and Oldner A (2001) Effects of the endothelin receptor antagonist bosentan on cardiac performance during porcine endotoxin shock. *Acta Anaesthesiol. Scand.* **45**:1262-1270.
- Wang JH, Scollard DA, Teng S, Reilly RM and Piquette-Miller M (2005) Detection of P-glycoprotein activity in endotoxemic rats by <sup>99m</sup>Tc-sestamibi imaging *J. Nucl. Med.* **46**:1537-1545.
- Watanabe Y and Kimura J (2000) Inhibitory effect of amiodarone on Na<sup>+</sup>/Ca<sup>2+</sup> exchange current in guinea-pig cardiac myocytes. *Br. J. Pharmacol.* **131**:80-84.
- Weiss M (1999) The anomalous pharmacokinetics of amiodarone explained by nonexponential tissue trapping. *J. Pharmacokinet. Biopharm.* **27**:383-396.
- Weiss M, Baek M and Kang W (2004) Systems analysis of digoxin kinetics and inotropic response in rat heart: effects of calcium and KB-R7943. *Am. J. Physiol. Heart Circ. Physiol.* **287**:H1857-1867
- Weiss M and Kang W (2002) P-glycoprotein inhibitors enhance saturable uptake of idarubicin in rat heart: pharmacokinetic/pharmacodynamic modeling. *J. Pharmacol. Exp. Ther.* **300**:688-694.
- Westfall TC and Westfall DP (2005) Chapter 10: Adrenergic agonists and antagonists, in *Goodman & Gilman's The Pharmacological Basis of Therapeutics* (Brunton LL ed) pp 235-295, McGRAW-HILL Companies, Inc., New York.
- Wu CC, Wang JH, Chiao CW and Yen MH (1999) Comparison between effects of dantrolene and nifedipine on lipopolysaccharide-induced endotoxemia in the anesthetized rats. *Chin. J. Physiol.* **42**:211-217.
- Xiao R, Zhu W, Zheng M, Cao C, Zhang Y, Lakatta EG and Han Q (2006) Subtype-specific  $\alpha$ 1- and  $\beta$ -adrenoceptor signalling in the heart. *Trends Pharmacol. Sci.* **27**:330-337.
- Yamada S, Yamamura HI and Roeske WR (1980) Characterization of alpha-1 adrenergic receptors in the heart using [<sup>3</sup>H]WB4101: effect of 6-hydroxydopamine treatment. *J. Pharmacol. Exp. Ther.* **215**:176-185.
- Zhong J, Hwang TC, Adams HR and Rubin LJ (1997) Reduced L-type calcium current in ventricular myocytes from endotoxemic guinea pigs. *Am. J. Physiol. Heart Circ. Physiol.* **273**:H2312-2324.

## **Acknowledgement**

My sincere gratitude and the greatest respect is expressed to Prof. Dr. Michael Weiss for his endless patience, generosity, attention, continual guidance, understanding and encouragement throughout my Ph.D. study.

My special appreciation is given to Ms. Dagmar Günther for her endless kindly help and encouragement.

I wish to thank Dr. Myoungki Baek for his helpfulness introducing me to the techniques using in this research.

I am appreciated Dr. Osama Abd Elrahman for his cooperation and kindly help.

I am deeply grateful to all colleagues (Ms. Monika Niebisch, Ms. Sylvia Heidl, Ms. Rana Hassna and Mr. Tobias Bednarek) for their helpfulness and friendliness.

The financial support provided by Commission on Higher Education of the Royal Thai Government is gratefully acknowledged.

I sincerely thank Assoc. Prof. Suvatana Chulavatnatol at Pharmacy Faculty, Mahidol University, Thailand for providing background knowledge of pharmacokinetic research.

I would like to give special thank to friends who always encourage me.

Finally, I would like to express my deeply gratitude to my beloved family for their love and supporting throughout my whole life.

## Curriculum Vitae

**Name** Pakawadee Sermsappasuk

**Date of Birth** 24 January 1976

**Place of Birth** Bangkok, Thailand

**Nationality** Thai

**Marital Status** Single

### Education

1992-1997 Bachelor of Science in Pharmacy,  
Mahidol University, Bangkok, Thailand

1997-2000 Master of Science in Pharmacy (Clinical pharmacy)  
Mahidol University, Thailand

2003-2007 Ph.D. course at Section of Pharmacokinetics,  
Department of Pharmacology,  
Martin Luther University Halle-Wittenberg

### Achievement

Pharmacist's license in 2000

### Employment

2000- Lecturer at Department of Pharmacy Practice,  
Faculty of Pharmaceutical Sciences,  
Naresuan University, Phitsanulok, Thailand

## **Publications resulting from the thesis**

Sermsappasuk P, Baek M and Weiss M (2006) Kinetic analysis of myocardial uptake and negative inotropic effect of amiodarone in rat heart. *Eur. J. Pharm. Sci.* 28:243-248.

Sermsappasuk P, Abdelrahman O and Weiss M (2007) Modeling cardiac uptake and negative inotropic response of verapamil in rat heart: Effect of amiodarone. *Pharm. Res.* 24:48-57.

Sermsappasuk P, Abdelrahman O and Weiss M. Cardiac pharmacokinetics and inotropic response of verapamil in rats with endotoxemia. *J. Pharm. Sci.* (in press)

## **Oral Presentation**

Sermsappasuk P and Weiss M. Quantification of alpha 1-adrenoceptor concentration, ligand binding kinetics and inotropic response in the perfused rat heart: a PK-PD modeling analysis; *Pharmaceutical Sciences World Congress 2007*. Amsterdam, The Netherlands, 22-25 April 2007.

## Declaration

I hereby declare that the work presented in this manuscript titled “Modeling of cardiac uptake, binding kinetic and inotropic response of amiodarone, verapamil and  $\alpha_1$ -adrenergic agents in isolated rat heart” is my own and was carried out entirely with help of literature and aid cited in the manuscript.

Halle (Saale), Germany

July 2007

.....  
(Pakawadee Sermsappasuk)